CREEM

Centre for Research into Ecological and Environmental Modelling

Evaluating the effect of measurement error in pairs of 3D bearings in point transect sampling estimates of density

Tiago A. Marques[1,2], Pedro Duarte[3], Telmo Peixe[4], David Moretti[5] and Len Thomas[1]

1. *Centre for Research into Ecological and Environmental Modelling, The Observatory, University of St Andrews, tiago.marques@st-andrews.ac.uk*

2. *Centro de Estatística e Aplicações, Departamento de Estatística e Investigação Operacional, Faculdade de Ciências, Universidade de Lisboa*

3. *Departamento de Matemática, Faculdade de Ciências, Universidade de Lisboa*

4. *Universidade de Lisboa, Departamento de Matemática, ISEG Lisbon School of Economics & Management; CEMAPRE Centro de Matemática Aplicada à Previsão e Decisão Económica*

5. *Naval Undersea Warfare Center (NUWC), Newport, RI*

CREEM REPORT 2018-1

March 2, 2018

The recommended citation for this document is

Marques, T. A., Duarte, P., Peixe, T. Moretti, D. & Thomas, L. 2018 Evaluating the effect of measurement error in pairs of 3D bearings in point transect sampling estimates of density. CREEM Report 2018-1. Report produced for LMR under the DECAF-TEA project.

Contents

1 Introduction

In this report we investigate how errors in estimating the 3D bearing angles within the DECAF-TEA sensor setting propagate through to density estimates considering conventional distance sampling, in particular point transect sampling.

We begin with a quick description of distance sampling and in particular point transect sampling in the presence of measurement errors. This is followed by presenting the DECAF-TEA main objectives and the data collection and analysis setting. Then a description of the geometry involved follows, together with insights about how one can estimate the position of a sound source detected by two 3D bearing sensors measured with error. Then we describe how errors in 3D bearings might be conceptualized and then simulated. Finally, we conclude with some exploratory simulations presenting the propagation of measurement error in 3D bearings to 3D location estimates, from these to 2D distances projected on the ocean's bottom, and from those all the way through to final density estimates.

This report builds heavily on material first described in Marques & Thomas (2017), including in particular the process for simulating the measurement error in the 3D bearings. Code for the simulation of measurement error was also adapted from there.

2 Distance sampling

Distance sampling is arguably the most widely used method for estimating animal abundance and density over wide survey regions (Buckland *et al.* 2001, 2015). In recent years the methods have been adapted to the context of passive acoustic density estimation (Marques *et al.* 2013). The most common applications involve either line transects or point transects. DECAF-TEA is an example of the later.

2.1 Conventional point transect sampling

In conventional point transect distance sampling an estimator of animal density is given by

$$\hat{D} = \frac{\hat{h}(0)n}{2\pi k}$$

where n represents the number of detected objects of interest, k is the number of point transects and $\hat{h}(0) = \hat{f}'(0)$ is the first derivative of the pdf of detected distances, evaluated at distance 0. In our passive acoustic monitoring context the n would correspond to the number of detected acoustic cues. Note that, to convert the above density of cues into an animal density we would also require the recording time and the cue rate, but we ignore that aspect here. The above quantity can be directly related to the concept of detection probability (P), i.e. the probability of detecting an object of interest, which might lead to a more intuitive density estimator:

$$\hat{D} = \frac{n}{k\pi w^2 \hat{P}}$$

where w represents a truncation distance beyond which no detections are possible to occur. In some sense, is as if we are correcting a large area over which detection could have occurred ($k\pi w^2$), leading to a smaller effective detection area due to imperfect detectability.

A common simplification used in a conventional distance sampling context is that while detections might occur in a 3D space, these are usually projected to the plane where the sensors are (e.g. the ground in a terrestrial context, the sea surface in a boat based survey, or the bottom of the ocean in the case of bottom mounted passive acoustic sensors). So here too we will focus on how errors propagate from the 3D bearing estimation to the 2D distance estimation.

When using a conventional distance sampling approach we typically consider a likelihood based on the observed distances to the point transect (note that strictly the integration in the denominator should not be in r to show that the expression is not a function of r, but we use the standard way in which these functions are presented in the distance sampling literature)

$$f(r) = \frac{rg(r)}{\int_0^w rg(r)dr}$$

where $g(r)$ represents the detection function, and the r is coming from the distribution of distances available to be detected, which given an assumption about random transect placement, we assume to be known (and triangular). This is actually a simplification of

$$f(r) = \frac{\pi(r)g(r)}{\int_0^w \pi(r)g(r)dr} = \frac{\frac{2r}{w^2}g(r)}{\int_0^w \frac{2r}{w^2}g(r)dr}$$

where the multiplying constants have canceled out.

Conventional distance sampling (CDS) requires a set of assumptions for unbiased estimates of density. Buckland *et al.* (2015) provide details about all of these. Not surprisingly, given that the detection function is estimated using the recorded distances, one of the key assumptions is that distances are measured without errors. In the presence of measurement error the estimators might become severely biased.

2.2 Distance sampling with measurement error

In the presence of measurement error, Borchers *et al.* (2010) proposed extensions to incorporate information coming from a model for the measurement error. This assumed then that the likelihood is based on the observed distances, themselves a function of the true (unobserved) distances. Despite being unobserved, we can integrate them out given a model for the error distances y, given the true distances, r, $f(y|r)$. We then have a likelihood that is expressed as a function of the observed distances with error

$$f(y) = \int_0^\infty f(y|r)f(r)dr$$

The required extra bit of information over conventional CDS is the measurement error model, $f(y|r)$.

What makes the current setting special is that the measurement error will not be radially symmetric, and so it might require that we develop new expressions which are a function of not only distance, but distance and angle. Actually, strictly speaking, the measurement error will be a function of distance, angle and depth, but below we assume that the depth component can be ignored. Preliminary results do seem to show that when looking at slices of the surface of the coeficient of variation (CV) of the error these appear remarkably constant across depths (perhaps because the potential variation in depth is small relative to the changes in distances).

From above, we could extend the formulation to include both angle (say θ), and radial distance

$$f(r,\theta) = \frac{\pi(r,\theta)g(r,\theta)}{\int_0^{2\pi}\int_0^w \pi(r,\theta)g(r,\theta)\ dr\ d\theta}$$

Despite it being now bivariate, we still assume that the detection itself is independent of angle and that the distribution in r and θ are independent, and, as usual in CDS, known by design. In particular we assume a random distribution in the circle for θ. Then we get

$$f(r,\theta) = \frac{\pi(r)\pi(\theta)g(r)}{\int_0^{2\pi}\int_0^w \pi(r)\pi(\theta)g(r)\ dr\ d\theta} = \frac{rg(r)}{\int_0^{2\pi}\int_0^w rg(r)\ dr\ d\theta} = \frac{rg(r)}{2\pi\int_0^w rg(r)dr} = \frac{f(r)}{2\pi}$$

and therefore, for a likelihood based on non-isotropic errors, we have a similar expression as above

$$f(y) = \int_0^\infty \int_0^{2\pi} f(y|r,\theta) f(r,\theta)\ d\theta\ dr = \int_0^\infty \int_0^{2\pi} f(y|r,\theta) \frac{f(r)}{2\pi}\ d\theta\ dr$$

3 DECAF-TEA

3.1 Setting overview

The objective of DECAF-TEA is to showcase a way to estimate density from bottom mounted fixed passive acoustic sensors in areas without existing Navy Instrumentation. After a search for a suitable hardware system, we determined that an optimal, cost-efficient system is one built in house at NUWC (see separate report) with two types of sensor units: (1) units with a single hydrophone, 1HU, and units with 4 hydrophones, 4HU, arranged close together in a tetrahedron, capable of providing a 3D bearing angle to sounds detected on the four hydrophones. Sampling (i.e. recording) points will be distributed over the area over which inferences are required, typically in a regular grid. Each sampling point will be called a node. A node can be composed of one or two units. There are two node types, designated n-nodes and p-nodes (Figure 1). Nodes with a single 1HU are called n-nodes, alluding to the fact that these nodes allow us to get counts of detected sounds, usually denoted in density estimation formulas using the symbol "n". These provide information about encounter rate, in distance sampling jargon. A pair of 4HUs placed close together are referred to as p-nodes. The "p" is the symbol typically used for detection probability in density estimation formulas. A pair of 3D bearing angles provides enough information to estimate a 3D location, and therefore to estimate the detectability of the sounds detected. Estimating detectability is the cornerstone of animal density estimatoin (naturally together with estimates of cue rate, and eventually false positives; that will be addressed elsewhere within the DECAF-TEA project). Ideally, all nodes would be p-nodes, but cost and logistics mean that only a subset might.

Note that under such a setting, the assumption is that the pairs of 4HUs are placed close together such that they generate a virtual point transect half way between the pair. The implications of this assumption are addressed below and we note that a possible alternative to this approach might be the use of spatially explicit capture recapture (SECR), a topic which will also be address in a separate document(s). As planned, beaked whales would be estimated using distance sampling, and fin whales would be estimated from SECR.

We note in passing that if that a 4HU was not much more expensive to build and deploy than a 1HU, then one might argue that n-nodes could be made of single 4HU instead of single 1HUs. This has an additional advantage because, although confounded with the distribution of depths at which animals vocalize, there is some information about detectability in the distribution of single individual 3D bearings (see separate subsection later where we explore this concept). However, there is an additional cost benefit analysis to be made when making such a choice. The main downside of having all the n-nodes with 4HUs is if the 4HUs are memory or battery constrained. As an example, if we could record on a 1HU for 4 months without servicing, yet we can only record on a 4HU for 1 month, then it is a cost benefit analysis in terms of servicing what is the most adequate setting for long term deployments of a grid with both n-nodes and p-nodes.

In particular, for a p-node we assume to have pairs of 4HUs capable of providing pairs of independent 3D bearings to detected whale sounds. From a single source, in the absence of measurement error, pairs of 3D bearings would intersect at a single point in 3D, and hence the position of the detected source would be known with certainty. However, in the presence of measurement error the two bearings will not cross and therefore, at best, an estimate of the most likely position for the source can be obtained. The quality of the estimate will depend on a number of factors affecting the relative geometry involved, and this will be investigated at length below.

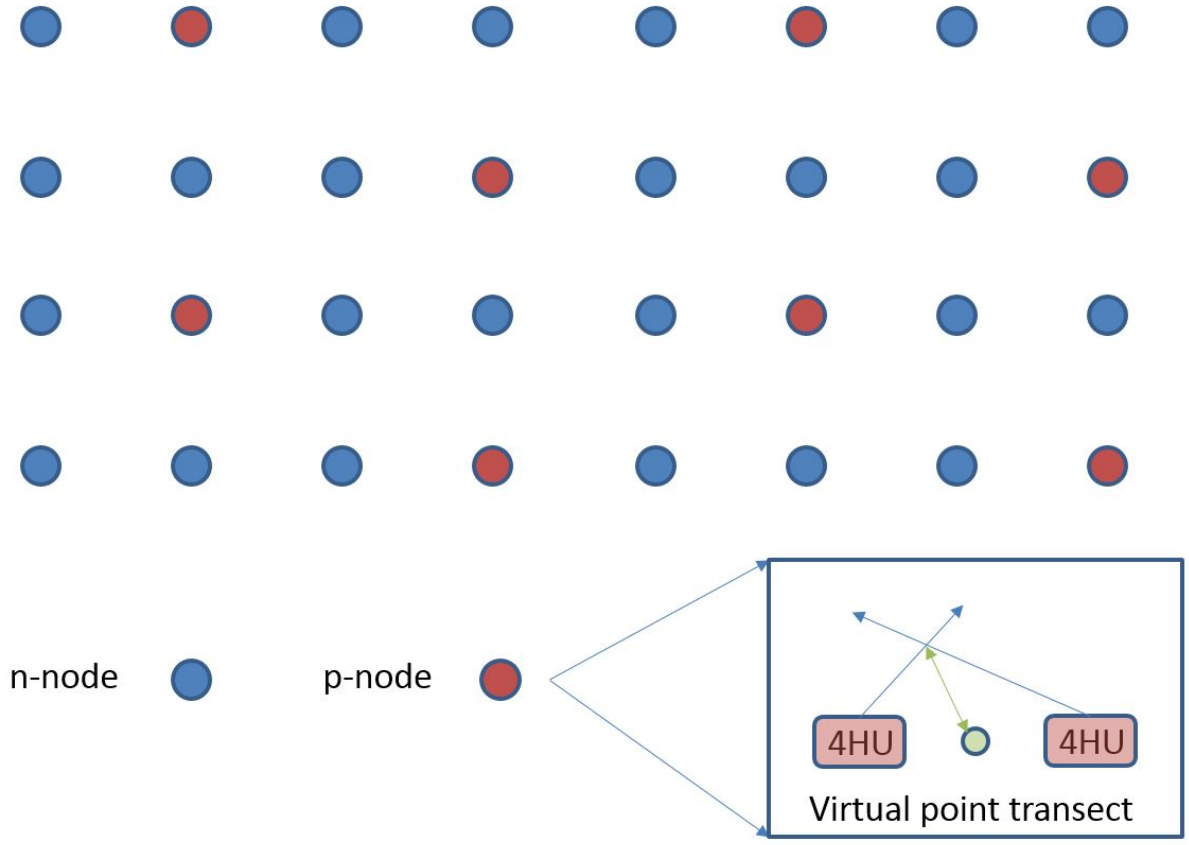

Figure 1: An example grid of nodes, with n-nodes and p-nodes, with a zoom in a p-node, showing the pair of 4 hydrophone units (4HU) and the corresponding virtual point transect half way in between the 2 4HU

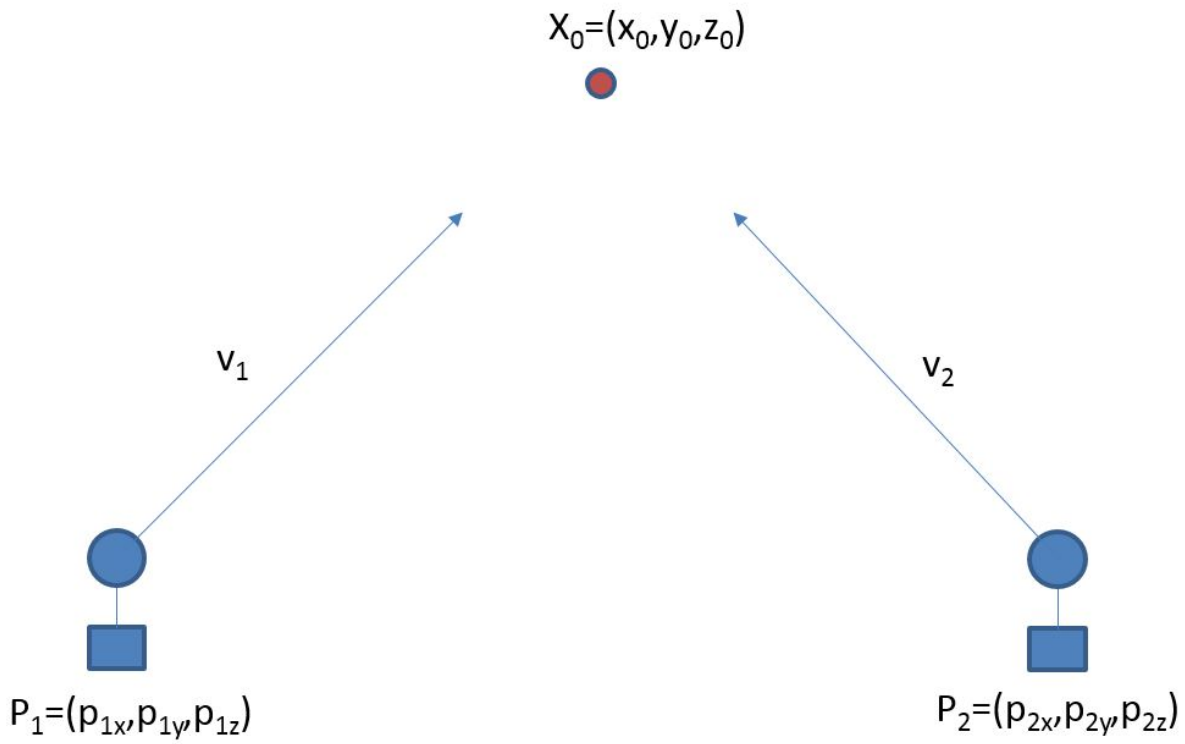

Figure 2: Bearing array geometry for estimating the location of a sound source location that we wish to given the location of a pair of 4 hydrophone units along with the resulting estimated 3D bearing to a detected sound source (red dot).

3.2 The geometry involved

Consider a sound source (here, a whale vocalizing) is located at $X_0 = (x_0, y_0, z_0)$ and that a pair of 4HUs, capable of providing 3D headings to detected sound sources, are available. Each 4HU location is known, at say $P_1 = (p_{1x}, p_{1y}, p_{1z})$ and $P_2 = (p_{2x}, p_{2y}, p_{2z})$, and each provides a 3D bearing, say respectively $v_1 = (v_{11}, v_{12}, v_{13})$ and $v_2 = (v_{21}, v_{22}, v_{23})$ (Figure 1). In the presence of measurement error the whale position must be estimated.

This is a problem akin to that described in Duarte *et al.* (2013). In that case a simpler 2D context was considered, and bearings (ranges in bearing) were assumed to be obtained without error, making it purely geometrical, i.e. non statistical, in nature. Nonetheless, the same objective of finding a whale's position given a pair of measurements was involved.

In the absence of measurement error the two 3D bearings would cross at a single point in 3D space, the whale position. Given that such 3D position is found, then one could project the position into the bottom of the ocean, and therefore obtain the required distance(s) to implement a distance sampling analysis. This is illustrated in figure 3.

However, in the presence of measurement error in the 3D bearings, the probability that the two 3D bearings cross in 3D space is zero. This is illustrated in figure 4, where a lateral view could lead us to think the bearings cross, but a vertical view shows that the bearings do not cross at any point.

Therefore, the problem is not really about finding the 3D position where the 2 3D bearings cross, but that of finding the more likely location of the whale given pairs of non-crossing 3D bearings. Intuitively, that

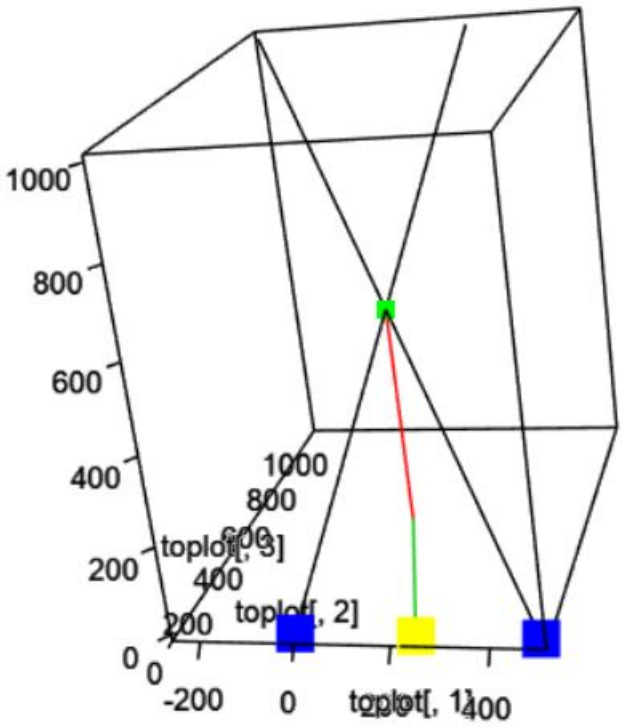

Figure 3: The geometric setting involved in a p-node. The 2 4HU are shown in blue, the virtual point transect in yellow, the sound source location and the 2D projected distance to the virtual point transect in green. The two true 3D bearings are shown in black.

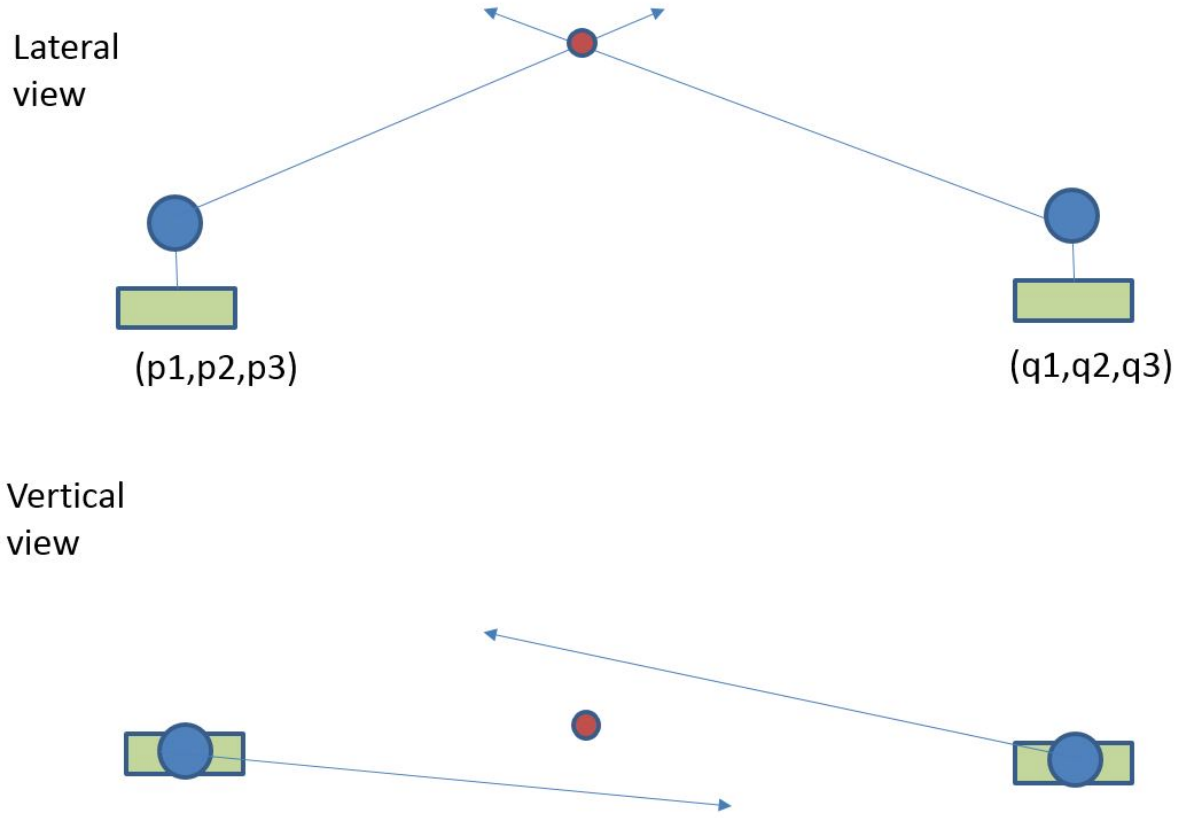

Figure 4: Illustrating how two 3D bearing angles do not cross in any point in 3D.

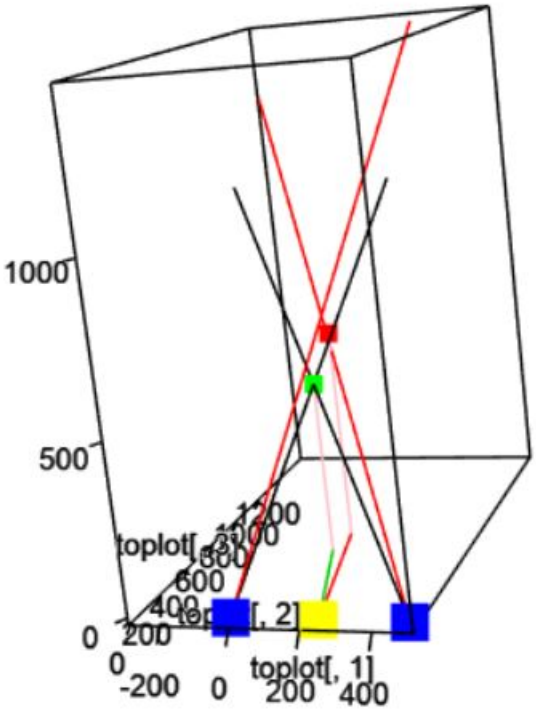

Figure 5: The true bearings to the true sound source position are shown as black solid lines, while the position of the sound source and the 2D projected distance to the virtual point transect are represented in green. The estimated bearings, the corresponding estimated position and 2D distance in the presence of errors in the bearings are shown in red.

corresponds to finding a position that minimizes the sum of the square of the distances between it and the 2 3D bearings.

Ideally we would like to obtain a function of the available quantities, P_1, P_2, v_1, v_2, returning the desired solution location X_0

$$X_0 = f(P_1, P_2, v_1, v_2)$$

Then, given this estimated position, we can again project downwards and obtain a 2D distance. This is illustrated in figure 5, where both the true position and 2D distance and the position and 2D distance estimated with errors are represented

3.3 The virtual sensor concept

Typically, point transect distance sampling would be conducted from a single point. In terrestrial applications this would correspond typically to a human observer. In the passive acoustic context, this would correspond to a single hydrophone. Given such a context, the recorded distances to the point are unambiguous and modelling a detection from these is straightforward.

In the current context, however, to obtain a localization and hence a projected 2D distance, we require at least 2 3D bearings, which means detections at 2 4HUs placed close together. Under such a context, we have two alternatives available to us: (1) consider a methodology that can treat the detections in each 4HU

independently, like SECR, or (2) consider a virtual point transect at half way between the pair of 4HUs. In this report we address only the later case.

That means that we must distinguish between what is a "detection" detection function, and a "localization" detection function. The former is what applies to each of the 4HUs. The later is the result of the compound process required for a localization, i.e., that a sound is detected by both units. To avoid the confusing terminology in this section we refer to "detection function" to the former and "localization function" to the later. In the remainder of the report we might simply use the term detection function when no confusion arises given the context.

If we assumes a common detection function for the 2 4HUs, the localization function, i.e. the detection function for a localization of a sound produced at X, $g_l(X)$ with respect to a virtual sensor at the center of the pair, would be given by the product of the detection functions for detecting the sounds in each unit (g_d)

$$g_l(X) = g_l(d) = g_d(X) \times g_d(X) = g_d(d1) \times g_d(d2)$$

where d represents the distance between the virtual sensor and the call, $d1$ represents the distance from the source to the first 4HU and $d2$ the distance from the source to the second 4HU.

We present below some resulting localization function examples, assuming a usual Half-Normal detection function for each 4HU. If the detection detection function has a wide shoulder, then the localization function might be well approximated by a function with the usual decreasing probability with distance pattern. We begin with an example with a large σ compared to the units separation, a σ the same as the units separation and a σ smaller than the units separation.

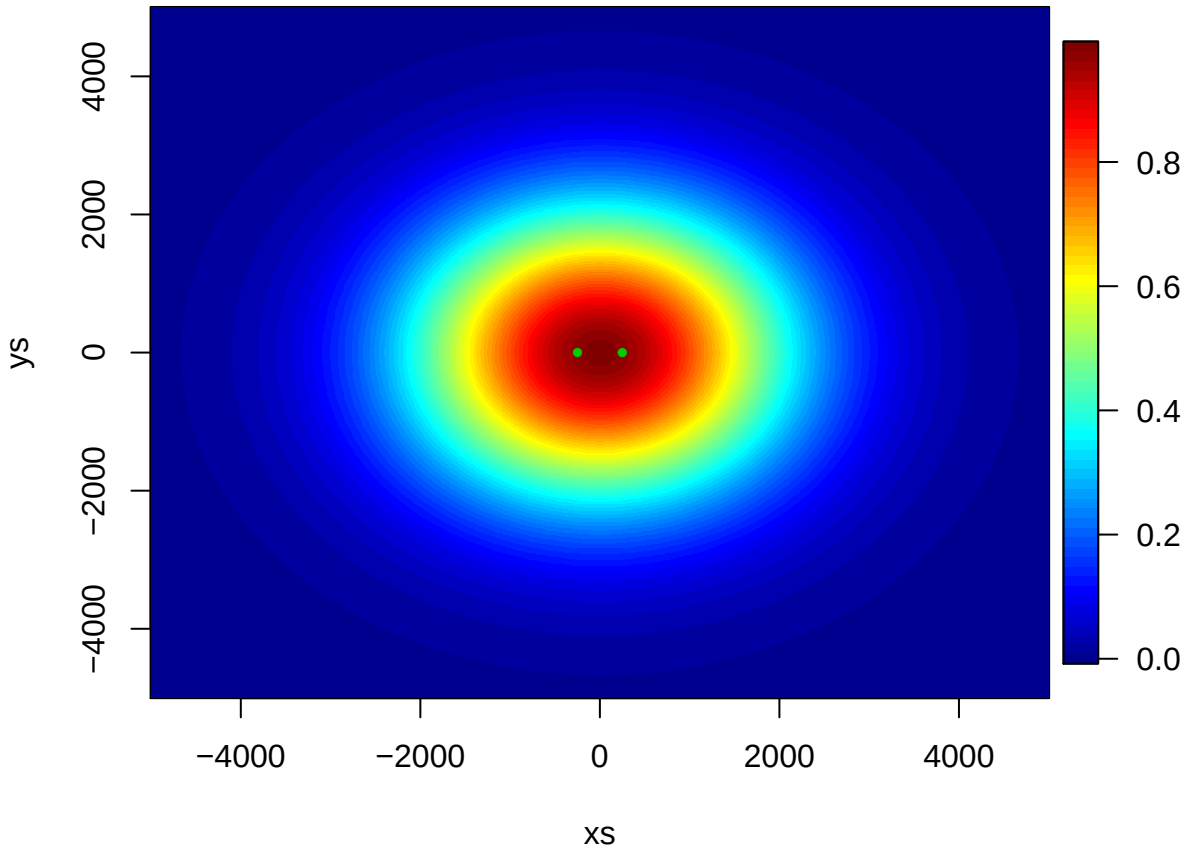

Figure 6: Localization function given a Half Normal detection function, where the scale parameter is larger than the 2 4HU separation.

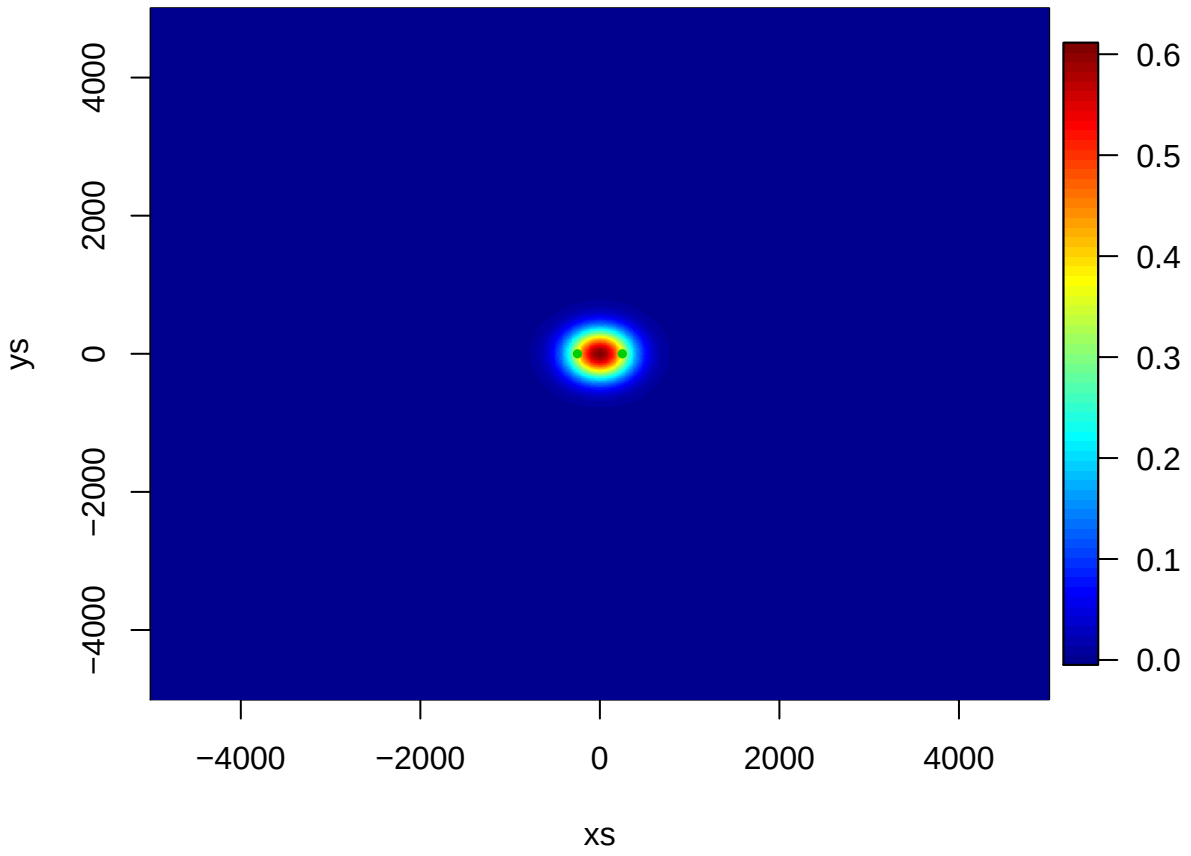

Figure 7: Localization function given a Half Normal detection function, where the scale parameter is the same as the 2 4HU separation.

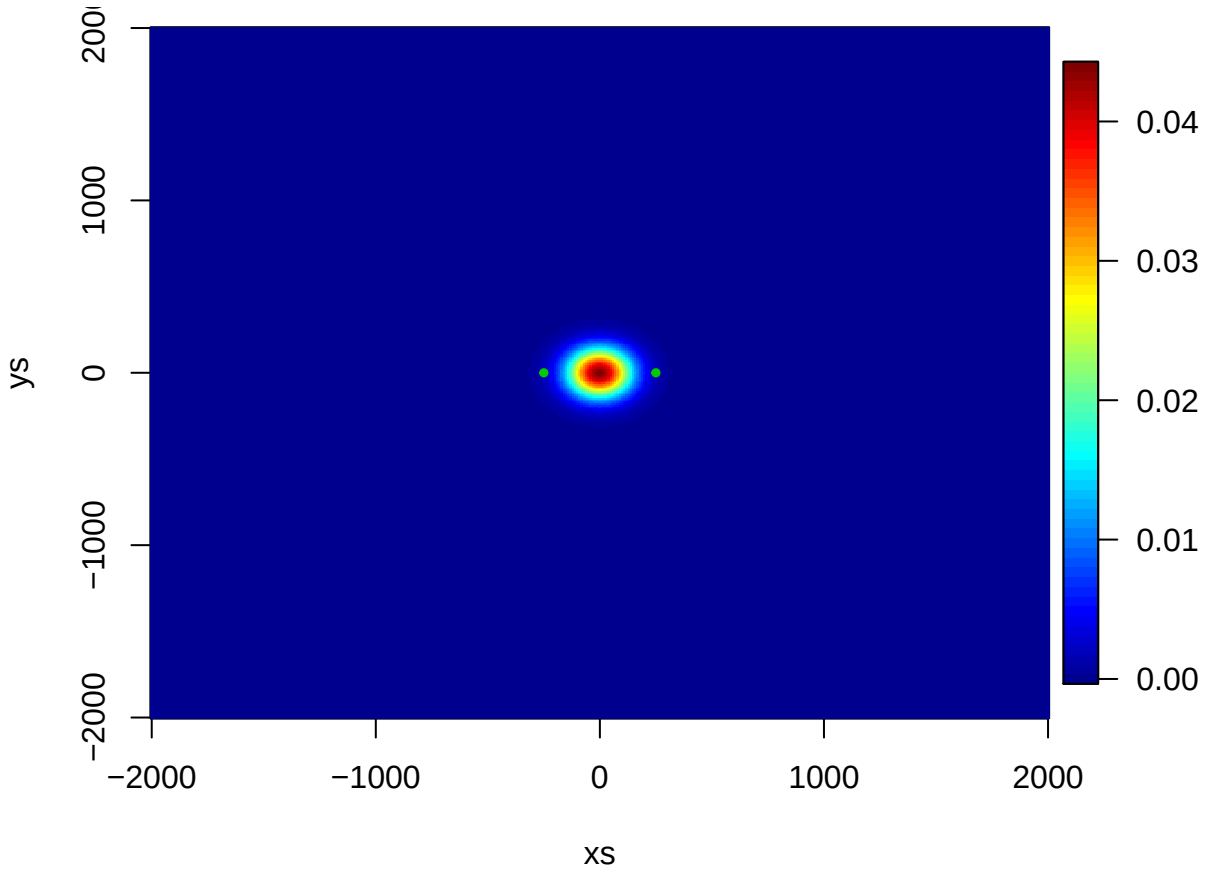

Figure 8: Localization function given a Half Normal detection function, where the scale parameter is smaller than the 2 4HU separation.

Of course if one considers less likely detection functions the resulting localization function might also not be what one would expect. The next example illustrates the use of a step function detection function (i.e. detection probability is 1 up to a given distance from the 4HU, then 0 beyond that)

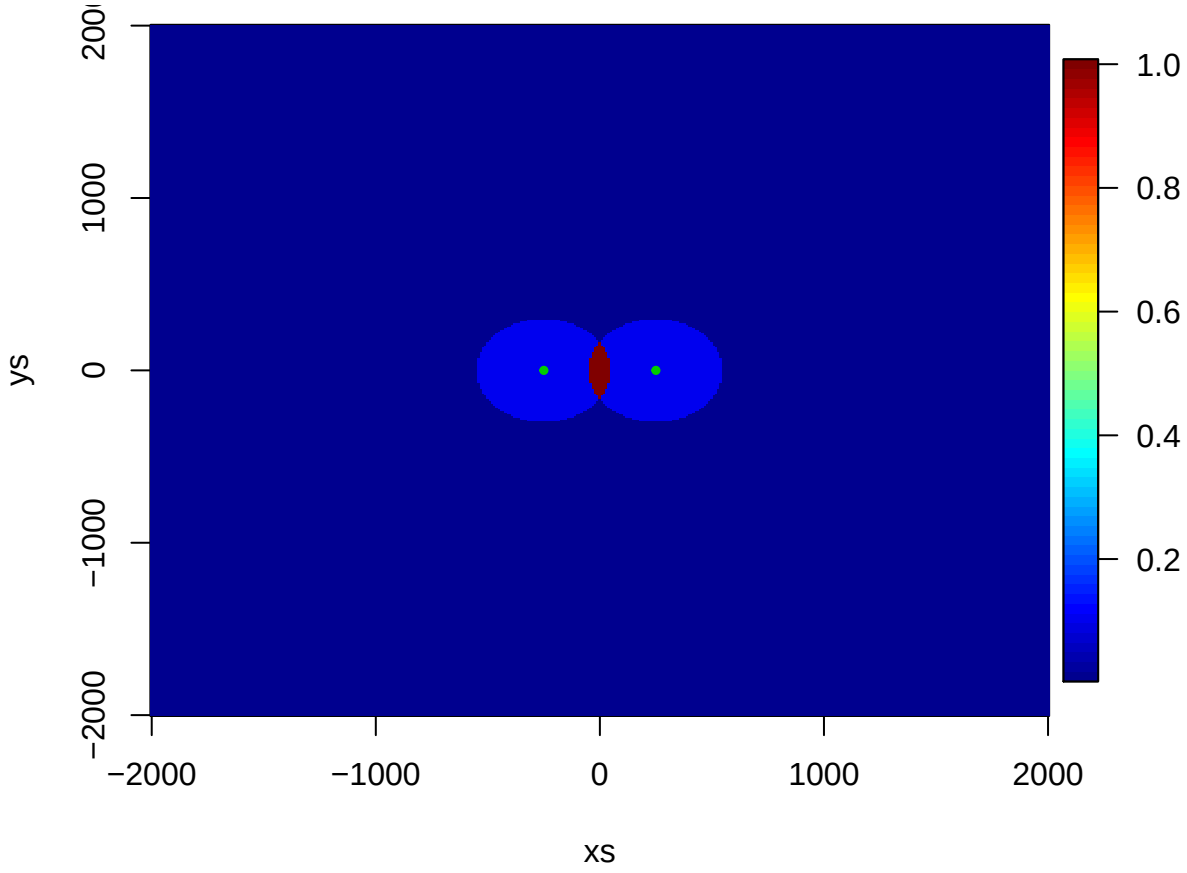

Figure 9: Localization function given a step function detection function

Finally, considering a hazard rate for the detection function leads to the following localization function.

In general we will assume that the localization function can be reasonably approximated by a detection function with respect to the virtual point transect.

4 Estimating a source's 3D location

Here we formalize the problem in terms of d 3D bearing sensors, but typically we will use only two sensors. We note however that it is possible that the test deployment will have 3 4HU placed in close vicinity, so that redundancy would be obtained - i.e. 3 3D bearings for some of the detected sources.

Consider a finite number of points $\{P_j = (p_{1j}, p_{2j}, p_{3j}) \in \mathbb{R}^3 \colon j = 1, \ldots, d\}$, where $d \geq 2$ sound sensors are placed.

When a sound is produced at a point $X_0 = (x_0, y_0, z_0)$ each sensor detects its 3D bearing as a unit vector $v_j = (v_{1j}, v_{2j}, v_{3j})$ which up to a small random error points to the sound's source. The problem is then to estimate the sound location $X_0 = (x_0, y_0, z_0)$ from the data $S := \{(P_j, v_j) \colon 1 \leq \ j \leq d\}$.

For each $j = 1, \ldots, d$ let V_j be the line through P_j parallel to v_j

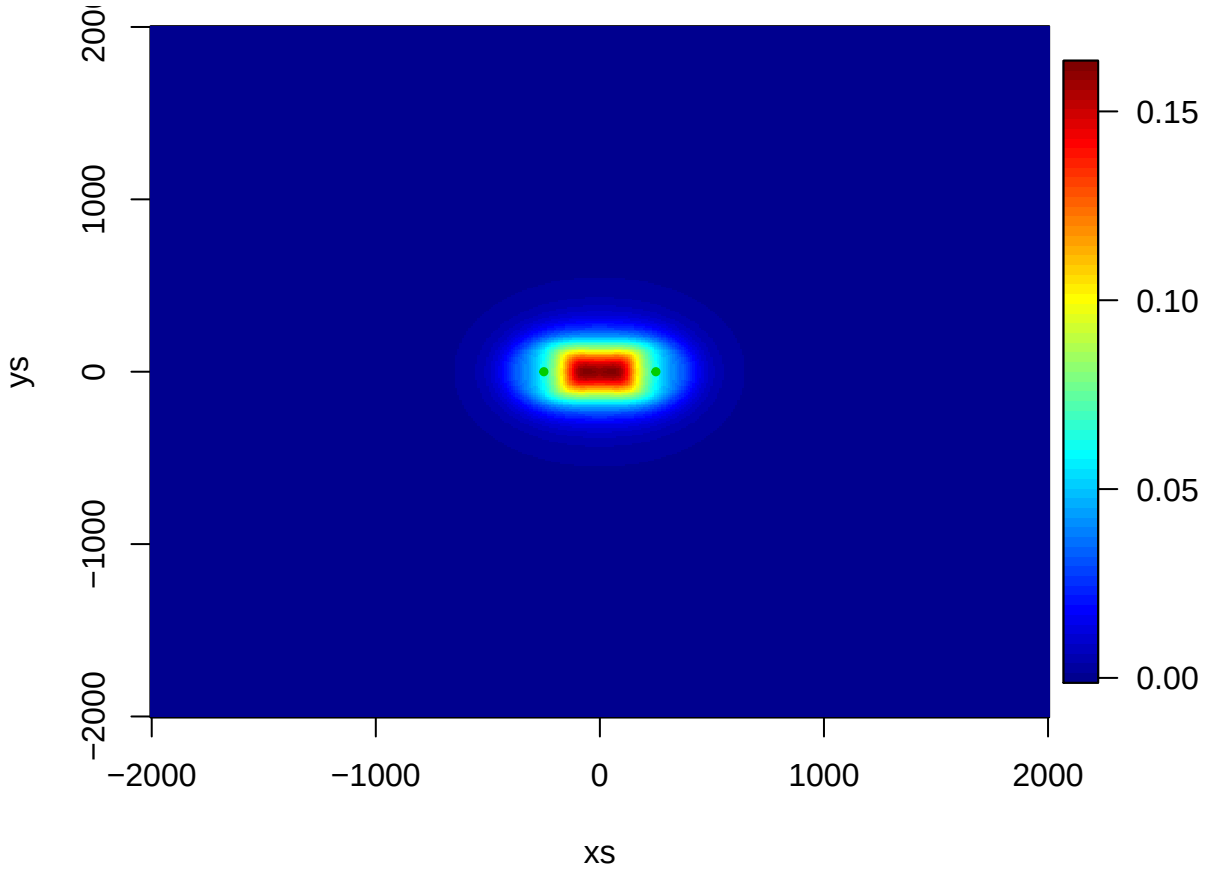

Figure 10: Localization function given a Hazard Rate detection function

$$V_j := \{P_j + tv_j : t \in \mathbb{R}\}.$$

Note a key but subtle difference: v_j is a unit vector, while V_j is not. We can now define an error function $E_S : \mathbb{R}^3 \to \mathbb{R}$ that represents the sum of the squared distance (dist) between each V_j and a given point in space, X:

$$E_S(X) := \sum_{j=1}^{d} \text{dist}(X, V_j)^2.$$

Given $X \in \mathbb{R}^3$, the value $E_S(X)$ measures the observation error when the source of the sound is $X_0 = X$. The function E_S is quadratic (i.e., polynomial in $X = (x, y, z)$ with degree 2) and positive semi-definite (i.e., $E_S(X) \geq 0$).

Set then

$$e(S) := \min_{X \in \mathbb{R}^3} E_S(X),$$
$$Q(S) := \text{argmin}_{X \in \mathbb{R}^3} E_S(X).$$

Clearly, in the absence of measurement error all the lines V_j are concurrent on the same point, and therefore only in that case $e(S) = 0$. When at least a pair of lines V_i and V_j with $i \neq j$ are not parallel then E_S is positive definite quadratic function whose minimum set $Q(S)$ reduces to a single point - our best estimate of the sound source location.

In the case where $d = 2$ we have that

$$e(S) = \frac{|(P_1 - P_2) \cdot (v_1 \times v_2)|^2}{||v_1 \times v_2||^2}.$$

Note that in the above "$\cdot$" corresponds to the usual vector product (in software R implemented by "%*%"") and $\times$ represents the cross product of two vectors (the cross product is not available in native R, therefore we created a dedicated function to implement it)

Moreover, defining

$$Q_1 := P_1 + \left(\frac{((v_1 \times v_2) \times v_1) \cdot (P_1 - P_2)}{||v_1 \times v_2||^2} \right) v_1$$
$$Q_2 := P_2 + \left(\frac{((v_1 \times v_2) \times v_2) \cdot (P_1 - P_2)}{||v_1 \times v_2||^2} \right) v_2$$

the line Q_1Q_2 is orthogonal to both V_1 and V_2. The minimum point $Q(S)$ is in this case the middle point of the segment $\overline{Q_1Q_2}$, i.e., $Q(S) = \frac{Q_1+Q_2}{2}$.

Intuitively, one can see that ψ=dist(Q_1, Q_2) is proportional to the uncertainty about the true location. If the error was very small said distance would be small, if the error was very large, said distance would be large.

Given one obtains an estimate of the 3D position based on the pair of 3D bearings with error, one can project downwards to obtain the 2D projected distance, which is typically what one would use in a conventional distance sampling setting.

5 Errors in 3D bearings

Models for measurement errors in observations of univariate random variables, for instance distances to detected animals in a conventional distance sampling context, are conceptually simple. Given such a model and a true distance, simulating distances contaminated with error is straightforward. In the case of DECAF-TEA, the errors will be associated with the 3D bearings. This requires some model for errors in 3D bearings, which is slightly less obvious, given that a vector in 3D is defined by 3 components with respect to a set of axes.

Collecting actual data on measurement error will be fundamental to understand what might be reasonable measurement error models. Here we present some alternatives based on first principles. These are guided by the notion that one can conceptualize the error defined as x degrees around the true 3D bearing.

We note upfront that for simplicity we assume that errors in the 3D bearings will be independent of the actual relative geometry of the sound source to the 4HU, but this is unlikely to be the case. The ability to provide a 3D angle should be dependent on the actual location of the source, and therefore we might want to revisit this assumption at a later stage.

To illustrate the complexity of quantifying measurement error in 3D, we introduce the first measurement error model that we naively considered: an unbiased (i.e. mean 0) Gaussian error with a given standard deviation, acting independently on each of the 3 components of vectors defining the 3D-bearings. That means that for a true bearing

$$B = (b_x, b_y, b_z)$$

the error bearing would be obtained as

$$B^* = B(1 + E) = B + BE = B(1 + e_x, 1 + e_y, 1 + e_z)$$

where E is a vector with 3 independent Gaussian distributions with mean 0, presumably leading to unbiased errors. Interestingly, this formulation could lead to considerably anysotropic patterns in the measurement error, because clearly the error depends on the original value. The reader is referred to Marques & Thomas (2017) for additional details.

An alternative approach, which might be more sensible and avoids the above mentioned artifacts, considers an error model that does not apply to each of the vector components independently.

Consider first the true heading that goes from a single 4HU to the sound source. Then define a set of additional auxiliary orthonormal vectors that can be used to define a plane perpendicular to this first true heading. Then generate a point on that plane according to the desired measurement error and select the 3D bearing errors resulting from the line that passes through the sensor and those points.

Unless otherwise stated all the vectors below are normalized. Consider $\vec{AB}$ to represent the direction between the sensors and given by $B - A$, and $\vec{v} = \frac{\vec{AP}}{||\vec{AP}||} =$ to represent the 3D-bearing between sensor A and the whale at position P.

Then, a reasonable second vector orthonormal to $\vec{v}$ is $\vec{u}$ obtained as

$$\vec{u} = \frac{\vec{AB} - (\vec{AB} \cdot \vec{v})\vec{v}}{||\vec{AB} - (\vec{AB} \cdot \vec{v})\vec{v}||}.$$

Finally we can get $\vec{w}$, a third orthonormal (to $\vec{v}$ and $\vec{u}$) auxiliary vector, as

$$\vec{w} = \frac{\vec{v} \times \vec{u}}{||\vec{v} \times \vec{u}||}$$

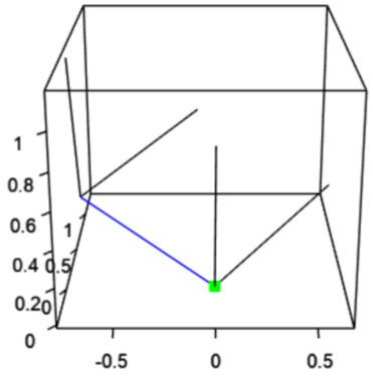

Figure 11: Defining a set of auxiliary vectors for generating 3D bearings with error. The sensor is shown in blue, the true 3D bearing between sensor and whale in green, and the pair of auxiliary orthogonal vectors are shown in black (these are shown both with respect to the sensor location and on the tangent of the unit sphere centred at the sensor)

For a specific example we can examine what these look like in space in figure 11. The original sensor to whale vector is shown in blue, the sensor location in green, and the two auxiliary axis are shown in black.

To generate an error in bearing we can now take a number of possible approaches, we consider explicitly two below.

Note that, since we are now going to generate errors on a plane perpendicular to the whale-sensor 3D bearing, a plane which approximates a unit sphere, we need to think about sensible units to use for the errors. If we want to generate errors with a given standard deviation in the 3D angle, what are the units to consider on the plane? Figure 12 helps to understand what is at stake.

We want to generate errors with magnitude $\tan\theta$. For small θ, $\tan\theta = \theta$, hence we can approximate the angle by its tangent. As an example, if we want to have a standard deviation of 2 degrees in 3D radial angle, we need to generate on the auxiliary plane a Gaussian with a standard deviation of $\tan\{\frac{2\pi}{360}\}$=0.017455 $\approx$ 0.017453.

5.1 Uniform direction and random angle

Generate a random direction θ (with respect to the original 3D bearing) and then a δ from the appropriate distribution (e.g. a Gaussian with mean 0 and standard deviation σ) and the resulting error vector $\vec{v_\delta}$ will be given by

$$\vec{v_\delta} = \vec{v} + \delta\cos(\theta)\vec{u} + \delta\sin(\theta)\vec{w}$$

5.2 Gaussian bivariate

Generate a bi-variate Gaussian (X, Y) with mean value (0,0) and standard deviation σ, then the resulting error vector $\vec{v_\delta}$ will be given by

$$\vec{v_\delta} = \frac{\vec{v} + X\vec{u} + Y\vec{w}}{||\vec{v} + X\vec{u} + Y\vec{w}||}$$

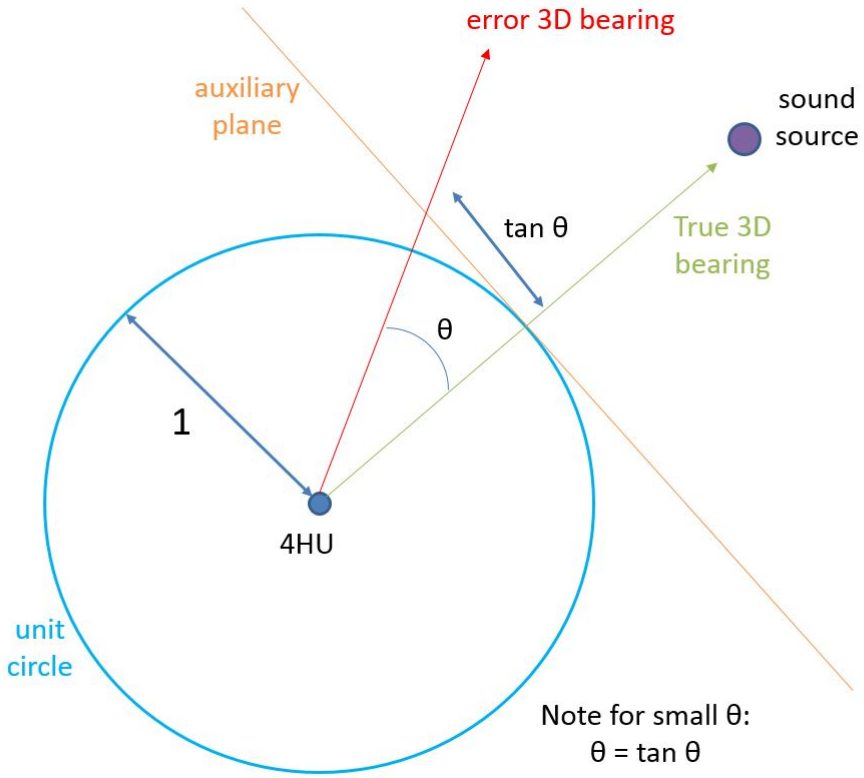

Figure 12: The trigonometry involved in the relation between the standard error of the desired angle errors and the standard error on the auxiliary plane used to generate the 3D bearings with error

These two approaches are not be equivalent since the second approach means does not result in a Gaussian distribution for the angles. Given that we model the error on the angle, the former approach might be more sensible than the later. Nonetheless, after looking analyzing real data we might re-evaluate this concept.

6 Propagating errors in 3D bearings to errors in 3D localization and 2D distances

It is not straightforward to represent analytically what the error will be as a function of the error in the 3D bearings. However, it is straightforward to evaluate via simulation what the observed errors will be. Here we implement simulations that illustrate the magnitude of the error under a set of scenarios.

Naturally, given the geometry involved, even a common error in the two 3D 4HU units, independent across units and independent of the source location, induces errors in 3D location and 2D distance to the virtual point transect which are dependent of the location of the sound source.

6.1 Required functions

We begin by creating a function that takes as input parameters the location of a pair of 3D-bearing sensors, and the corresponding observed 3D bearings to a detected sound source, in this setting assumed the location of a whale producing a sound, and returns the most likely 3D position for the whale.

```
get3DP=function(sensor1,sensor2,heading1,heading2){
  #function that calculates most likely position for a whale given
  #sensor1 - x,y,z coordinates of the first sensor
  #sensor2 - x,y,z coordinates of the second sensor
  #heading1 - the 3D bearing from the first sensor to the whale
  #heading2 - the 3D bearing from the second sensor to the whale
Q1=sensor1+as.vector((vector.cross(vector.cross(heading1,heading2),heading1) %*%
(sensor1-sensor2)/(vector.cross(heading1,heading2) %*%
vector.cross(heading1,heading2))))*heading1
Q2=sensor2+as.vector((vector.cross(vector.cross(heading1,heading2),heading2) %*%
(sensor1-sensor2)/(vector.cross(heading1,heading2) %*%
vector.cross(heading1,heading2))))*heading2
P3D=(Q1+Q2)/2
return(P3D)
}
```

The above function requires that the cross product between pairs of vectors is evaluated, which surprisingly does not exist in native R (see Marques *et al.* (2017) for details), therefore we coded a dedicated one.

```
vector.cross <- function(a, b) {
#function that calculates cross product of two vectors of length 3
#and length 3 only!

      if(length(a)!=3 || length(b)!=3){
        stop("Cross product is only defined for 3D vectors.");
    }
    i1 <- c(2,3,1)
    i2 <- c(3,1,2)
    return (a[i1]*b[i2] - a[i2]*b[i1])
}
```

6.2 Simulations

It is well known that errors in distance estimation can have an impact on the density estimates themselves, depending on the magnitude of the errors.

In this section we will use the functions defined above to evaluate how measurement error in 3D bearings impacts the estimation of a whale position, under relevant scenarios, and consequently how the errors in the 3D bearings propagate towards the distance that would be used in a conventional distance sampling analysis, i.e. the 2D horizontal distance as projected on the sea floor.

To begin we look at particular locations under specific scenarios. Afterwards we will look at specific scenarios over all possible source locations.

6.2.1 Setting the scene

Without loss of generality, we always assume that the first sensor defines the origin of a Cartesian system, so it is located at (0,0,0).

Within DECAF-TEA we are interested in evaluating two different scenarios:

1. A high frequency deep diving odontocete, for which we will in particular consider beaked whales as an example. Beaked whales high frequency clicks should be good candidates for obtaining a 3D bearing with reasonable precision. These animals produce most of their clicks while deep diving, so here we consider cue production depths to be around 800-1200 m deep (but note that these animals might dive even deeper, all the way to the bottom where the sensors will be deployed).
2. A low frequency shallow diver baleen whale, for which we will in particular consider fin whales as an example. Fin whales low frequency calls will be harder to localize than beaked whale's clicks. Also, fin whales will typically produce their sounds close to the surface. Here we consider animals to produce their cues in the 0-100 m range (based on Stimpert *et al.* (2015)). We note that if, as planned, we use SECR for fin whales density estimation, the localization of fin whale sounds will be less relevant, since SECR can bypass the need for localization. Nonetheless arrival angles could be used.

Both scenarios consider sensors at the bottom, somewhere around the SCORE range (so about 800-1700m deep).

We note that the depth constraints for the location of the detected whales are not used in the localization procedure itself, which could be something to consider at some point.

For the measurement error model we assume an unbiased (i.e. mean 0) Gaussian error with a given standard deviation, acting independently on each of the 3 components of vectors defining the 3D-bearings. As described above in section 5, this is perhaps not the more sensible way to model errors in 3D bearings, but it was considered adequate for an initial investigation.

6.3 Beaked whales

Accurate bearing estimates for high frequency beaked whales echolocation clicks should be more straight forward to obtain as compared to lower frequency baleen calls. Here we assume an unbiased Gaussian error with a standard deviation of 1%, acting independently on each of the 3 components of vectors defining the 3D-bearings.

We investigate the following scenarios:

- a best case scenario, namely a nearby whale with a good (relative) geometry
- an intermediate scenario, namely a whale close with a sub-optimal geometry
- an intermediate scenario, namely a whale mid-range with a sub-optimal geometry
- an intermediate scenario, namely a whale far with a sub-optimal geometry

- a worst case scenario, namely a relatively far whale with a poor geometry

6.3.1 Close by and good geometry

In this scenario we consider that the second sensor is 500 m east of the first sensor, and that the whale is 500 m above the sea floor (assume say 1700 m deep ocean floor and a deep diving whale producing a sound at 1200m), 500 meters north of the point that is 1/4th of the way between the two sensors. The scenario geometry, with the true 3D bearings and animal position, as represented in figure 3.

Note in particular that the true 2D distance (i.e. the distance as projected on the bottom of the ocean, represented by the green line in the previous figure) between the whale and the center of the sensors was 515.39m.

We first simulate errors 3D bearing errors, and then estimate the whale position given these. Figure 13 shows the distribution in estimated 2D position and depth.

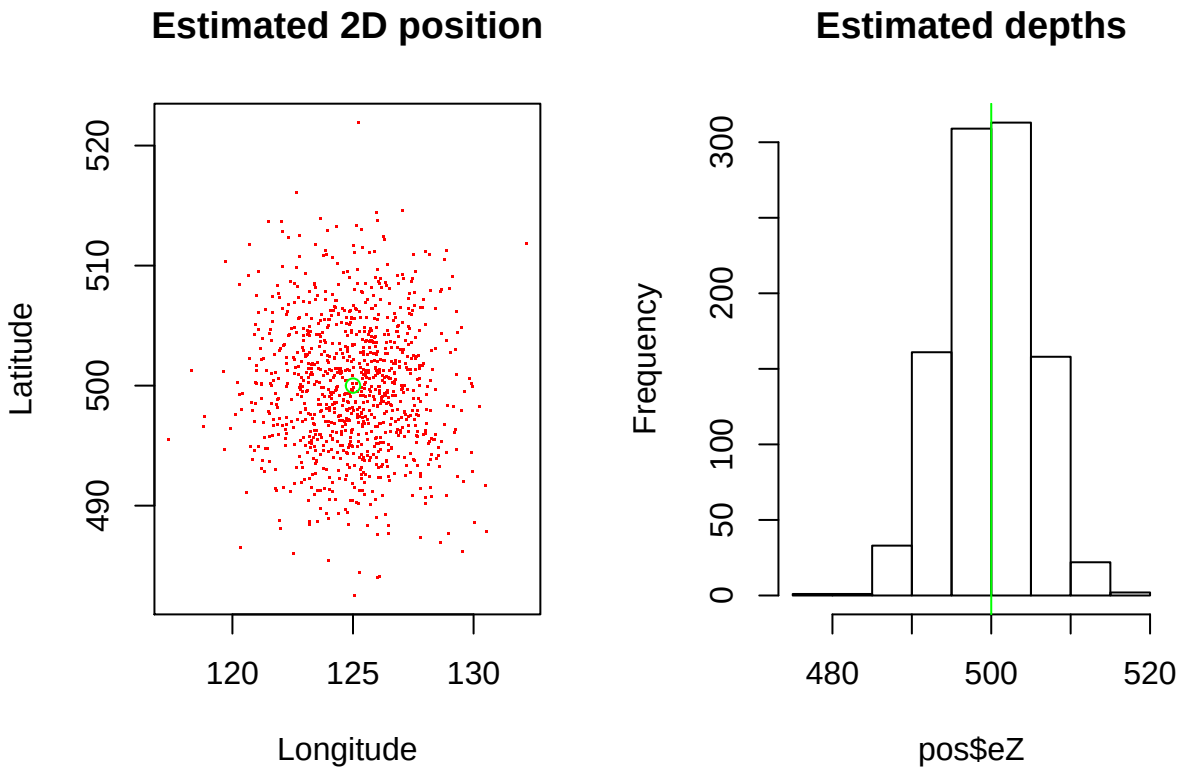

Figure 13: Estimated 2D positions and estimated depth. Green represents the truth. Sensors are 500 meters apart and whale is one fourth of the way between and 500 meters above the units. Measurement error is Gaussian (with a standard deviation of 1) in each of the components defining the 3D bearings.

Figure 14 shows the 3D estimated positions of the whale (in red) and the true whale location (in green), showing that under this scenario the errors in the position are quite small.

A plot of the histogram of the projected 2D error distances, with the true distance for reference is given (Figure 15). The mean distance is for practical purposes unbiased in this case, implying that such errors in distances would not be relevant in a density estimation exercise.

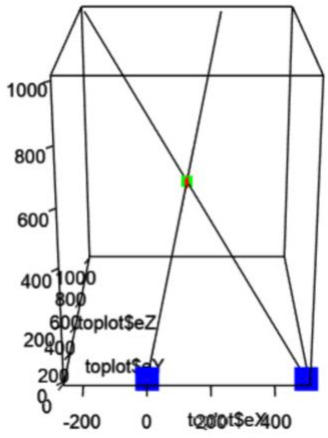

Figure 14: The 3D estimated positions of the whale (in red) and the true whale location (in green), under the 'Close by and good geometry' scenario

However, this setting is complex because the same measurement error in 3D bearings and distance from the source could lead to very different errors in distance, depending on the relative geometry (i.e the angles) of the whale position with respect to the arrays.

Arguably, the ideal position would be over the line that passes midway between the sensors, and perpendicular to the line that passes through the sensors.

This corresponds to a measurement error CV of about 1.05 %, which would be unlikely to cause problems in a distance sampling context.

6.3.2 Close by and sub-optimal geometry

Here we aim for a scenario such that the whale is at the same depth as before, same distance from the virtual point transect, but close to along the line joining the sensors. Lets assume that say it will be 50 meters from that line, i.e., at (x,50,500). Then simple trigonometry returns us the missing x coordinate, since the true distance being 515.39m means that it must be at x=762.96m.

Note in particular that the true 2D distance (i.e. the distance as projected on the bottom of the ocean, represented by the green line in figure 16) between the whale and the center of the sensors is again, for this particular scenario, the same 515.39 m.

We now simulate errors in 3D bearings, and then estimate the whale position given errors in bearings. These are shown in figure 17, first looking at the 2D position and then in depth.

Figure 18 shows us the 3D estimated positions of the whale (in red) and the true whale location (in green). Under this scenario the errors in the position are still overall quite small, but with a wider spreading than the 2 previous scenarios.

We plot the histogram of the projected 2D error distances, with the true distance on top. The mean distance is for practical purposes also unbiased in this case (Figure 19), implying that such errors in distances would not be relevant in a density estimation exercise.

This corresponds to a measurement error CV of about 2.11 %, which again would be unlikely to cause problems (based on back of the envelope calculations!).

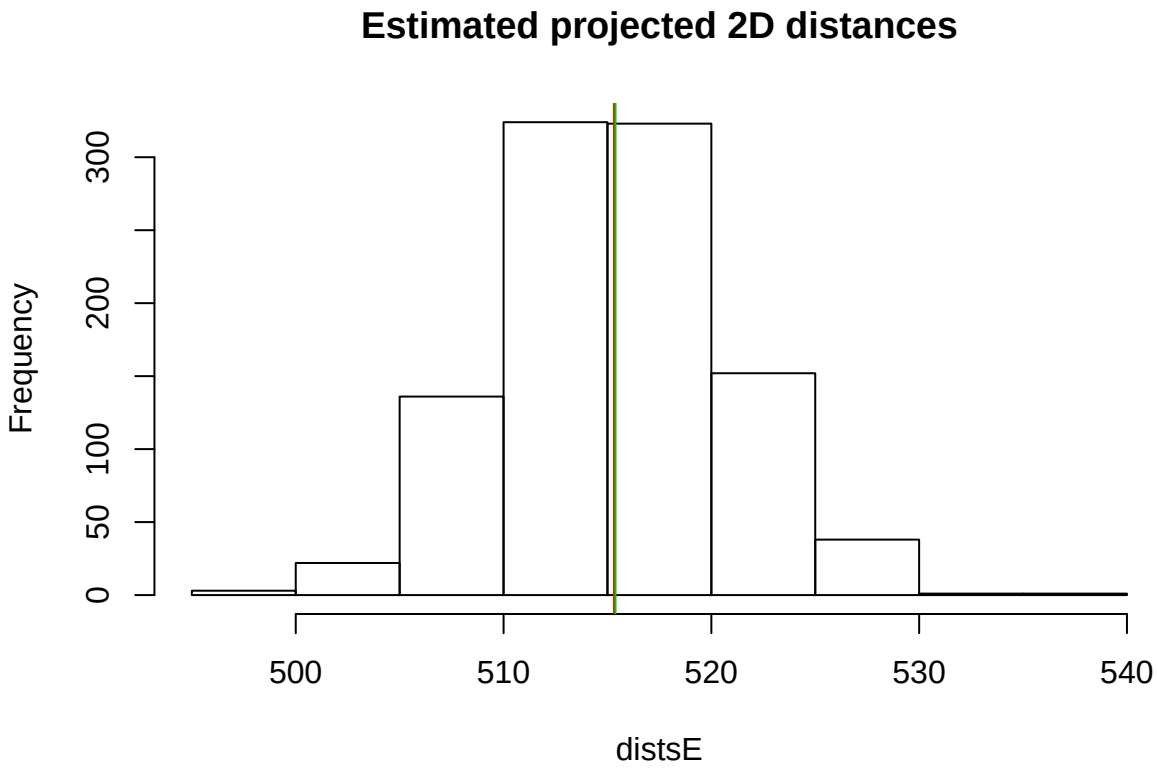

Figure 15: The 2D estimated distances between the whale and the virtual point transect. Sensors are 500 meters apart and whale is one fourth of the way between and 500 meters above the units. Measurement error is Gaussian (with a standard deviation of 1) in each of the components defining the 3D bearings. The green line represents the true distance, the red line represents the mean estimated distance in the presence of errors.

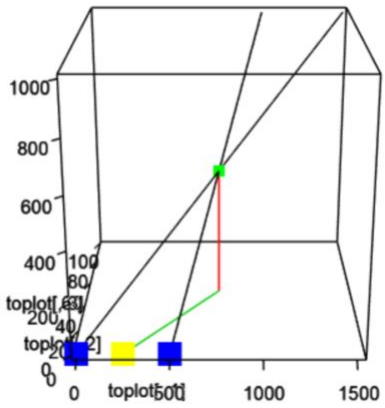

Figure 16: [The geometry involved in the 'Close by and sub-optimal geometry' scenario

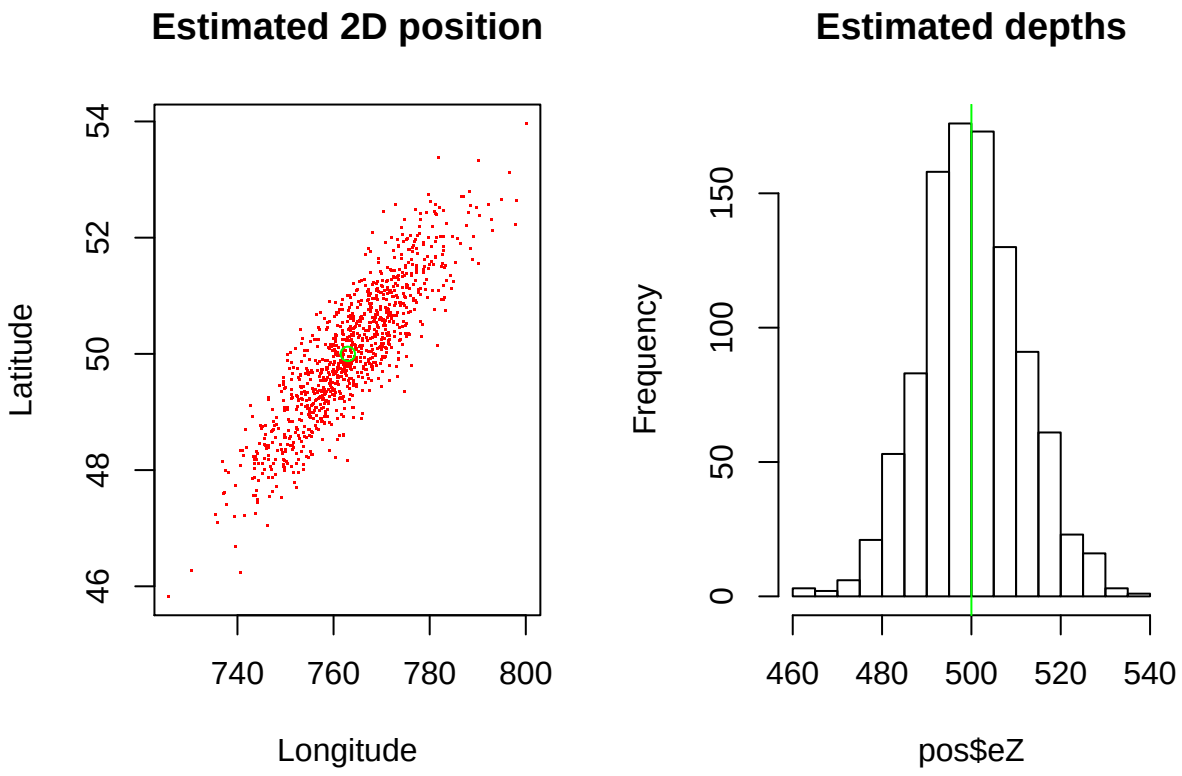

Figure 17: Estimated 2D positions and estimated depth. Green represents the truth. Sensors are 500 meters apart and whale 500 meters above the units, at the same 515 m 2D distance from the virtual point sensor as in the previous scenarion, but closer to the line joining the sensors than before. Measurement error is Gaussian (with a standard deviation of 1) in each of the components defining the 3D bearings.

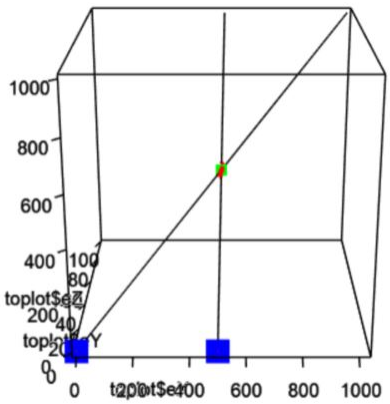

Figure 18: The 3D estimated positions of the whale (in red) and the true whale location (in green), under the 'Close by and sub-optimal geometry' scenario

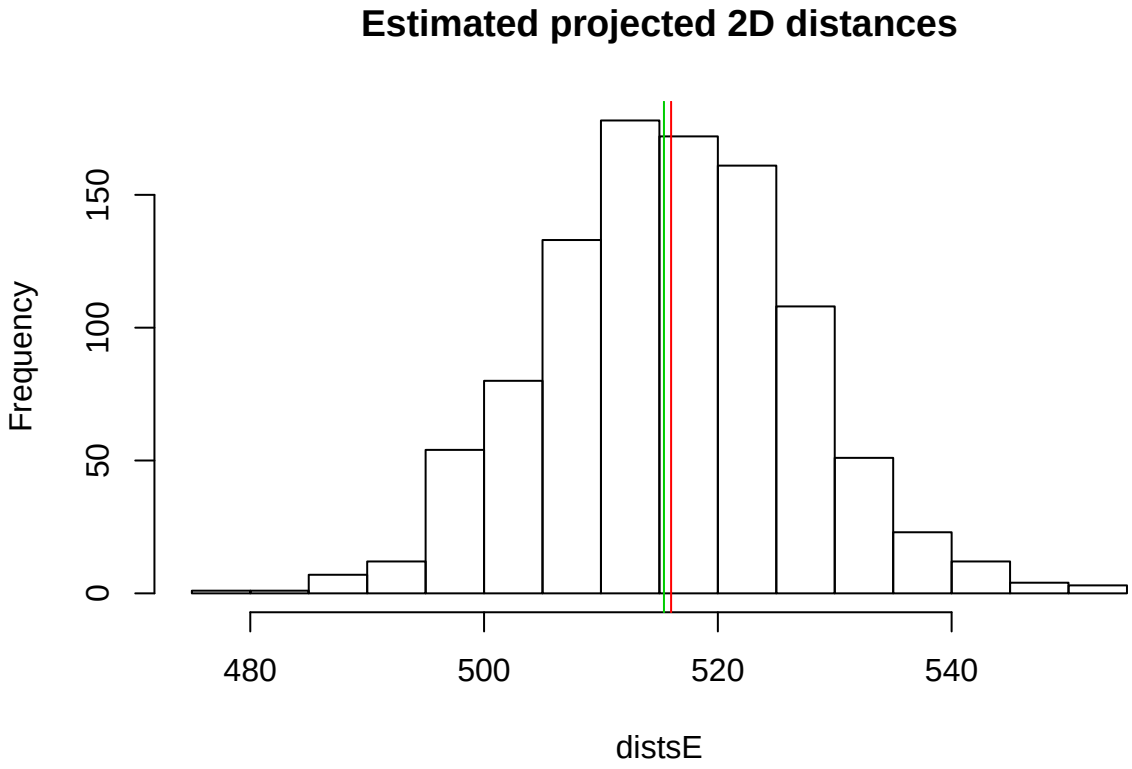

Figure 19: Estimated 2D distance. Sensors are 500 meters apart and whale 500 meters above the units, at the same 515 m 2D distance from the virtual point sensor as in the previous scenarion, but closer to the line joining the sensors than before. Measurement error is Gaussian (with a standard deviation of 1) in each of the components defining the 3D bearings.

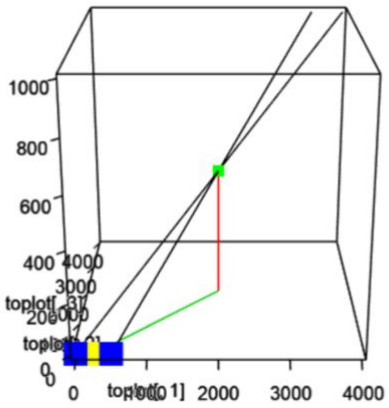

Figure 20: The geometry involved in the 'Mid-range and sub-optimal geometry' scenario

6.3.3 Mid-range and sub-optimal geometry

Here we aim for a scenario where that the whale is at the same depth as before, but far away from the virtual point. We assume that it will be about 2000 meters north and west of the first sensor. This is represented in figure 20.

Note now the true 2D distance (i.e. the distance as projected on the bottom of the ocean, represented by the green line in the previous figure) between the whale and the center of the sensors is 2657.54 units. This is 5.32 times the sensor baseline, and we would not expect reasonable localizations at such ranges.

We now simulate errors in 3D bearings, and then estimate the whale position given errors in bearings. These are shown in figure 21, which show the estimated 2D position and depth.

Figure 22 shows the 3D estimated positions of the whale (in red) and the true whale location (in green). For this scenario the errors in the position are still quite small.

The histogram of the projected 2D error distances, with the true distance on top (Figure 23) shows that the mean distance is for practical purposes unbiased, implying that such errors in distances would not be relevant in a density estimation exercise.

Note that while the plot above might suggest that the errors in the estimated distance are quite large, this actually corresponds to a measurement error CV of about 6.95 %, which would be unlikely to cause serious problems (based on back of the envelope calculations!).

6.3.4 Far and sub-optimal geometry

Keeping everything the same, we now assume the whale is 5000 meters north and 6000m west of the first sensor. As before, the corresponding estimated position in 2D and the estimated depths are shown in figure 24.

Note the true 2D distance (i.e. the distance as projected on the bottom of the ocean, represented by the green line in the previous figure) between the whale and the center of the sensors is 8003.91 units. That means that this is 16.01 times the sensor baseline, and we would not expect reasonable localizations at those ranges any way.

We simulate errors in 3D bearings, and estimate the whale position given errors in bearings. Figure 25 shows estimated 2D position and depth.

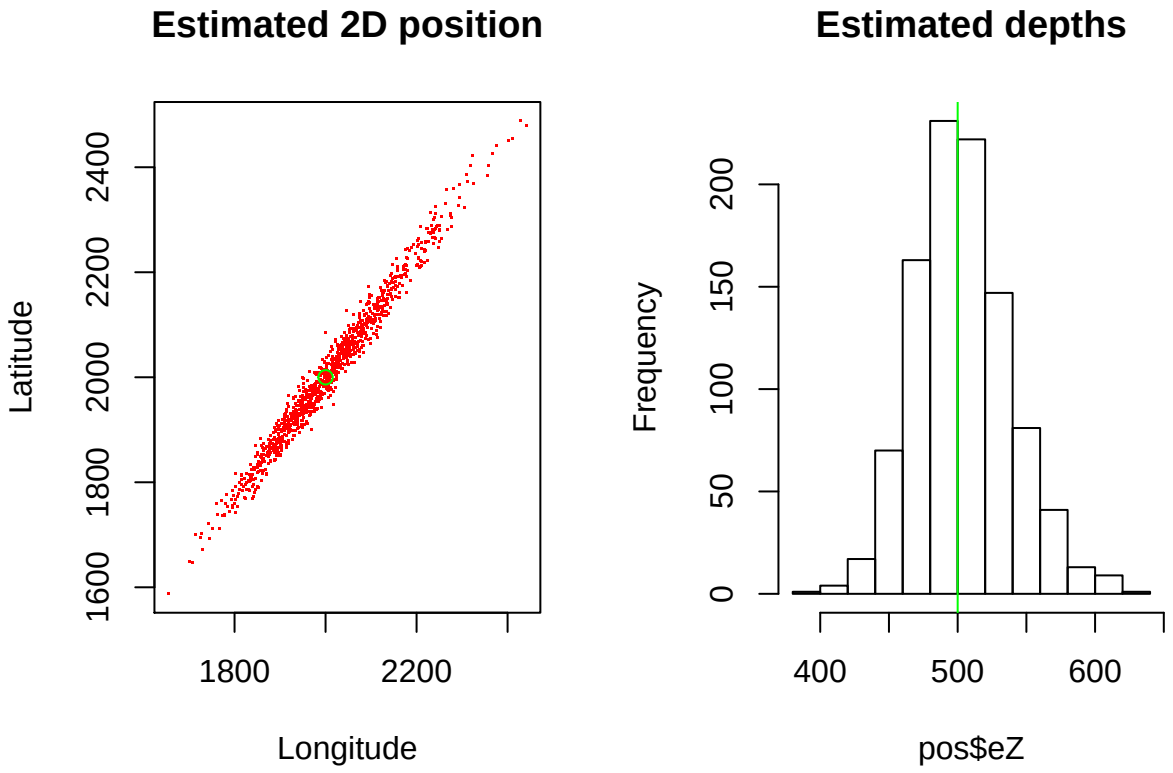

Figure 21: Estimated 2D positions and estimated depth. Green represents the truth. Sensors are 500 meters apart and whale 500 meters above the units and 2000 m East and North of the reference sensor. Measurement error is Gaussian (with a standard deviation of 1) in each of the components defining the 3D bearings.

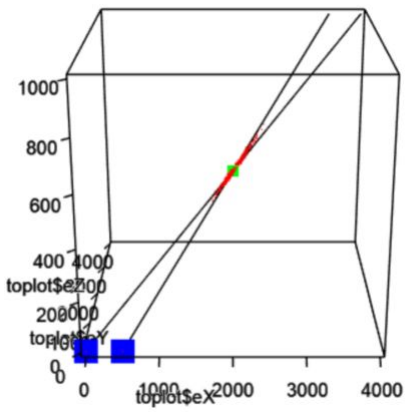

Figure 22: The 3D estimated positions of the whale (in red) and the true whale location (in green), under the 'Close by and sub-optimal geometry' scenario

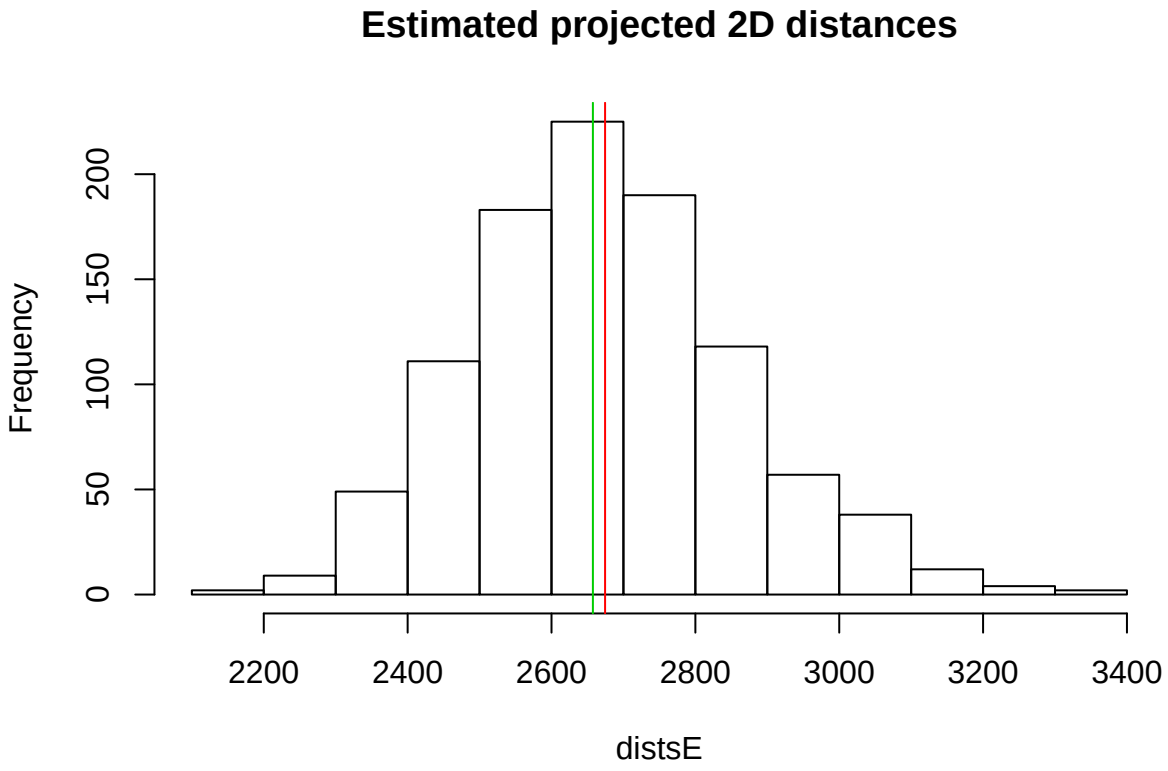

Figure 23: Estimated 2D distance. Sensors are 500 meters apart and whale 500 meters above the units and 2000 m East and North of the reference sensor. Measurement error is Gaussian (with a standard deviation of 1) in each of the components defining the 3D bearings.

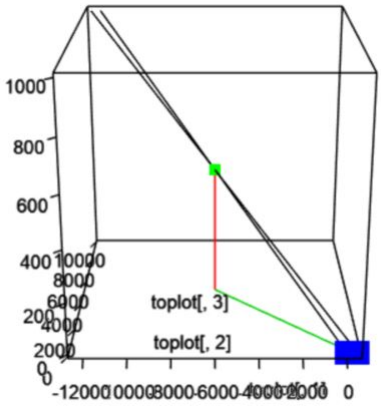

Figure 24: The geometry involved in the 'Far and sub-optimal geometry' scenario

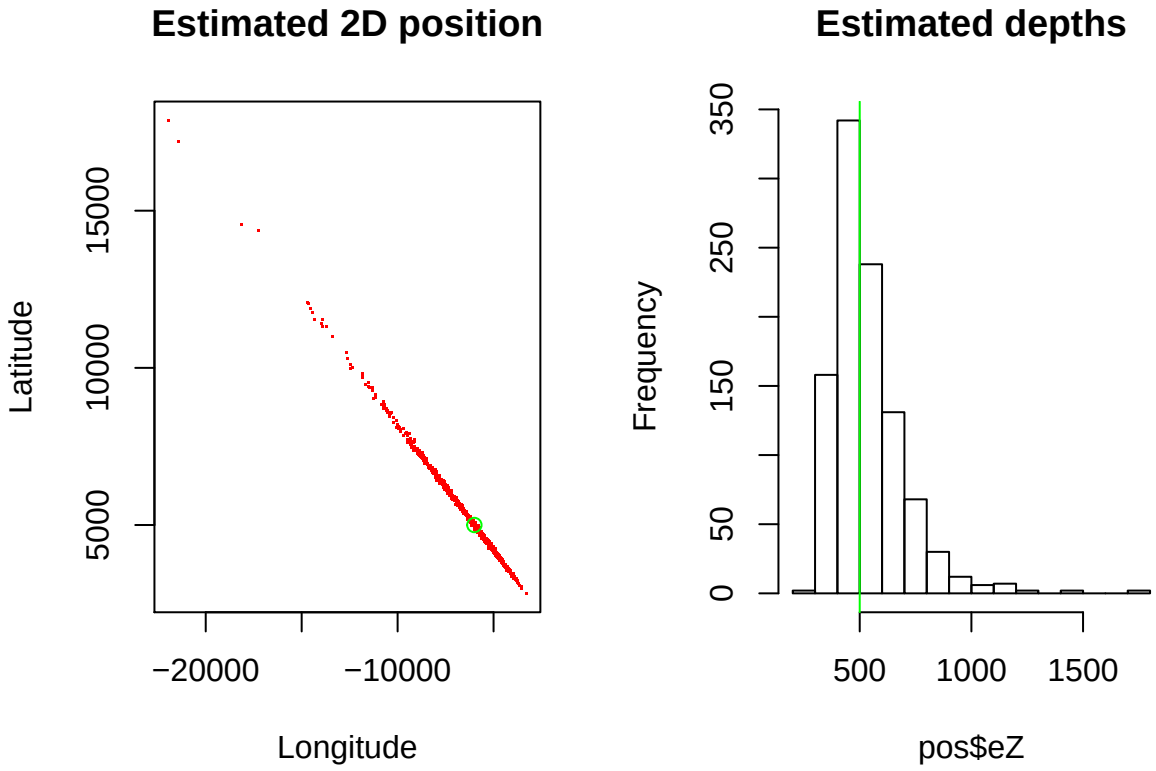

Figure 25: Estimated 2D positions and estimated depth. Green represents the truth. Sensors are 500 meters apart and whale 500 meters above the units and 6000 m West and 5000 m North of the reference sensor. Measurement error is Gaussian (with a standard deviation of 1) in each of the components defining the 3D bearings.

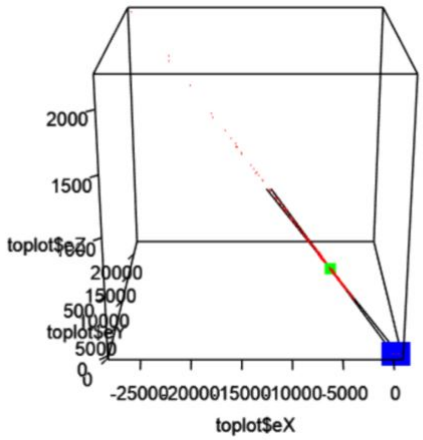

Figure 26: The 3D estimated positions of the whale (in red) and the true whale location (in green), under the 'Far and sub-optimal geometry' scenario

Figure 26 presents the 3D estimated positions of the whale (in red) and the true whale location (in green), showing that under this scenario the errors in the position estimate are large and th3erefore can not be ignored.

We plot the histogram of the projected 2D error distances, with the true distance on top (Figure 27). We now have a considerably biased distance, with a quite long and heavy right tail. Everything else being equal this would lead to an overestimation of distances, which we expect to correspond to an underestimation of density via conventional distance sampling.

Under this scenario, the true 2D distance between the whale and the center of the sensors is 8003.91 units. That means that this is 16.01 times the sensor baseline, and we would not expect reasonable localizations at those ranges any way.

This corresponds to a measurement error CV of about 32.66 %, which would likely cause serious problems in density estimation (based on back of the envelope calculations!).

6.3.5 Far and poor geometry

Still keeping everything else equal, we now assume the whale is 500 meters north and 6000m west of the first sensor. As before, the corresponding estimated position in 2D and the estimated depths are shown below.

Note now the true 2D distance (i.e. the distance as projected on the bottom of the ocean, represented by the green line in the previous figure) between the whale and the center of the sensors is 6269.97 units. That means that this is 12.54 times the sensor baseline, and we would not expect reasonable localizations at those ranges. While the geometry might seem more challenging, the distance alone is smaller than in the previous scenario, and hence the errors will be less.

We now simulate errors in 3D bearings, and then estimate the whale position given errors in bearings. These are shown in figure 28.

Figure 29 shows the 3D estimated positions of the whale (in red) and the true whale location (in green), showing that under this scenario the errors in the position estimate are no longer negligible.

We plot the histogram of the projected 2D error distances, with the true distance on top (Figure 30). We now have a considerably biased distance, with a long and heavy right tail. Everything else being equal this would lead to an overestimation of distances, which we expect to correspond to an underestimation of density via conventional distance sampling.

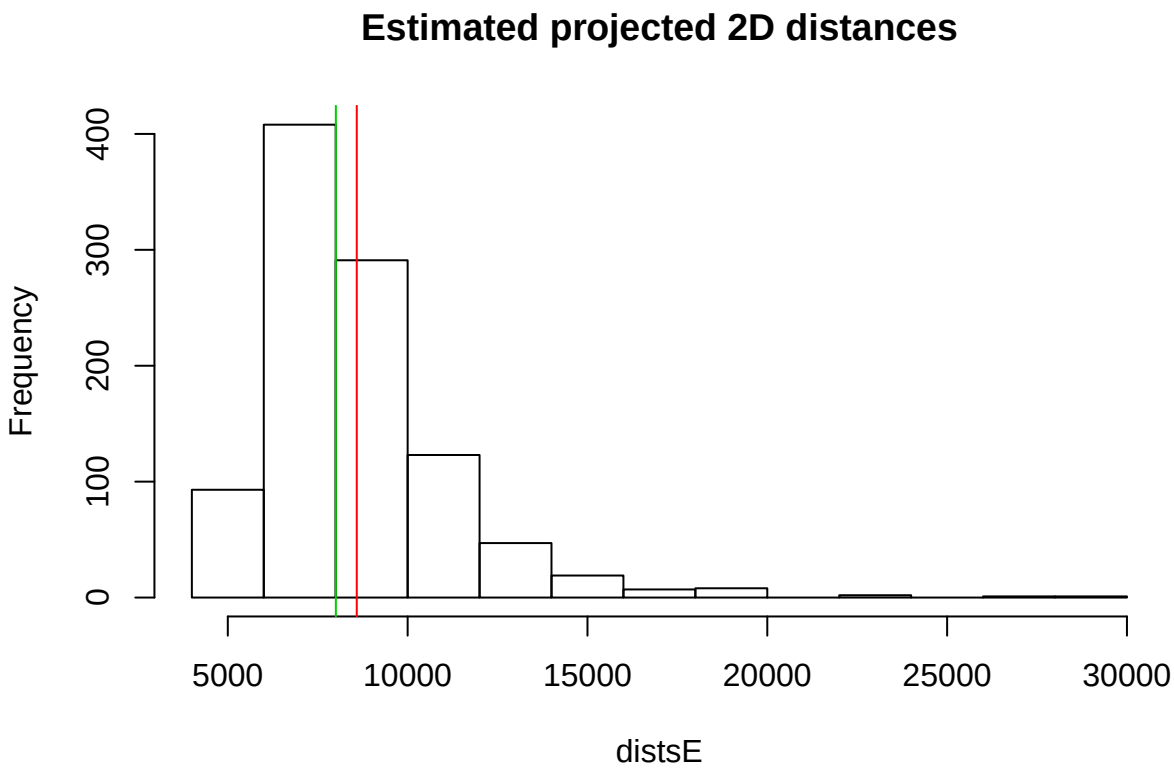

Figure 27: Estimated 2D distances. Green represents the truth. Sensors are 500 meters apart and whale 500 meters above the units and 6000 m West and 5000 m North of the reference sensor. Measurement error is Gaussian (with a standard deviation of 1) in each of the components defining the 3D bearings.

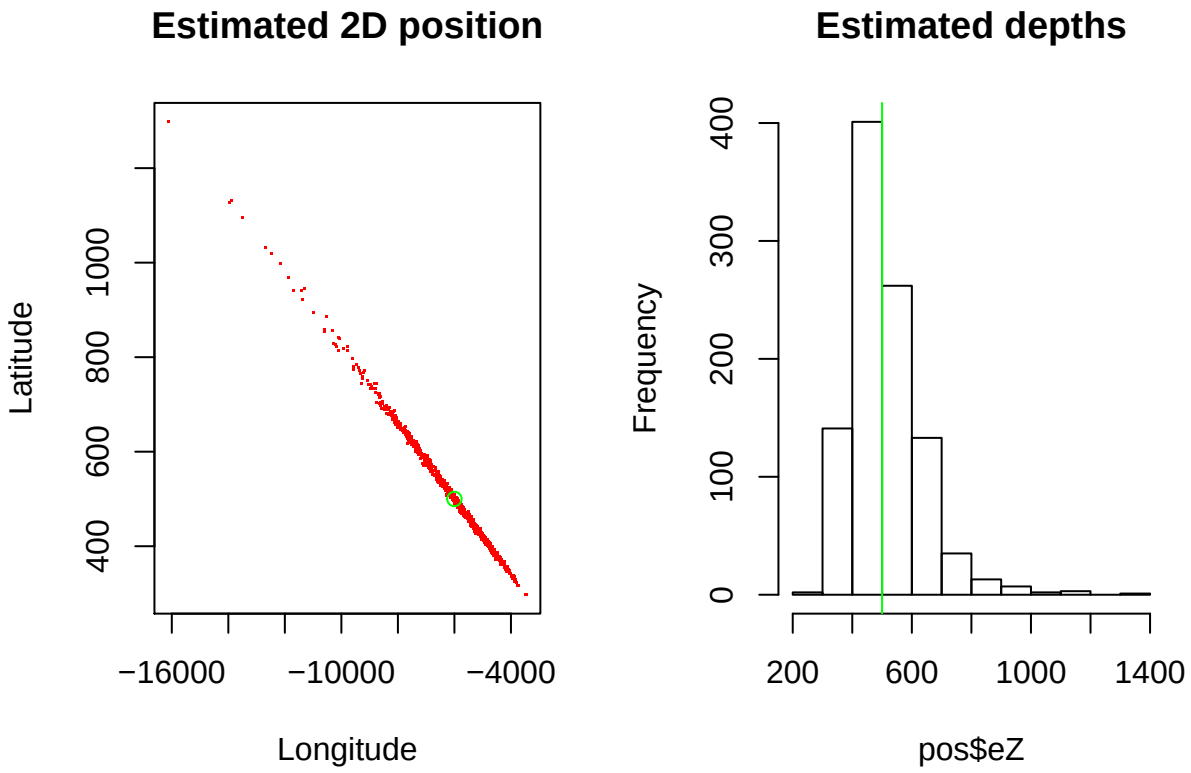

Figure 28: Estimated 2D positions and estimated depth. Green represents the truth. Sensors are 500 meters apart and whale 500 meters above the units and 6000 m West and 500 m North of the reference sensor. Measurement error is Gaussian (with a standard deviation of 1) in each of the components defining the 3D bearings.

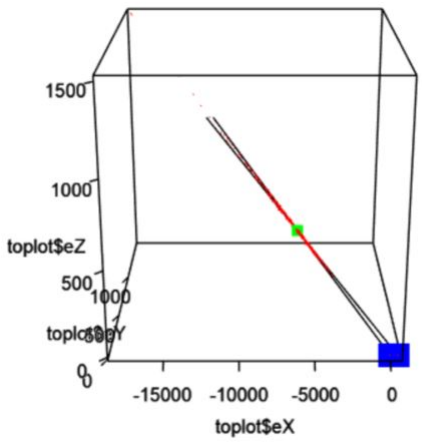

Figure 29: The 3D estimated positions of the whale (in red) and the true whale location (in green), under the 'Far and poor geometry' scenario

Under this scenario, the true 2D distance between the whale and the center of the sensors is 6269.97 m. This is 12.54 times the sensor baseline, and we would not expect reasonable localizations at those ranges.

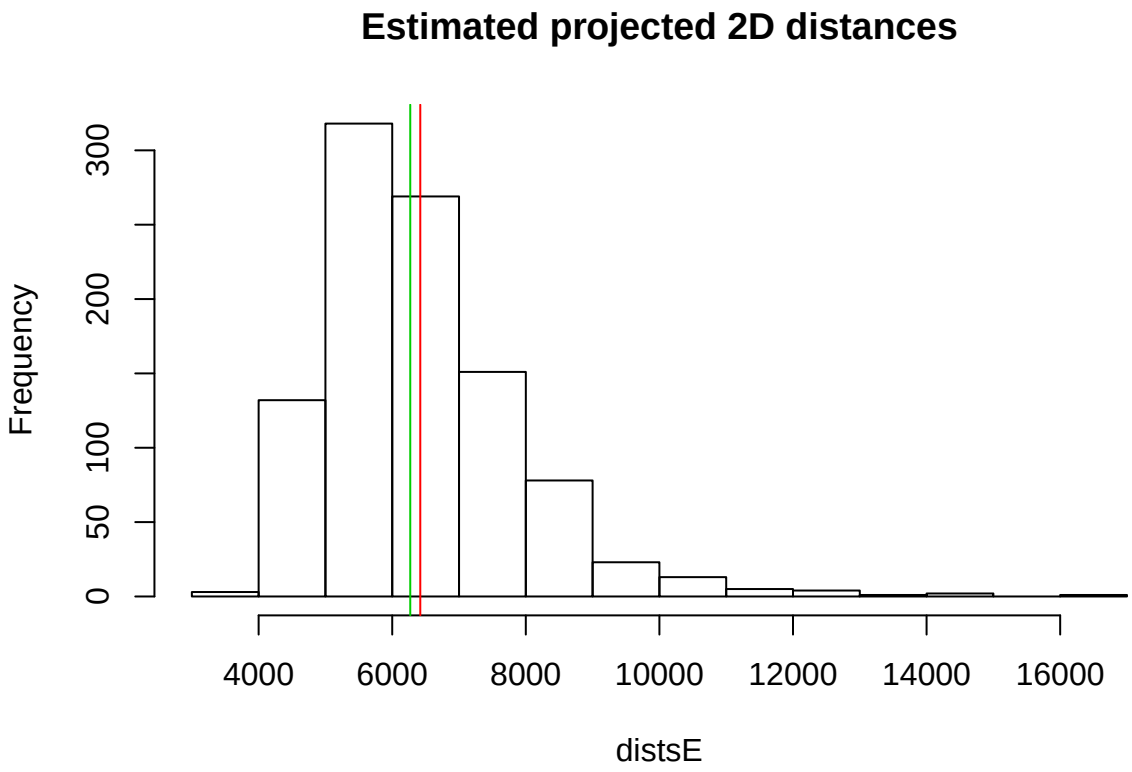

Figure 30: Estimated 2D distances. Green represents the truth. Sensors are 500 meters apart and whale 500 meters above the units and 6000 m West and 500 m North of the reference sensor. Measurement error is Gaussian (with a standard deviation of 1) in each of the components defining the 3D bearings.

This actually corresponds to a measurement error CV of about 23.89 %, which would very likely cause serious problems in density estimation.

6.3.6 Geometric dilution of precision

The previous simulations look at particular scenarios for a whale location, but it might be more informative to investigate how these change as a function of the whale position in 3D space.

Here we consider, for the same sensor placing considered above (two sensors separated by 500m), as well as for the same assumed whale depth (500 meters above the sensors), the calculation of the CV of the errors (cf. left plot below) and the mean error (cf. right plot below) as a function of the position of the whale with respect to the sensors, in a range of locations around the sensors.

As a simplification we define the units locations such that the center of the virtual point transect is at (0,0,0). Therefore, given the 500 meter separation between units, a 4HU will be at -250 and the other at 250 (in the x dimension, while both at $y = z = 0$).

Interestingly, the CV results show almost vertical stripes of equal precision, which was unexpected. Might this be because we have not looked far out enough in the y dimension. We repeat the process, this time

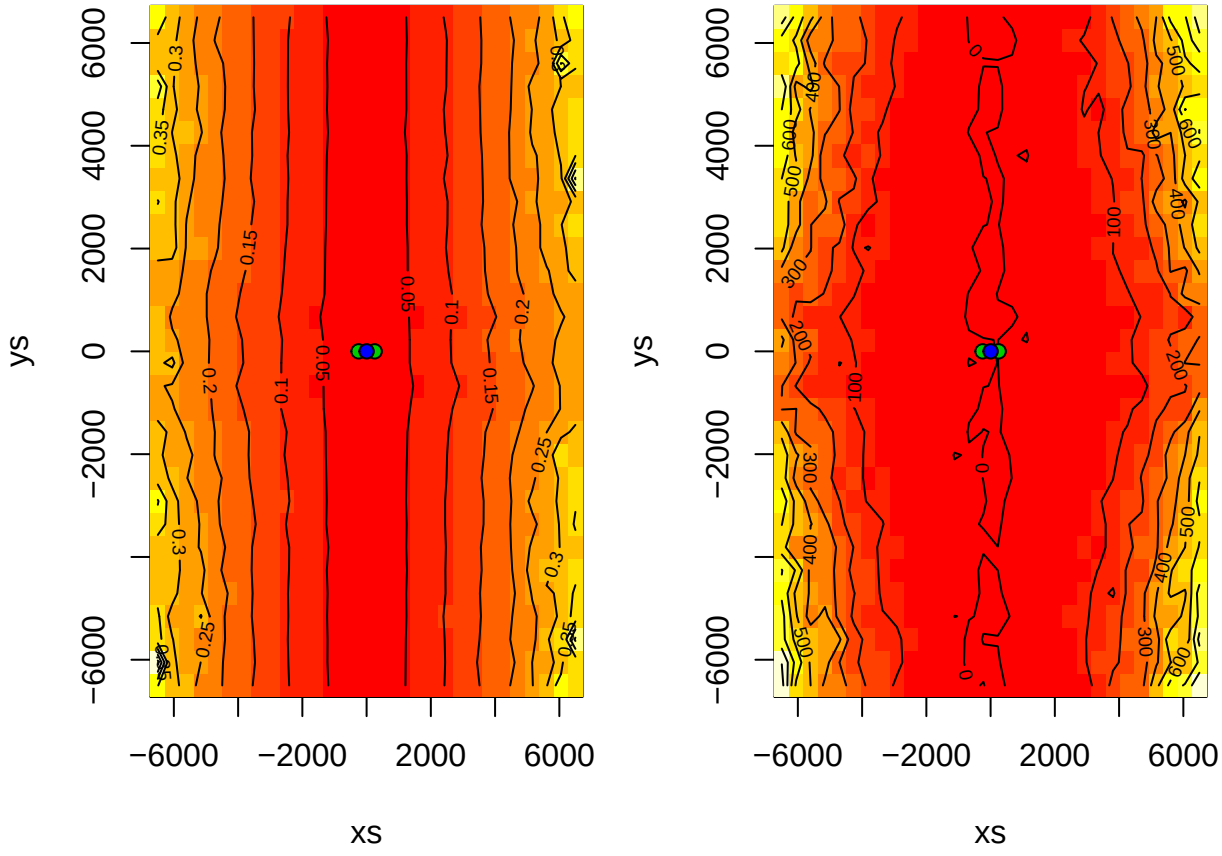

Figure 31: Geometric dillution of precision (gdop) plot, for two units 500 meters apart and whales 500 meters above the units.

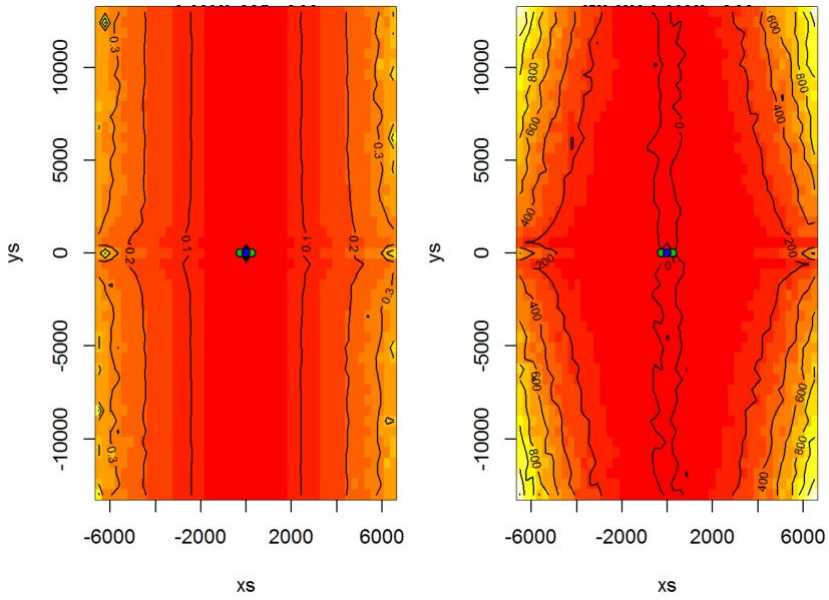

Figure 32: Geometric dillution of precision (gdop) plot, expanding the search area and the number of grid point with respect to the previous gdop plot.

increasing the range of the y's but also considering 5000 simulated positions (rather than the 1000 considered above). We also increase the number of points in the grid over which we search. This is shown in figure 32.

We run an additional simulation to evaluate how things would change for slightly larger values of x. This also considered explicitly looking into the errors in 3D distances (and not only 2D, distances projected on the bottom of the ocean). No surprises show up; some artifacts of the implementation of the contour plot near the boundaries present in the above plots are no longer present in the plots below. The patterns in 3D distances (bottom row plots) are not different from those in 2D distances, which is after the fact not surprising given that the distances in 3D are mostly driven by variance in 2D (i.e. depth is rather constant).

We then varied the vertical separation between the sensors and the whales. We first decreased it to 50 (Figure 34), 100 (Figure 35) and 250 meters (Figure 36), then increased it to 1000 meters (Figure 37), and then to 1500 meters (Figure 38).

The 6 sets of plots above are consistent across depths. At this scale, the process is not higly dependent on the depth of the whale. A comparison of the 6 CV plots (Figure 39) and the 6 absolute error plots (Figure 40) helps to confirm that pattern.

We repeat the process assuming the whale is again at 500 above the sensors, but increase the unit spacing: a unit will be at -500 and the other at 500 (in the x dimension, while both at $y = z = 0$). The results should be the same, but with smaller magnitude CV's (since it is just a matter of scaling).

The results are as expected (Figure 41), with low CVs on the estimated positions. Now, we move the whale shallower in the water column: keeping everything the same as before, but the whale at 1000 meters above the sensors (Figure 42).

Finally, we present a situation in which sensors are only 250 meters apart and hence our ability to obtain reliable distances with low CVs decreases fast with distance from the point (Figure 43). The performance degraded extremely fast, with such a scenario leading to errors that would likely lead to unreliable inferences.

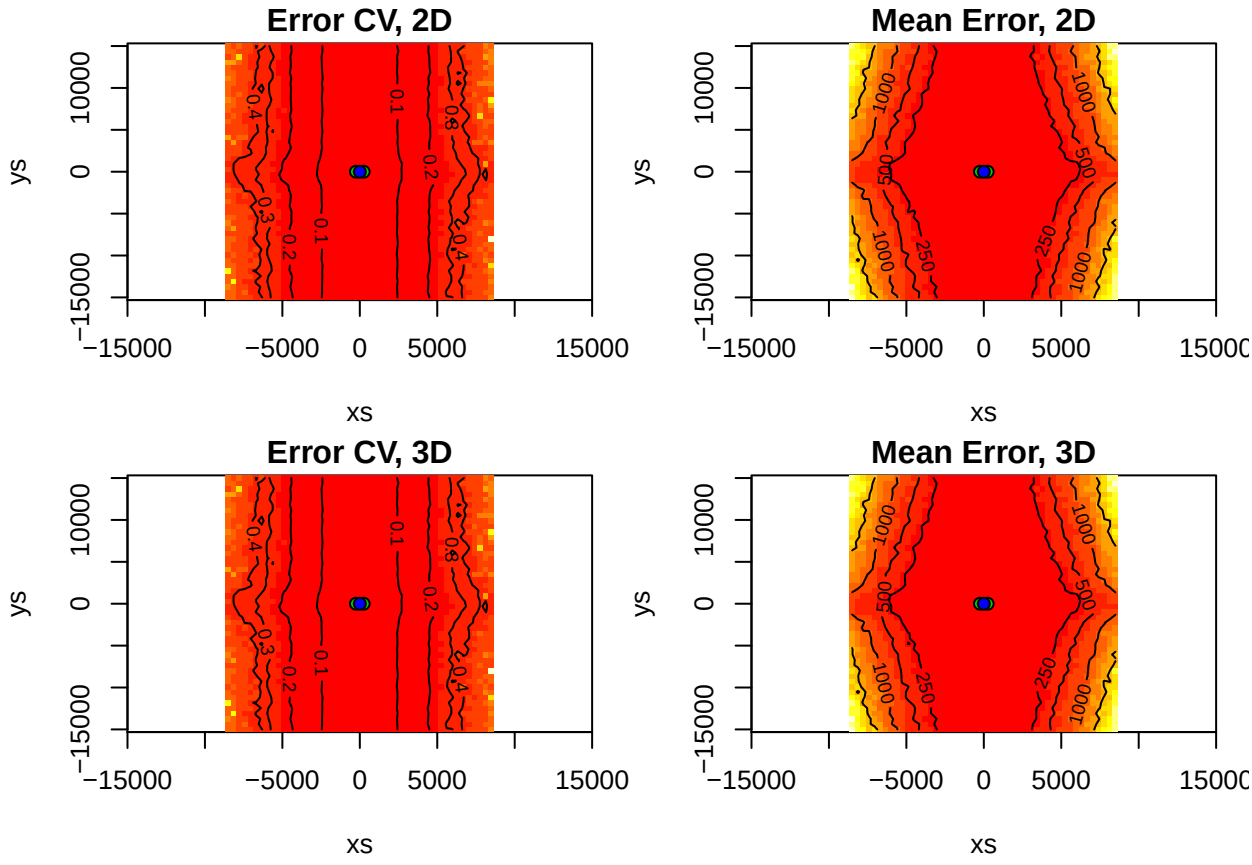

Figure 33: Geometric dillution of precision (gdop) plot, for two units 500 meters apart and whales 500 meters above the units.

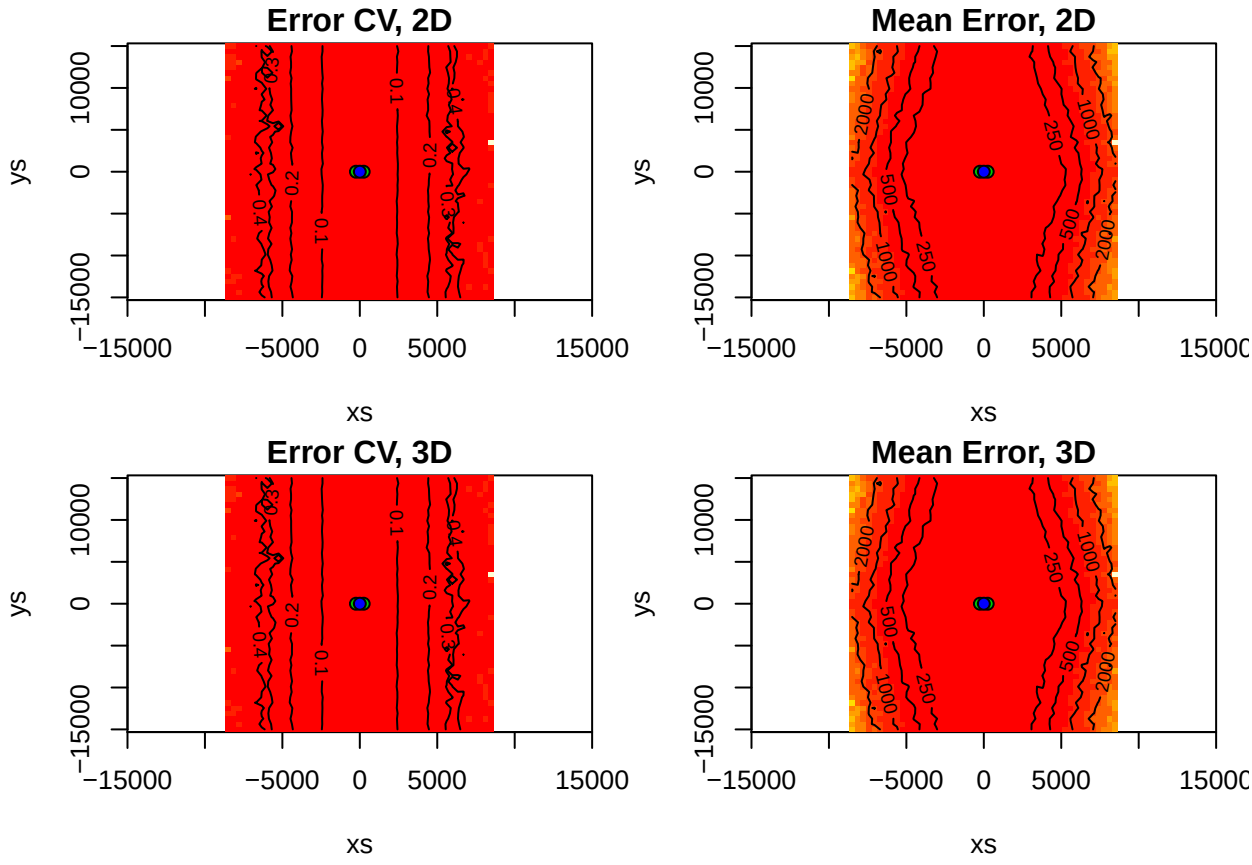

Figure 34: Geometric dillution of precision (gdop) plot, for two units 500 meters apart and whales 50 meters above the units.

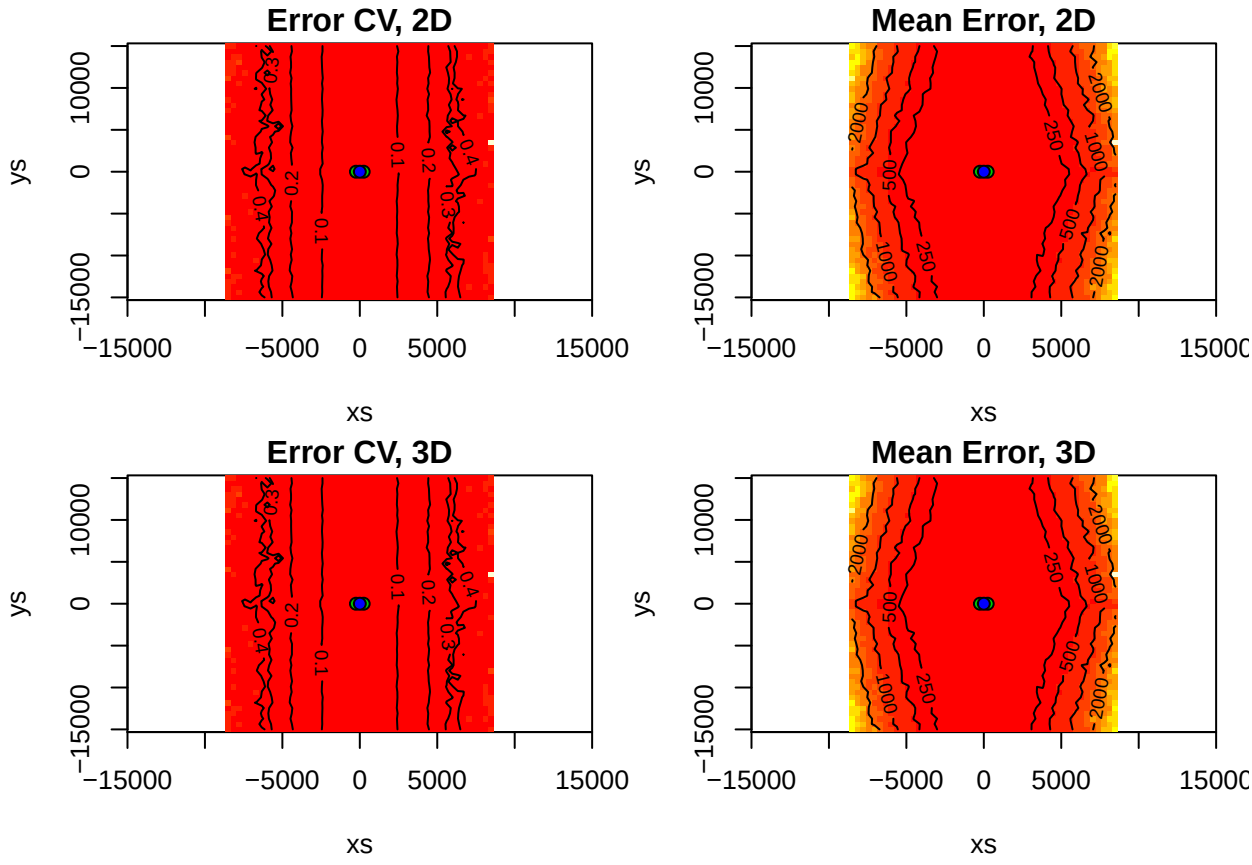

Figure 35: Geometric dillution of precision (gdop) plot, for two units 500 meters apart and whales 100 meters above the units.

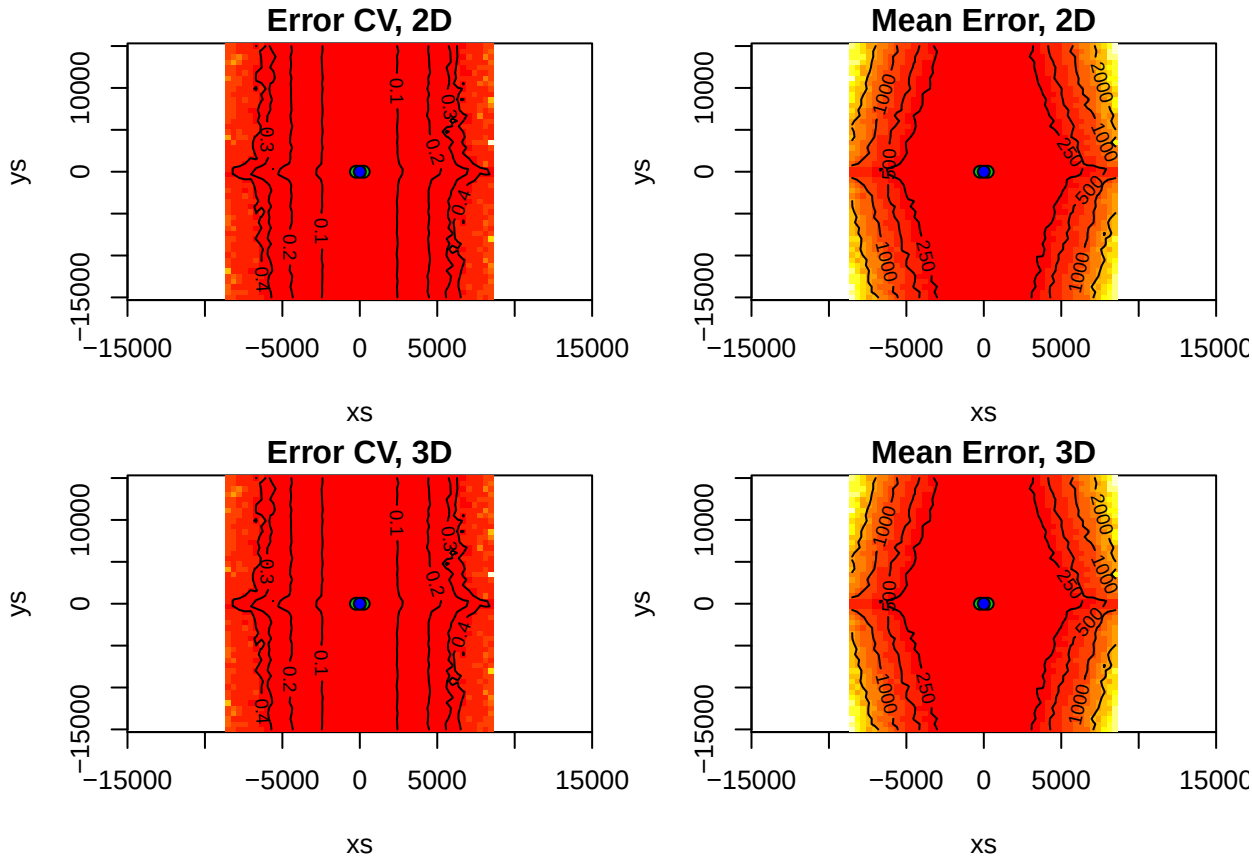

Figure 36: Geometric dillution of precision (gdop) plot, for two units 500 meters apart and whales 250 meters above the units.

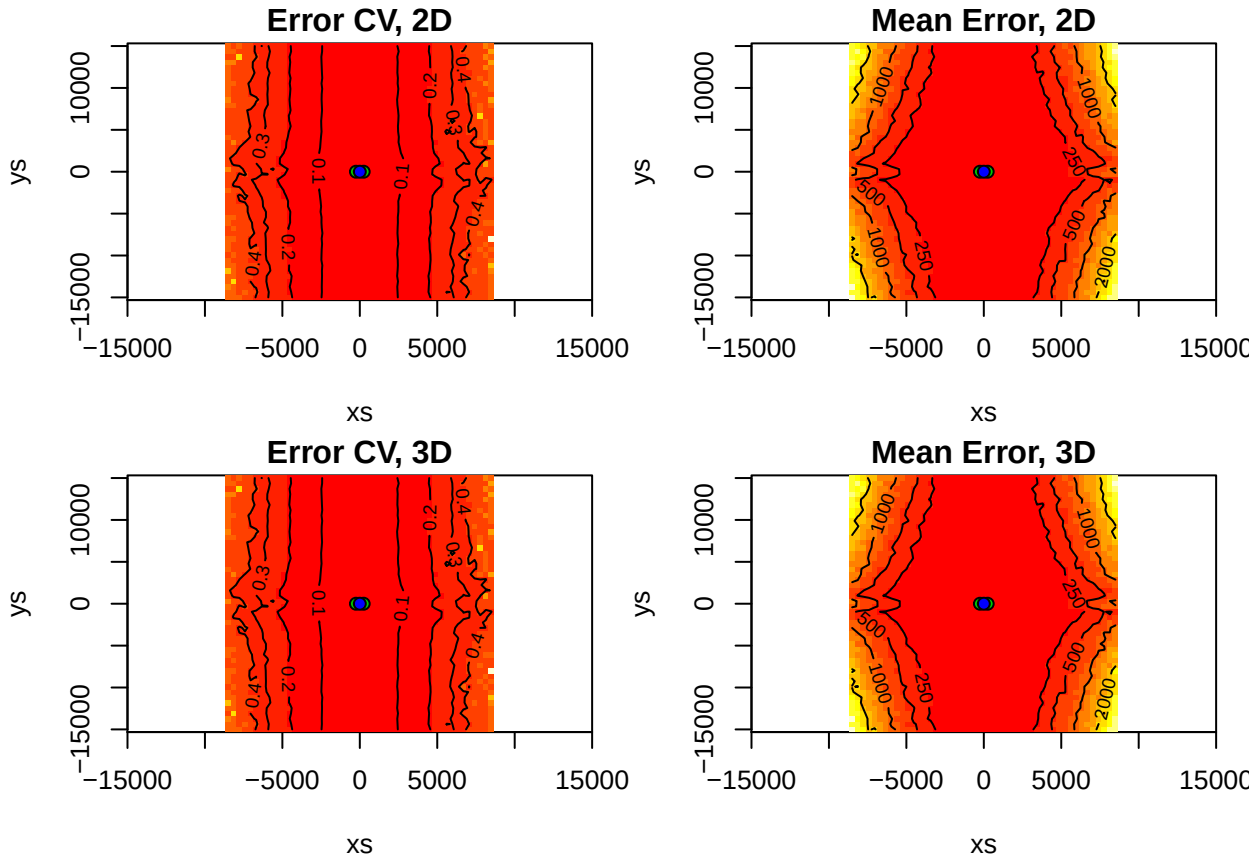

Figure 37: Geometric dillution of precision (gdop) plot, for two units 500 meters apart and whales 1000 meters above the units.

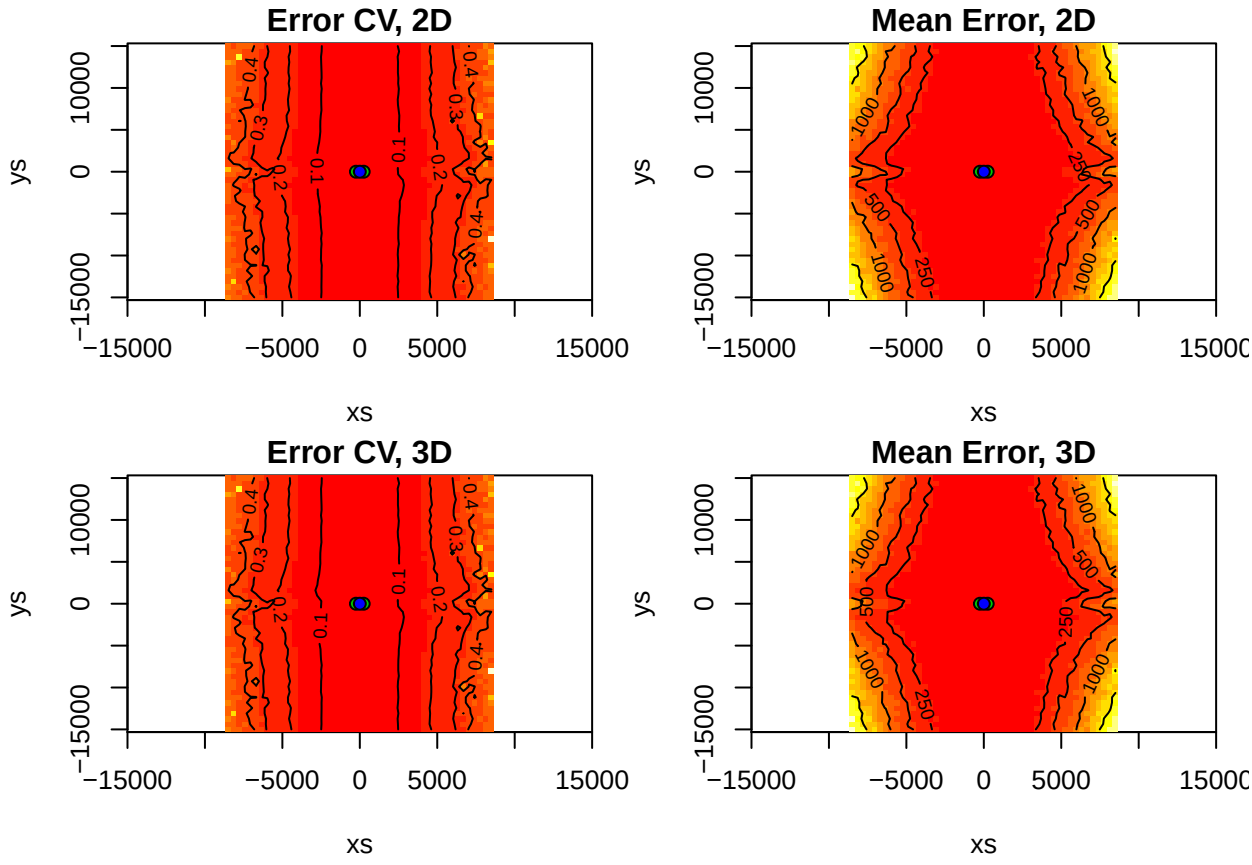

Figure 38: Geometric dillution of precision (gdop) plot, for two units 500 meters apart and whales 1500 meters above the units.

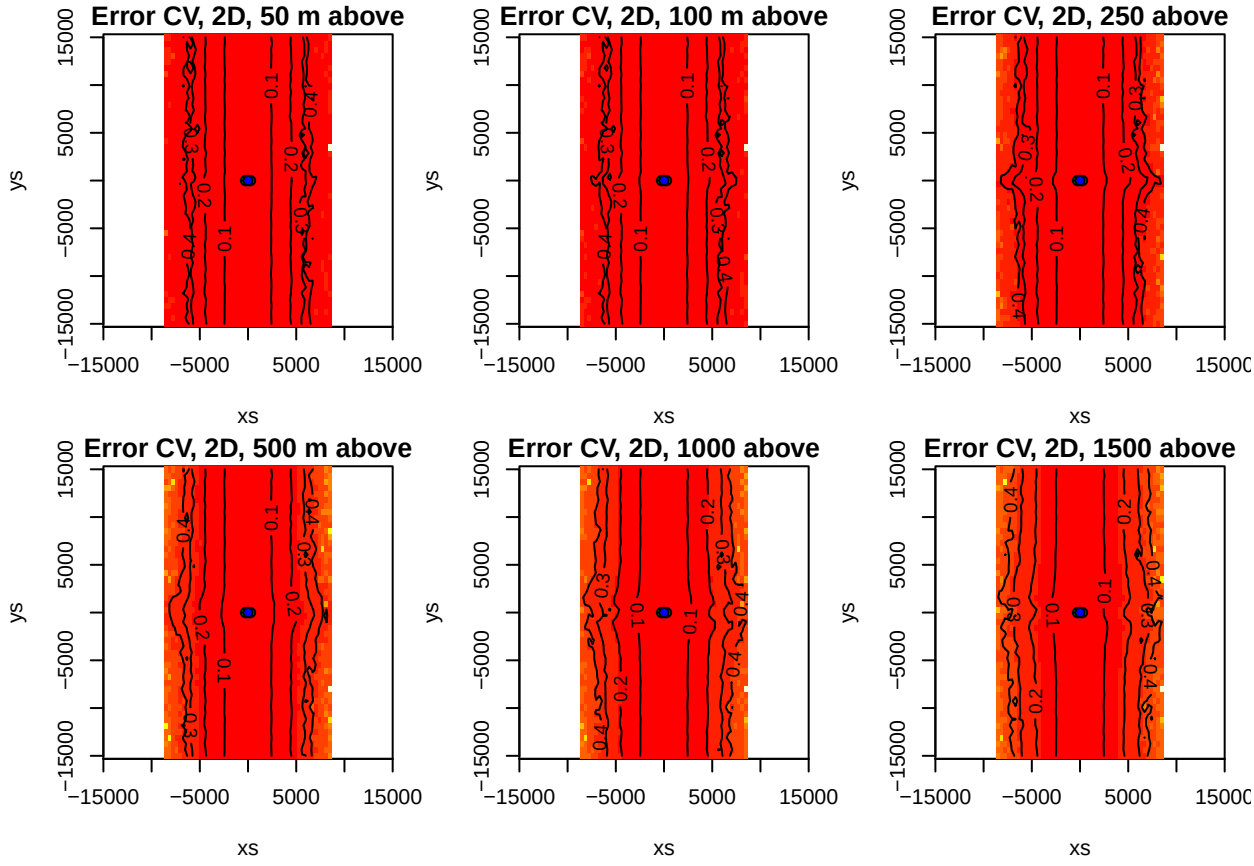

Figure 39: Geometric dillution of precision (gdop) plot, in terms of error CV, for two units 500 meters apart and whales at 6 different distances (50,100,250,500,1000,1500 meters) above the units.

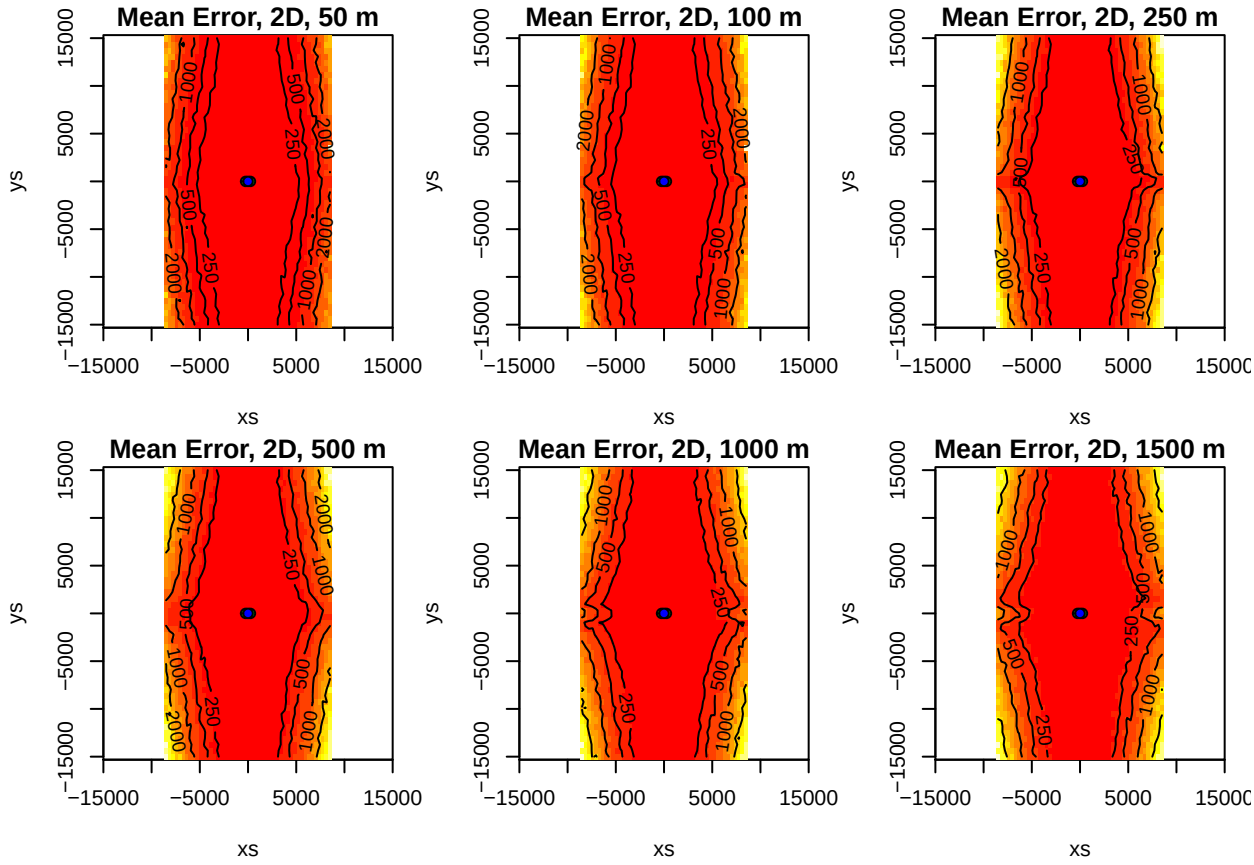

Figure 40: Geometric dillution of precision (gdop) plot, in terms of absolute error, for two units 500 meters apart and whales at 6 different distances (50,100,250,500,1000,1500 meters) above the units.

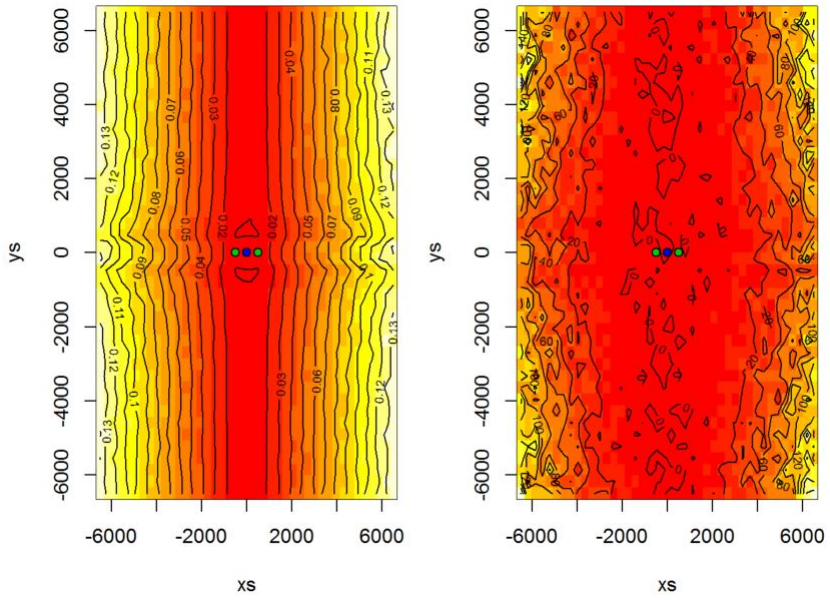

Figure 41: Geometric dillution of precision (gdop) plot. Units 1000 meters apart and whale 500 meters above units.

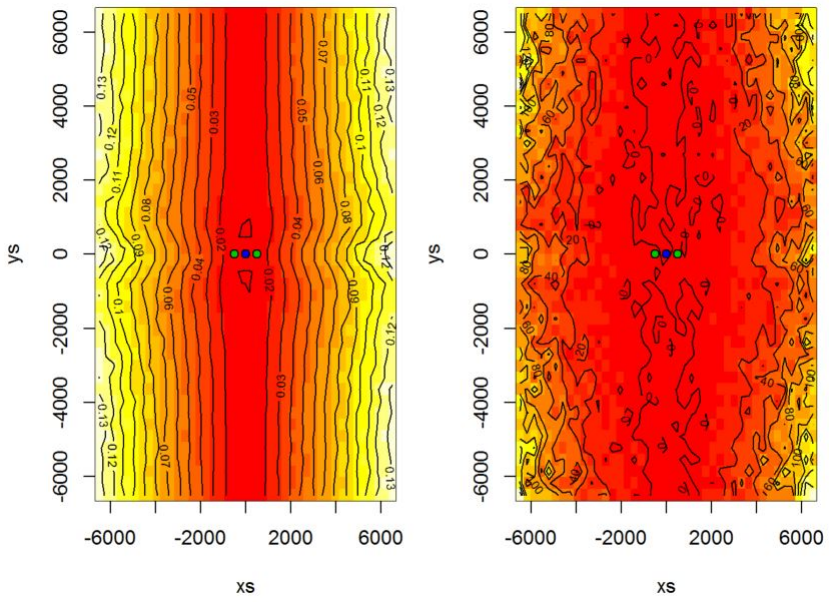

Figure 42: Geometric dillution of precision (gdop) plot. Units 1000 meters apart and whale 1000 meters above units.

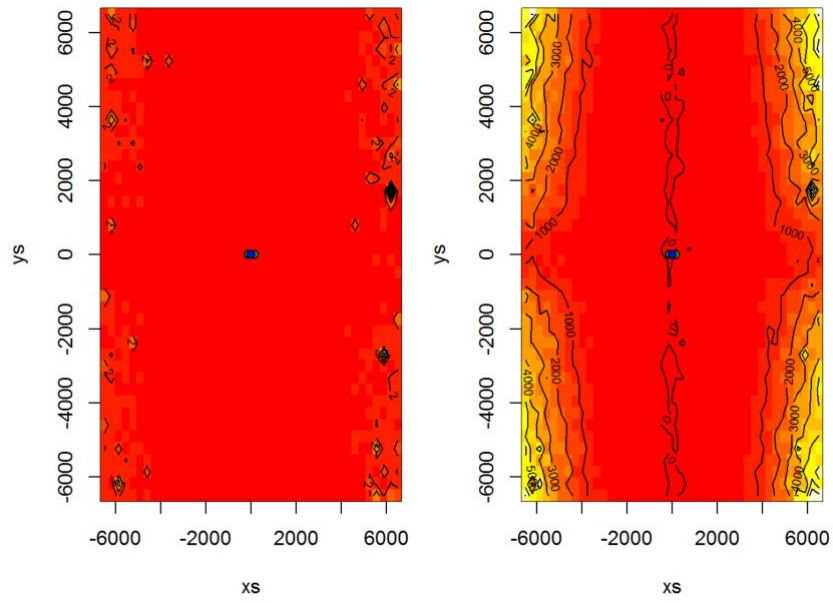

Figure 43: Geometric dillution of precision (gdop) plot. Units 1000 meters apart and whale 250 meters above units.

6.4 Fin whales

Note that the fin whale simulations are somewhat deprecated, as we moved to investigate aspects which were species independent.

In the case of fin whales, we assume that the whales call near the surface, while the sensors remain at the bottom. Stimpert *et al.* (2015) reported that for a set of 14 tagged fin whales, no dives deeper than 100 meters had calls recorded (cf. their figure 2).

We consider that the second sensor is 500 m east of the first sensor, and that the whale is near the surface (assume say 1700 m deep ocean floor).

The key difference between fin whales and beaked whales will be that the lower frequency calls of the former will mean calls will travel further, resulting in potentially much higher detection distances, but at the same time also make the corresponding calls harder to localize. Hence, instead of the 1 % error we associated with beaked whale call bearings, here we assume an unbiased Gaussian error with a standard deviation of 3%. As before, errors are assumed to act independently on each of the 3 components of vectors defining the 3D-bearings to the detected calls.

We consider 4 specific scenarios with fin whales:

- Near optimal geometry, close
- Near optimal geometry, far
- Close by, kind of good geometry
- Medium range, kind of good geometry

6.4.1 Near optimal geometry, close

The whale is located 1500 meters north and halfway between the sensors. The estimated 2D location and the estimated depth of the whale for 1000 sets of random errors is shown in Figure 44.

Figure 45 represents the estimated 3D positions of the whale (in red) and the true whale location (in green), showing that under this scenario the resulting errors in the position are moderate.

Figure 46 shows estimated 2D projected distance to the virtual point transect for 1000 realizations of the assumed error process in the 3D bearings. Note that now we have a biased distance, with a left tail, which would presumably lead to an underestimation of distances, which we expect to correspond to an overestimation of density via distance sampling (all else being the same).

6.4.2 Near optimal geometry, far

The whale is now located 7500 meters north and halfway between the sensors. The estimated 2D location and the estimated depth of the whale for 1000 sets of random errors is shown in Figure 47.

Figure 48 shows us the estimated positions of the whale (in red) and the true whale location (in green), showing that under this scenario the errors in the position are moderate.

Note that now we have a biased distance, with a left tail (Figure 49), which would presumably lead to an underestimation of distances, which we expect to correspond to an overestimation of density via distance sampling (all else being the same).

6.4.3 Close by, good geometry

The whale is located now 1000 meters north and 2000m west of the first sensor, and still the same 1700m above the sensors. The estimated 2D location and the estimated depth of the whale for 1000 sets of random errors is shown in Figure 50.

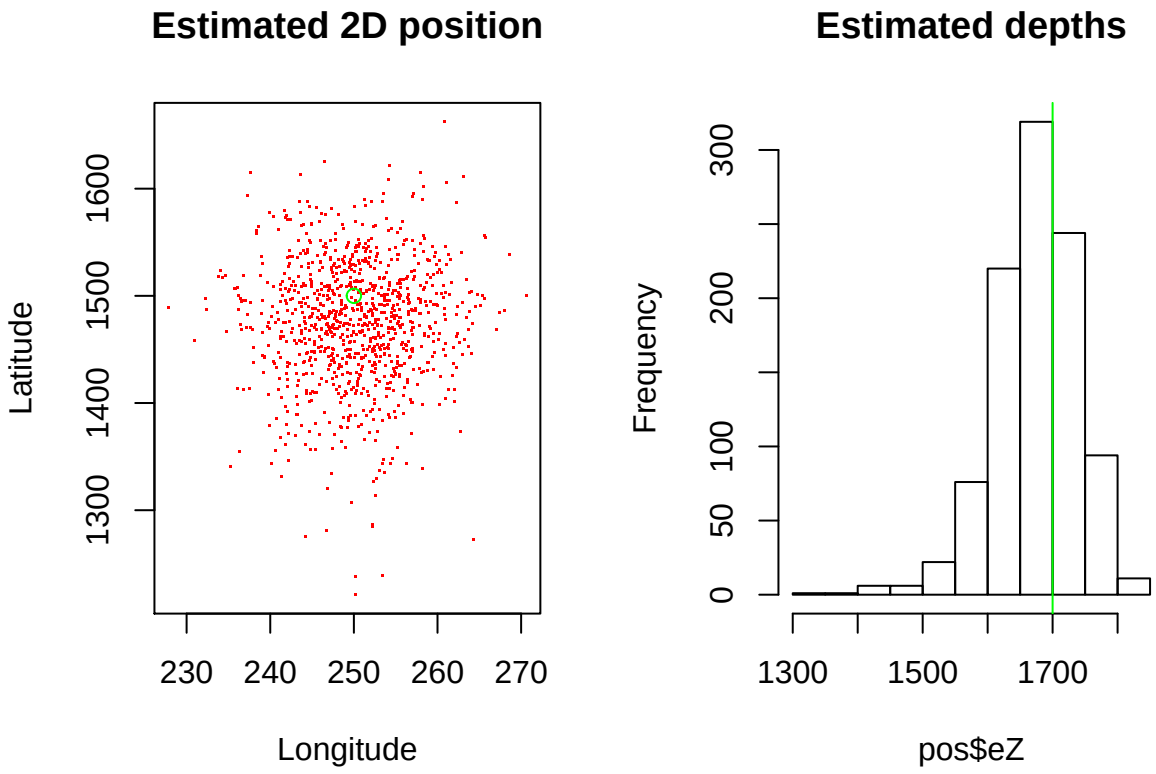

Figure 44: Estimated 2D positions and estimated depth of a fin whale. Green represents the truth. Sensors are 500 meters apart and whale is half way between units, 1500 m north and 1700 m above the units. Measurement error is Gaussian (with a standard deviation of 3) in each of the components defining the 3D bearings.

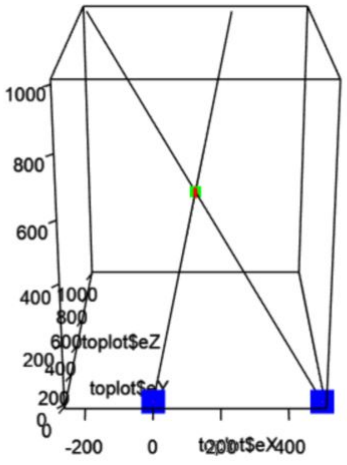

Figure 45: Estimated locations of fin whales under the 'Near optimal geometry, close' scenario.

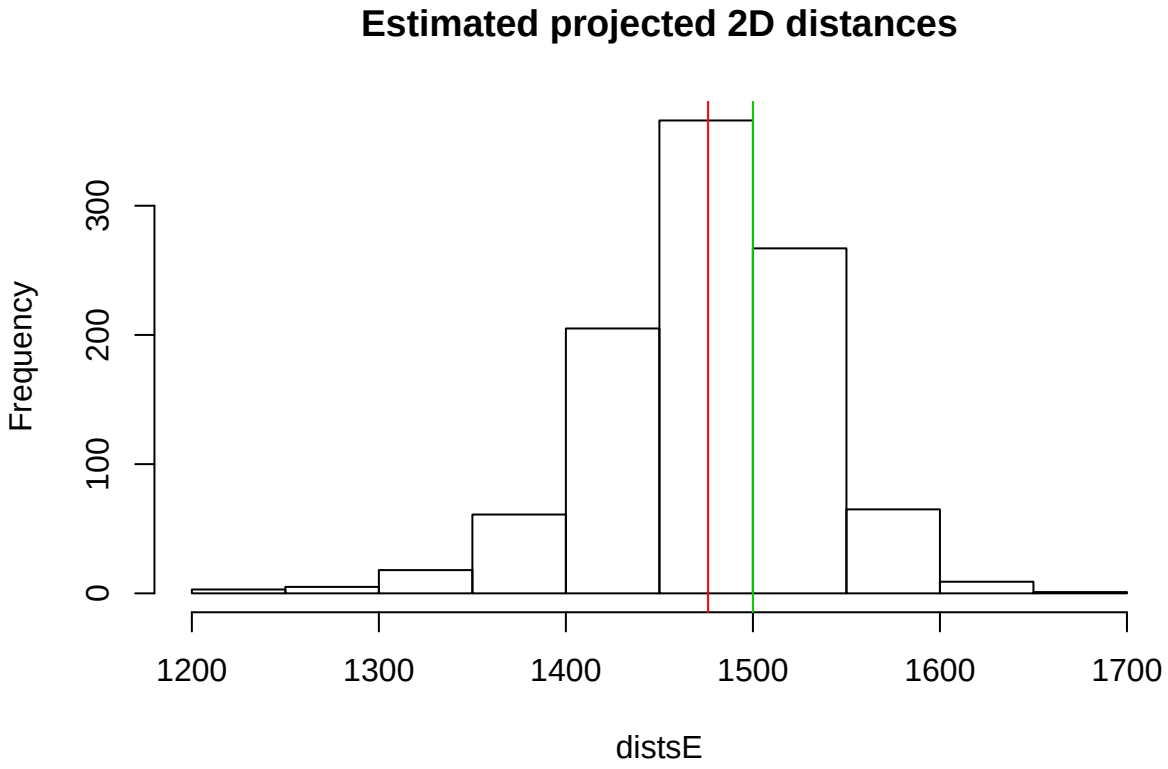

Figure 46: Estimated 2D distance between a fin whale and a virtual point transect. Green represents the truth. Sensors are 500 meters apart and whale is half way between units, 1500 m north and 1700 meters above the units. Measurement error is Gaussian (with a standard deviation of 3) in each of the components defining the 3D bearings.

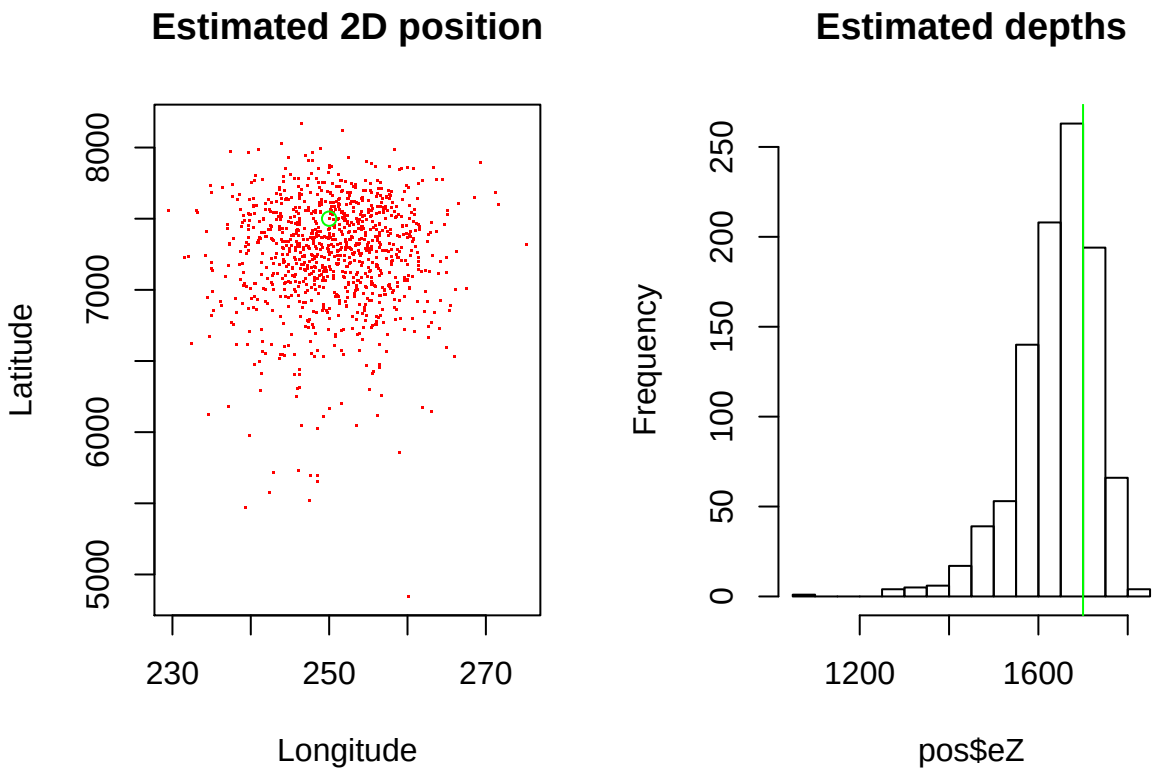

Figure 47: Estimated 2D positions and estimated depth of a fin whale. Green represents the truth. Sensors are 500 meters apart and whale is half way between units, 7500 m north and 1700 m above the units. Measurement error is Gaussian (with a standard deviation of 3) in each of the components defining the 3D bearings.

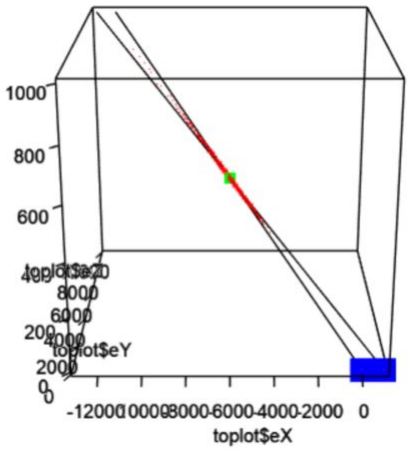

Figure 48: Estimated locations of fin whales under the 'Near optimal geometry, far' scenario.

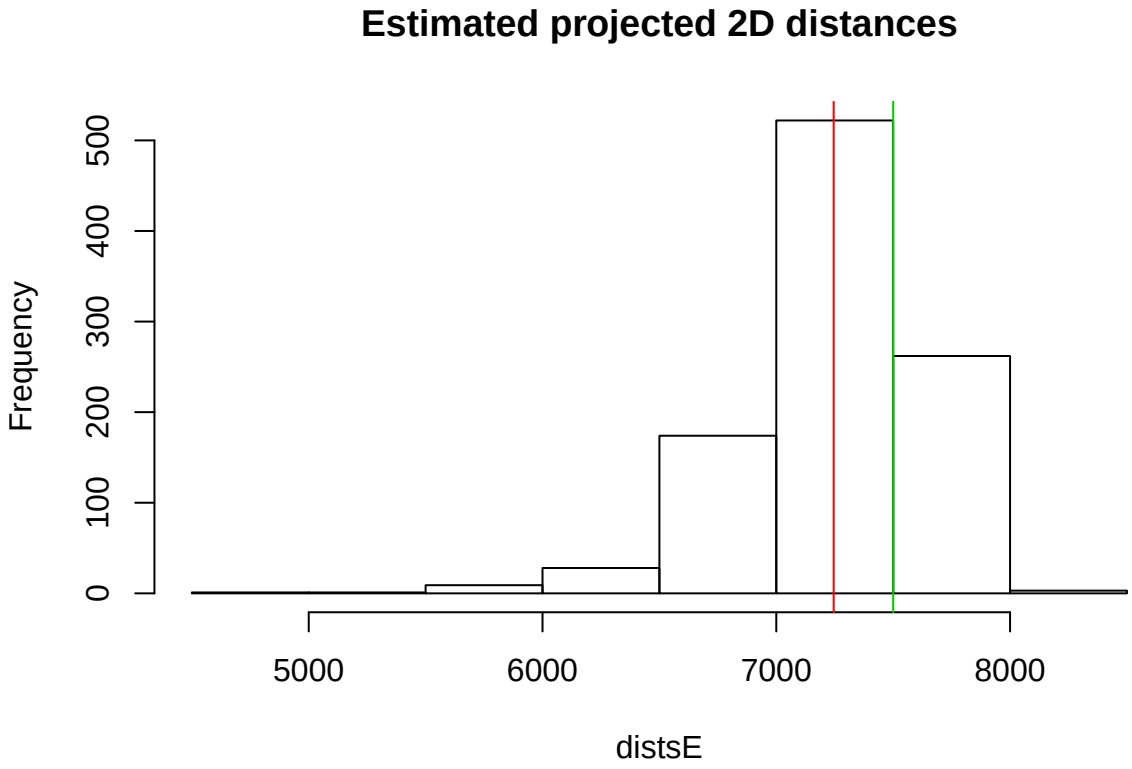

Figure 49: Estimated 2D distance between a fin whale and a virtual point transect. Green represents the truth. Sensors are 500 meters apart and whale is half way between sensors, 7500 m north and 1700 meters above the sensors. Measurement error is Gaussian (with a standard deviation of 3) in each of the components defining the 3D bearings.

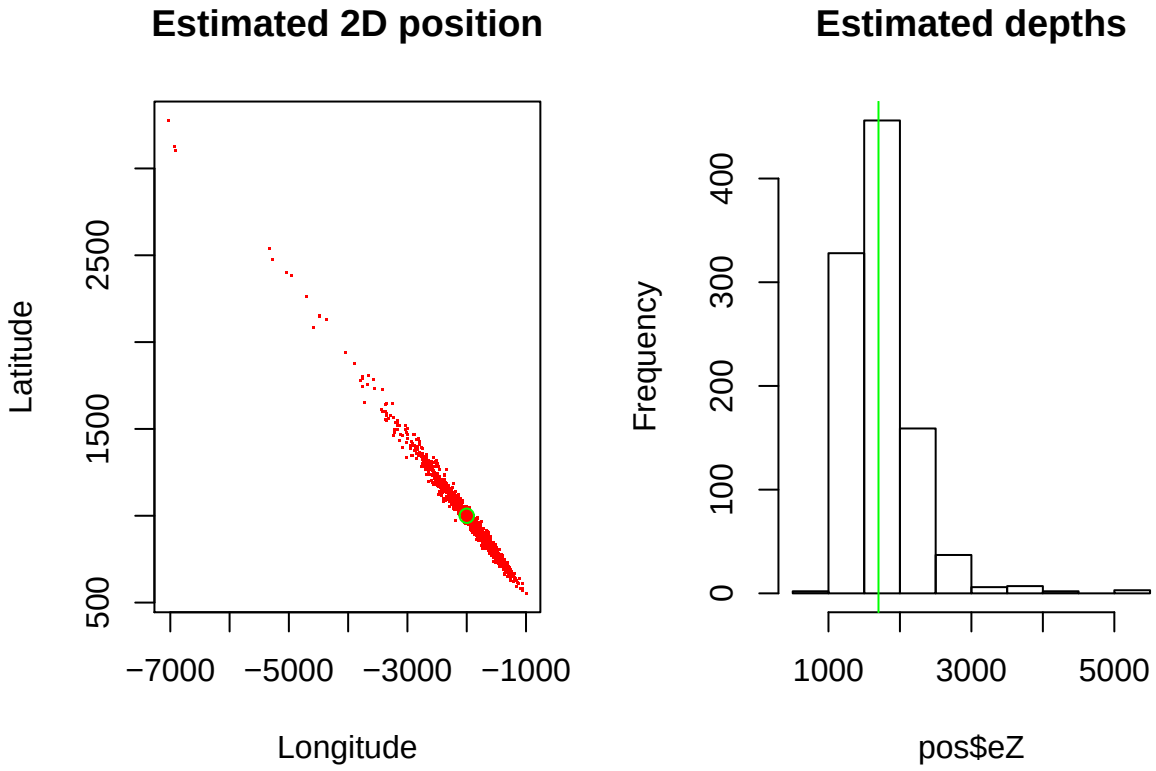

Figure 50: Estimated 2D positions and estimated depth of a fin whale. Green represents the truth. Senosors are 500 meters apart and whale is 1000 meters north and 2000m west of the first sensor and 1700 m above the sensors. Measurement error is Gaussian (with a standard deviation of 3) in each of the components defining the 3D bearings.

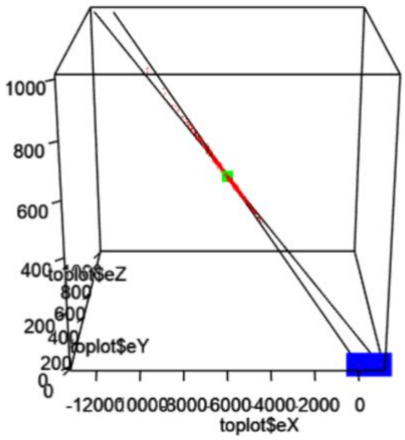

Figure 51: Estimated locations of fin whales under the 'Close by, good geometry' scenario.

Figure 51 shows the estimated positions of the whale (in red) and the true whale location (in green), showing that under this scenario the errors in the position are quite large.

Note that now we have a biased 2D distance, with a quite long and heavy right tail (Figure 52), which would presumably lead to an overestimation of distances, which we expect to correspond to an underestimation of density via distance sampling (all else being the same).

6.4.4 Medium range, good geometry

To illustrate a medium range scenario with good geometry, the whale was located 5000 meters north and 4000m west of the first sensor. Note this is a small distance for possible detections of low frequency fin whale calls. The estimated 2D location and the estimated depth of the whale for 1000 sets of random errors is shown in Figure 53.

Figure 54 shows the estimated positions of the whale (in red) and the true whale location (in green). Under this scenario the errors in the position can be extremely large.

Note , this results in apotentially extremely biased distance, with a long and heavy right tail (Figure 55), that would presumably lead to an overestimation of distances, in turn resulting in an underestimation of density via distance sampling (all else being equal).

In particular, some estimates which locate the whale under the bottom of the sea are obtained, but these are inadmissible estimates caused by the two bearings "diverging" on the positive depths. This is illustrated in figure 56, with the estimated bearings shown in red. Estimated distances become larger and larger as the two 3D bearings become closer to parallel. However, when they diverge the resulting depth is beneath the ocean floor. While this is clearly indicative of an estimated distance that is quite far, it provides little information about the actual distance as the best estimate then becomes infinity!

7 Propagating errors in 3D bearings to density estimates

In the previous section we investigated the effect of errors in 3D bearings and how they induce errors of 3D location and 2D projected distances. However, our main interest is on how these errors propagate through to density estimates from distance sampling, if the measurement error is ignored.

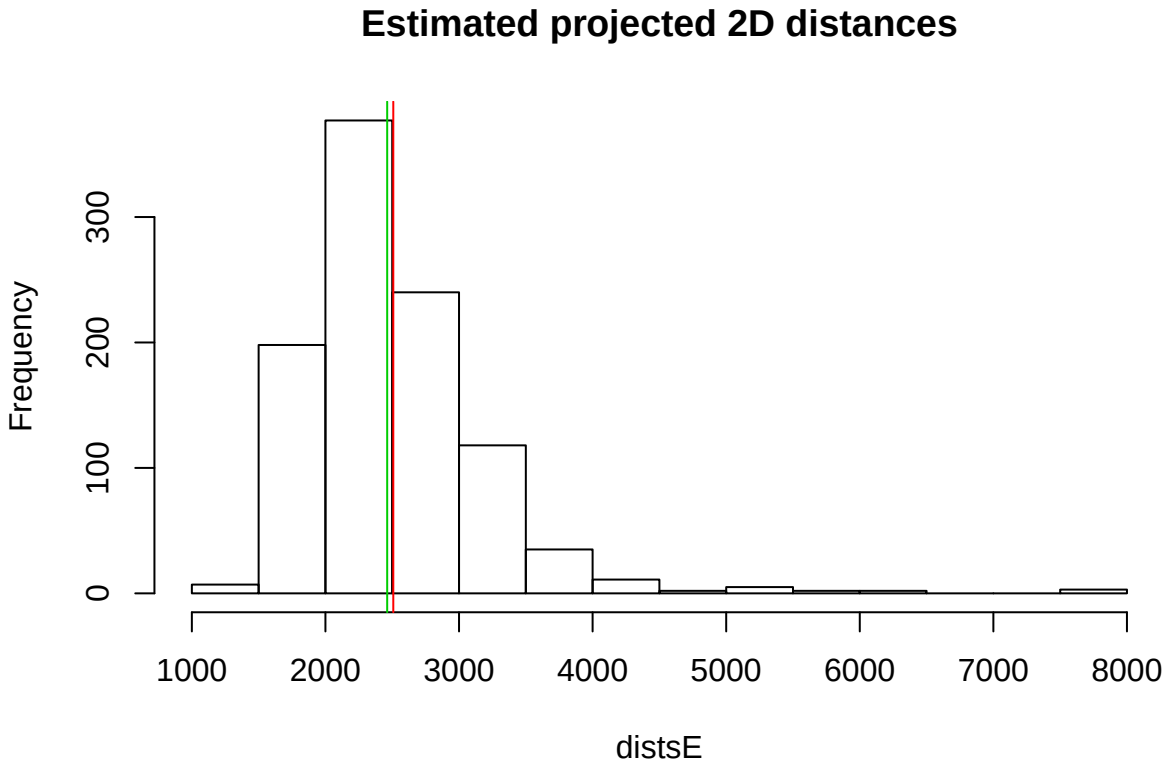

Figure 52: Estimated 2D distance between a fin whale and a virtual point transect. Green represents the truth. Sensors are 500 meters apart and whale is 1000 meters north and 2000m west of the first sensor and 1700 m above the units. Measurement error is Gaussian (with a standard deviation of 3) in each of the components defining the 3D bearings.

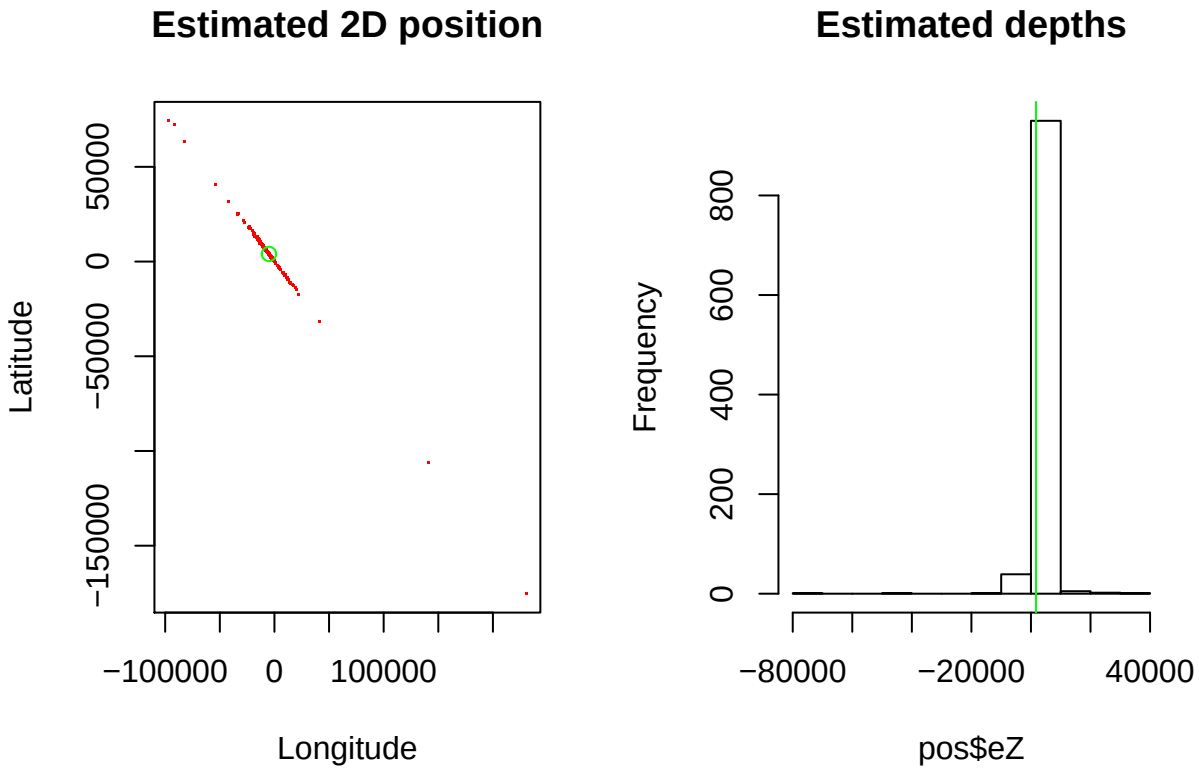

Figure 53: Estimated 2D positions and estimated depth of a fin whale. Green represents the truth. Sensors are 500 meters apart and whale is 5000 meters north and 4000m west of the first sensor and 1700 m above the sensors. Measurement error is Gaussian (with a standard deviation of 3) in each of the components defining the 3D bearings.

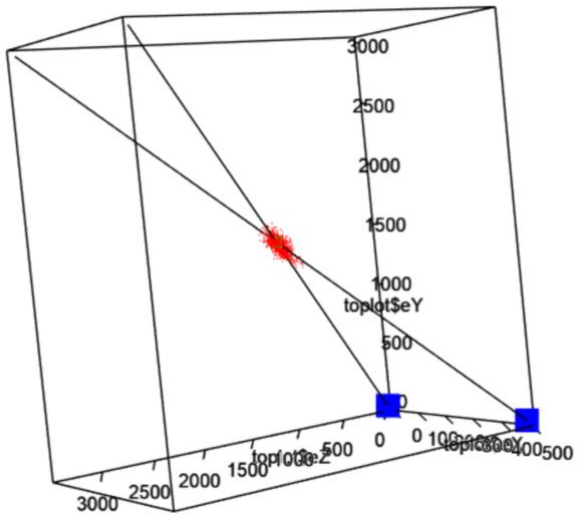

Figure 54: Estimated locations of fin whales under the 'Medium range, kind of good geometry' scenario.

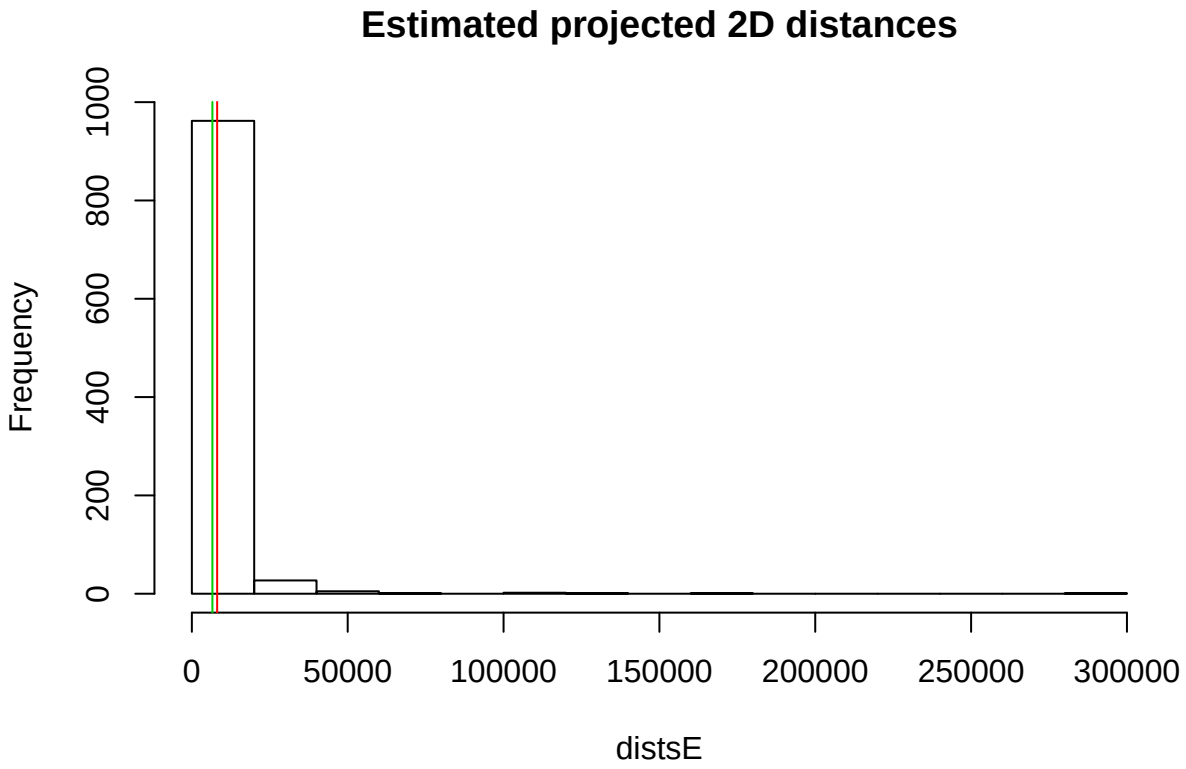

Figure 55: Estimated 2D distance between a fin whale and a virtual point transect. Green represents the truth. Units are 500 meters apart and whale is 5000 meters north and 4000m west of the first sensor and 1700 m above the units. Measurement error is Gaussian (with a standard deviation of 3) in each of the components defining the 3D bearings.

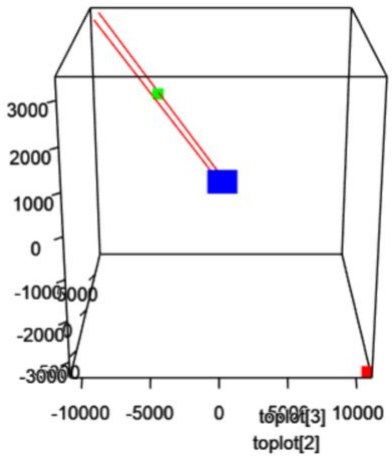

Figure 56: The estimated location of a fin whale under the sea bottom, obtained under the under the 'Medium range, good geometry' scenario.

We assume the sensors are at a 2000 m depth, on a flat ocean bottom, and separated by 500 m. Then we assume whale sounds to occur at depths sampled from a uniform distribution between 1500 and 1000 m deep (i.e. between 500 to 1000 m above the sensors depth). We will assume that 10000 calls are produced in a squared area of 8k km around the single virtual sensor (edge effects can be safely ignored given the parameters used). We will assume the detection function from the virtual sensor to be well approximated by a half-normal with 3km sigma. This is consistent with the detection function for on-axis beaked whale clicks estimated at AUTEC as described in Marques *et al.* (2009).

We created two dedicated functions to generate the auxiliary vectors required to simulate the vectors with errors.

An example of the resulting distances from such a survey assuming no measurement error is shown in figure 57.

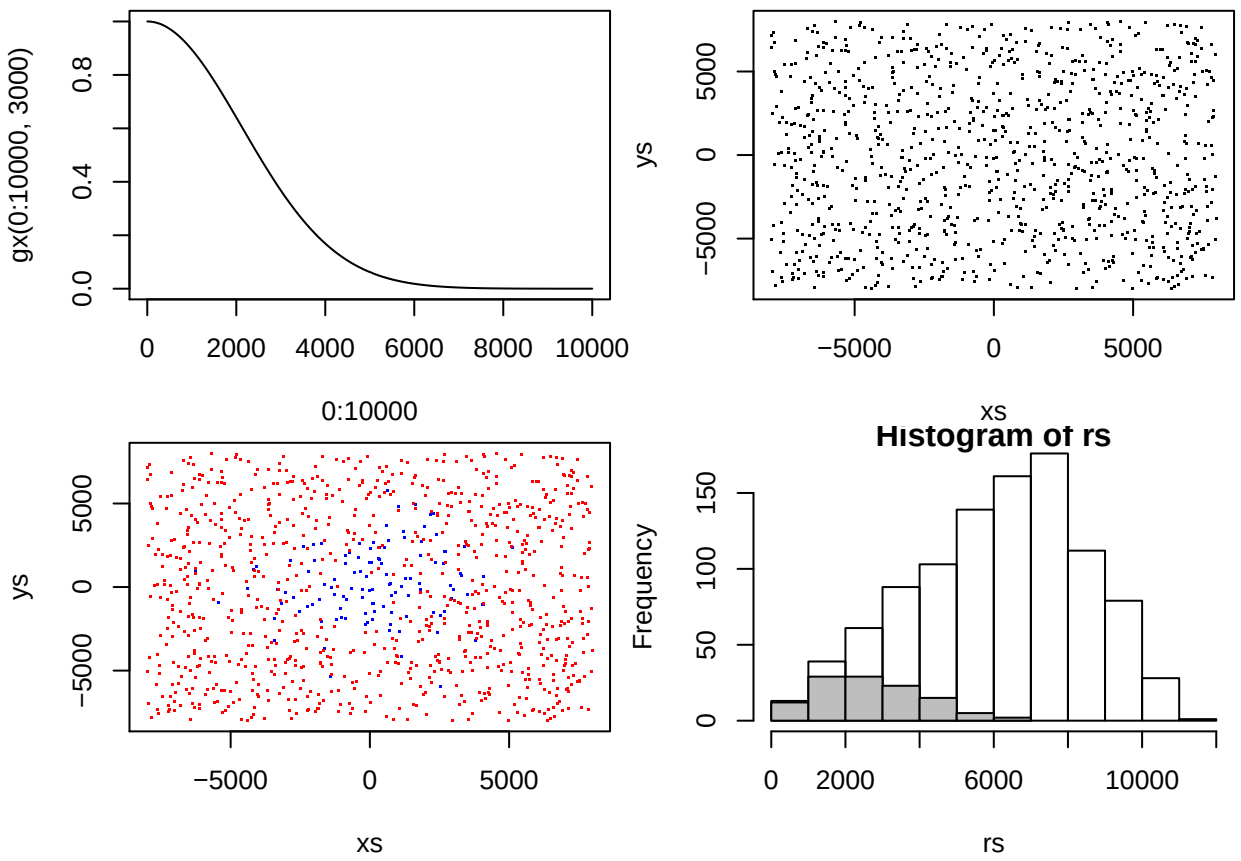

Figure 57: An example survey. Top left is the half-normal detection function. Top right are all the sound sources locations, projected on 2D. Bottom left represents the detected sound sources highlighted in blue. Bottom right presents the available and detected 2D projected distances.

As expected, assuming a known probability of detecting an animal in a circle around the sensor (and a known probability of an animal being in the circle, given that it is in the square that just includes the circle), we obtain an unbiased estimator of abundance (Figure 58).

Our goal is to repeat this process in the presence of measurement errors in the 3D bearings, while estimating P, to evaluate empirically what the potential bias might be.Note that in the example above, the 3rd dimension (i.e. depths) was ignored, but in the following we will consider it explicitly, with source locations being located uniformly between 500 and 1000 meters above the sensors. We run this simulation scenario a single time as an example (Figure 59).

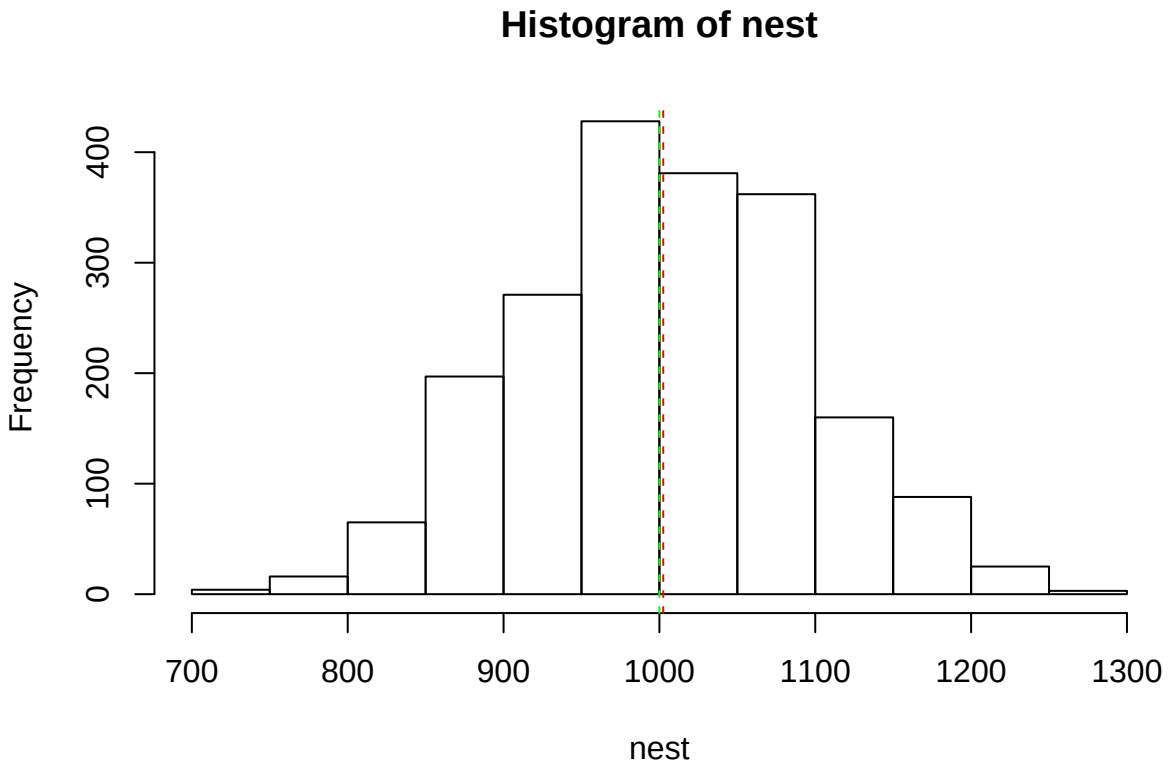

Figure 58: Repeating a survey 1000 times. Note P is assumed known

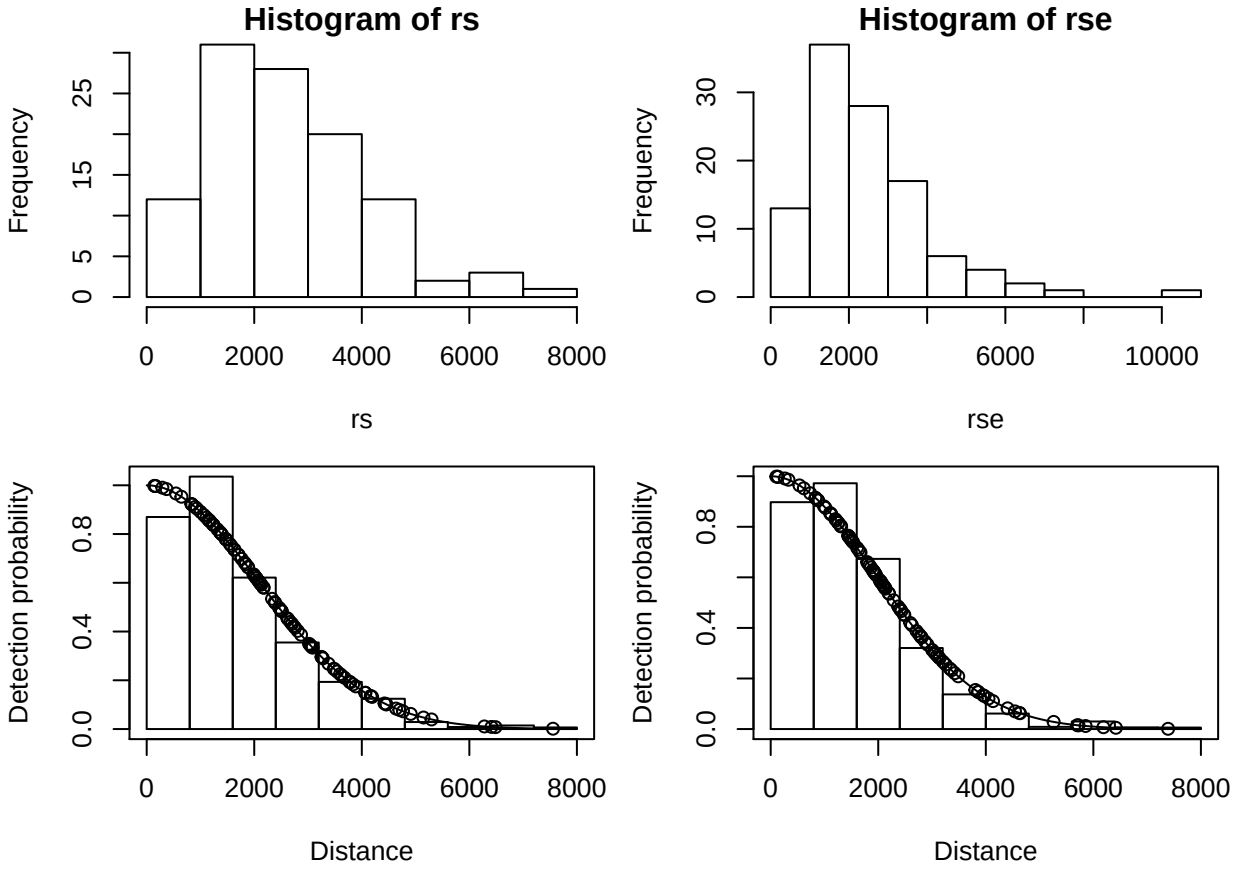

Figure 59: Projected distances between detected sound sources and the virtual point transect, with the corresponding estimated detection functions below. Left column are true distances, right column are distances measured with error

Under this scenario, the true probability of detection was 0.141. With no errors we estimated it to be 0.135, but with the errors we estimate it to be 0.121. This is only one instance, but does indicate a possible bias, as expected. Next we repeated this a few thousand times for a couple of scenarios.

7.1 Scenario 1

We ran the above scenario 1000 times. The results are shown in figure 60.

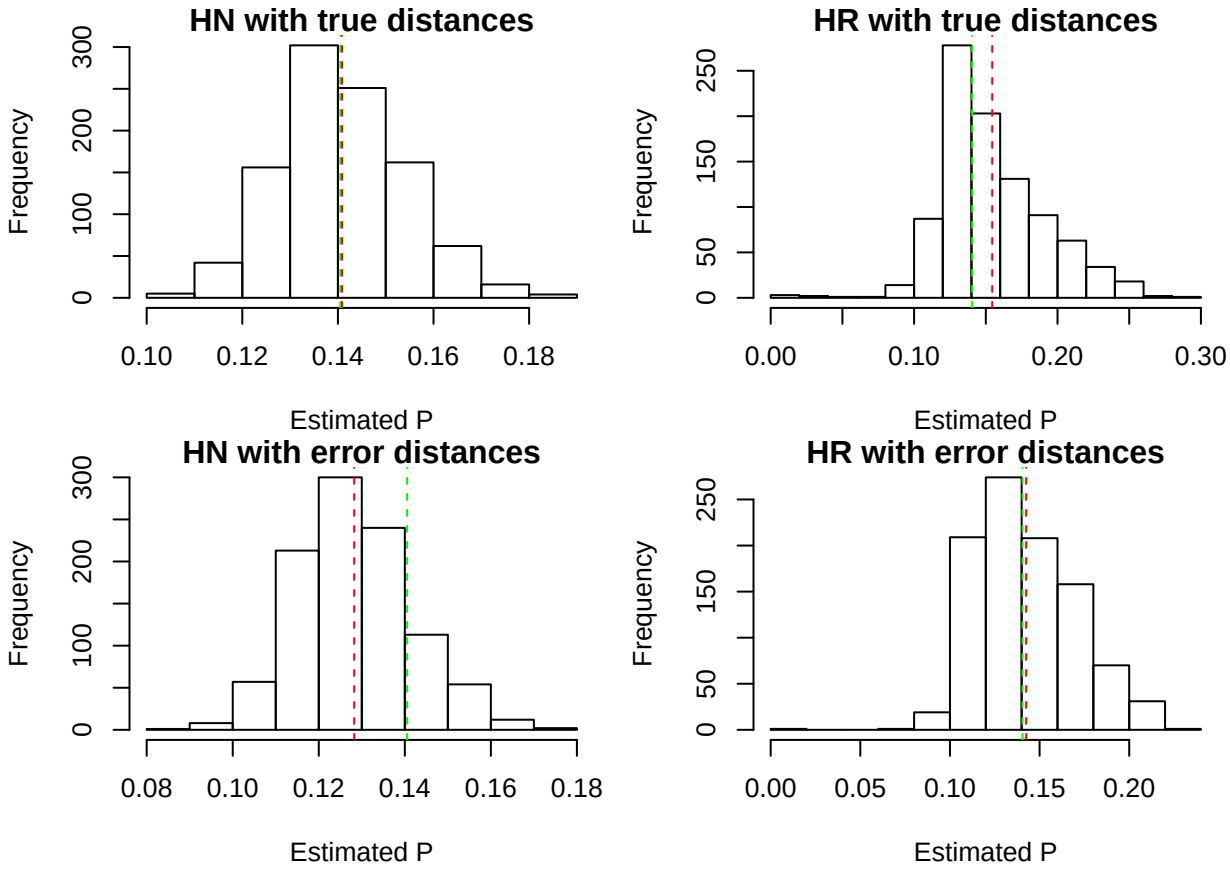

Figure 60: Density estimates under the first density estimation scenario. True detection function is a half-normal with scale parameter 3000. The 4 analysis options represent the factorial crossing of true model or wrong model (hazard-rate) and true distances or error distances.

Fitting simply the true model (half normal with no adjustments) leads to approximately unbiased results, as expected (red line - mean estimated value of P, green line - true value of P) (bias in P: 0.25; bias in N :0.621). Considering still the true distances, but a hazard rate model (with the possibility of adjustments via AIC), P is biased up, so $N \approx 1/p$ would be biased down (bias in P: 9.933; bias in N :-1.835). This reflects the effect of using the wrong model, and perhaps partially the effect of model selection (as in Gonzalez *et al.* (2017)). When considering the error distances and the true model, P is biased low (-8.733), which would lead to a positive bias in N (of 10.714). Finally, and likely just a coincidence, the two biases seem to cancel out when one uses the wrong model with the error distances (bias in P: 1.444; bias in N :4.347).

7.2 Scenario 2

We ran a second scenario, just increasing the sigma of the detection function to 4500 (cf. above 3000). The corresponding results are shown in figure 61.

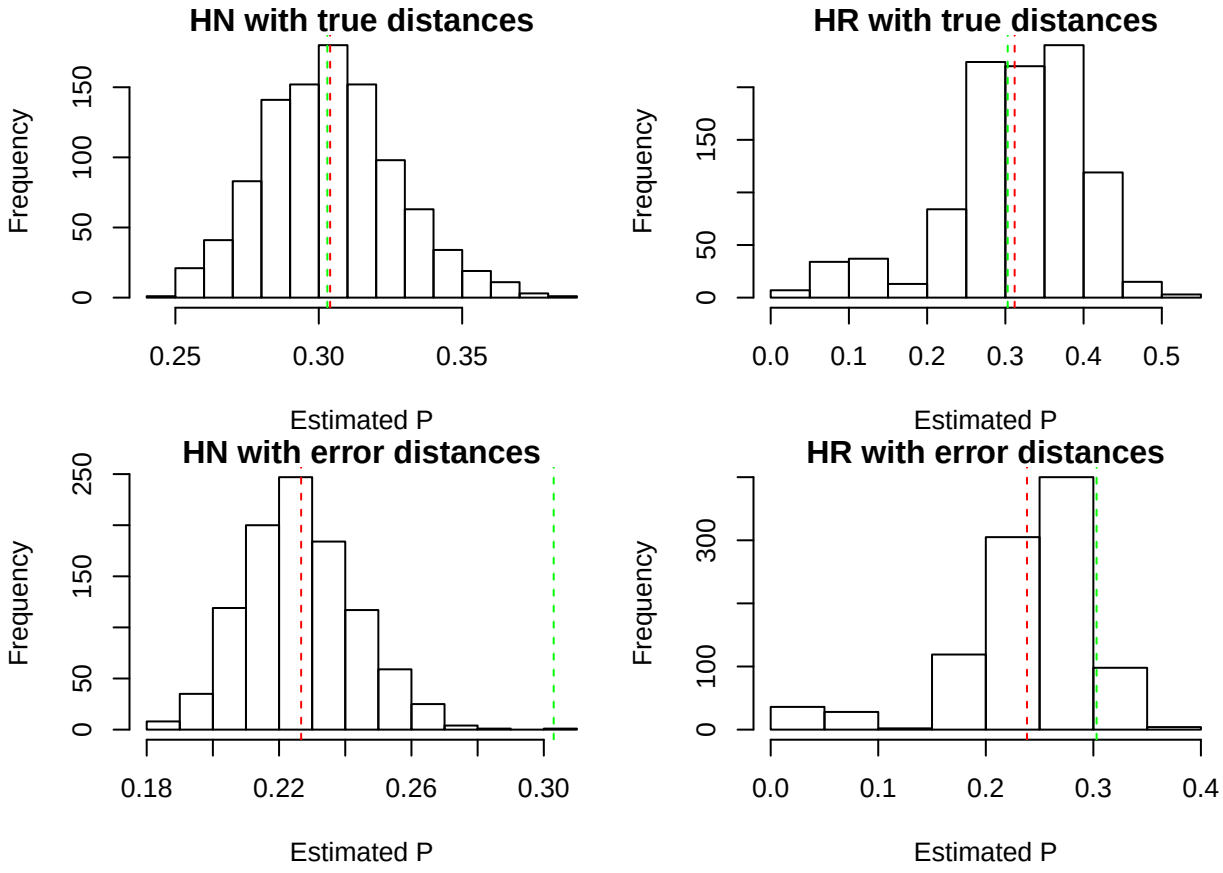

Figure 61: Density estimates under the second density estimation scenario. True detection function is a half-normal with scale parameter 4500. The 4 analysis options represent the factorial crossing of true model or wrong model (hazard-rate) and true distances or error distances.

Fitting simply the true model (half normal with no adjustments) leads to approximately unbiased results, as expected (red line - mean estimated value of P, green line - true value of P) (bias in P: 0.32; bias in N :0.259). Considering still the true distances, but a hazard rate model (with the possibility of adjustments via AIC), P is slight biased up, so $N \approx 1/p$ would be biased down (bias in P: 2.927; bias in N :19.595). Noticeably, the effect is less than before. When considering the error distances and the true model, P is considerably biased low (-25.189), which would lead to a positive bias in N (of 34.382). This effect is stronger than before, which is not surprising since the wider detection means more large distances, where measurement is larger. Finally, the two biases only partially cancel out when one uses the wrong model with the error distances, and the bias in N is extremely large (bias in P: -21.357; bias in N :119.648). On first sight some of these results were non-intuitive, and we suspected something might be wrong in the code. After double checking, the odd numbers seem real: they are a consequence of occasional very low estimated P's, which leads to large estimated N's. This was an effect which had already been noted in Gonzalez *et al.* (2017), which led us to report median biases there. To see the impact of the different statistics being reported for bias, median bias for the final scenario is -17.091 for P and 20.614 for N.

8 From a model in 3D bearings errors to a model for errors in 2D distances

As described in earlier sections, errors in 3D bearings will propagate to errors in 3D locations, which will then propagate to errors in 2D distances from a virtual point transect.

To implement a distance sampling measurement error approach along the lines of Borchers *et al.* (2010) requires a model of $f(y|r)$, where r represents the true distance, and y the distance observed with error. Conceptually, it might be possible to establish, from first principles and conditional on an assumed distribution for the errors in the 3D bearings $(V_1, V2)$, a distribution for X_t, the true location in 3D, $f(X_t|V_1, V2)$. Then, it might also be possible to get $f(X_e|X_t)$, i.e. a pdf describing the probability of observing a 3D location X_e given the true location X_t. This could then potentially be marginalized to finally obtain something like $f(y|r)$.

Naturally, $f(X_e|X_t)$ will be a complex distribution in 3D, because it will depend on the true 3D location of the sound source. As we have illustrated with simulations, the same error structure will result in localization errors quite distinct for good geometries, e.g., sources half way between units, vs. bad geometries, e.g., sources approximately along the line going through the sensors. Note in particular that for a source exactly along that line even in the absence of measurement error no position estimate would be possible, since we would get two 3D parallel bearing angles. That ambiguity fades away given that in general the whale will not be on the same plane, i.e. at the same depth, as the units, but in practice that might not be enough for a reliable position estimate.

An alternative approach might be to assume a distribution for the errors in the 3D bearings - or, better to estimate it based on data - and then simulate the error process and collect the resulting true distances r and error distances y. One could then simply consider a regression approach to describe $f(y|r)$. This would, in a single step, correspond to the marginalization process required, which, if tackled algebraically, could become extremely complex.

An example of this simulation approach to estimate the measurement error model follows. Naturally, the success of such an approach will depend critically on our ability to represent the tridimensional complex function with a one dimensional density dependent on radial distance alone.

9 Estimating the 2D projected distance error model by simulation

Consider a situation where the 2 4HUs are 500 meters apart, and sound sources are located around these, uniformly in 2D space, and 500 to 1000 meters above the sensors. An example of the true and estimated 3D location of a source under such a setting is shown in figure 62.

As an example, we consider a full realization of the above scenario, for 10000 simulated sources.

For the simulation we actually access to the true distances as well as the error distances. Therefore, we can ignore the 3D process, and try to directly model the 1D process that describes the error model, i.e. $f(y|r)$, using a standard regression approach.

We start by considering a Gamma response with a log link function (Figures 63 and 64).

The fit does not look adequate, with the the goodness-of-fit (GOF) showing considerable departure from the assumed model. Additionally we tried the inverse link function (i.e. the gamma canonical link function), but it fails fit.

Another option might be considering the log link function to force positive predictions, but within a Gaussian family (Figures 65 and 66). This is unlikely to be a sensible approach since we know the variance of the errors to increase with distance, which this formulation would not account for.

The fit continues to be less than ideal. Clearly the link function assumed implies a curvature on the response scale that the data simply do not present.

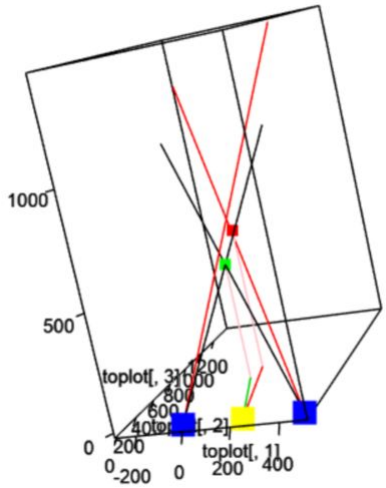

Figure 62: The true bearings to the true sound source position are shown as black solid lines, while the true position of the sound source and the 2D projected distance to the virtual point transect are represented in green. The estimated bearings, the corresponding estimated position and 2D distance in the presence of errors in the bearings are shown in red. The virtual point transect is shown in yellow and the 2 4HUs are shown in blue. In this example, the true 2D distance was 515.4 and the estimated distance with error is 643.4.

We could also consider a Gaussian distribution with the identity link, but that will actually lead to a model that could induce non-admissible (i.e. negative) predictions (Figures 67 and 68).

Of all the above, the gamma with the log link function is by far the best model given AIC (17991.2, vs. 19453.9 and 19424.4 for the Gaussian models). Therefore in the following we use this model for illustration (see below for a couple of additional considerations).

In practice, what does this mean in terms of an error model $f(y|r)$? For example, the distribution $f(y|r)$ is a Gamma with mean value $exp(a + b \times r)$, and with dispersion parameter as provided by the `glm`. In practice, the `glm` estimation of the dispersion parameter, which is also the inverse of the shape parameter in the Gamma, is deficient. The library `MASS` provides an alternative function, `gamma.shape` that works over a `glm` object. This case is illustrated by the following examples. Assume a pair of observed distances at 10 and 1000 m. As examples, $f(10|r)$ and $f(1000|r)$ are given by the functions represented in figure . Note that, scale aside, the process is essentially the same, independent of distance.

The pertinent question is whether there is enough variability represented by any of the chosen models for the measurement error to ensure that using them provides efficiency gains over simply ignoring the measurement error process.

9.1 Details to keep in mind

Given that we can estimate a measurement error model in such a simulation context, i.e. $f(y|r)$, the next step is to implement the methods of Borchers *et al.* (2010) using the error distances and the estimated model for measurement error. This will be a slightly artificial situation in that we have fitted a model using thousands of pairs of real and error distances, that are not available in practice. However, it does provide insight for whether or not we can correct the bias.

As illustrated above, in practice, the measurement error structure is quite complex. If we define the errors on the 3D bearings as a Gaussian 3D angle and a uniform (in the circle) angle, the combination of two error 3D bearings provide an estimate of the animal position in 3D. The uncertainty about that position is a 3D

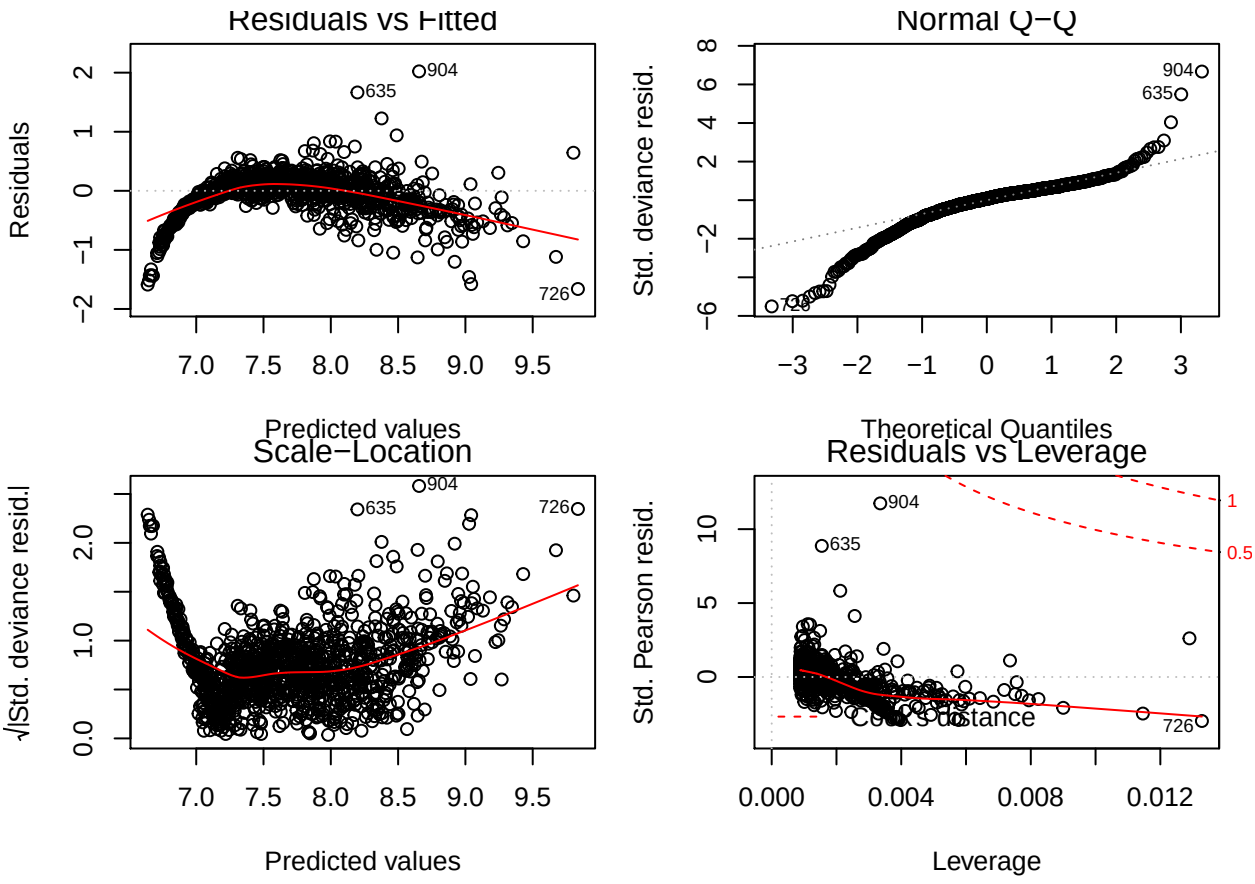

Figure 63: Fitting a gamma (log link) measurement error model to 10000 simulated pairs of true and error 2D distances to a virtual point transect. Model diagnostics.

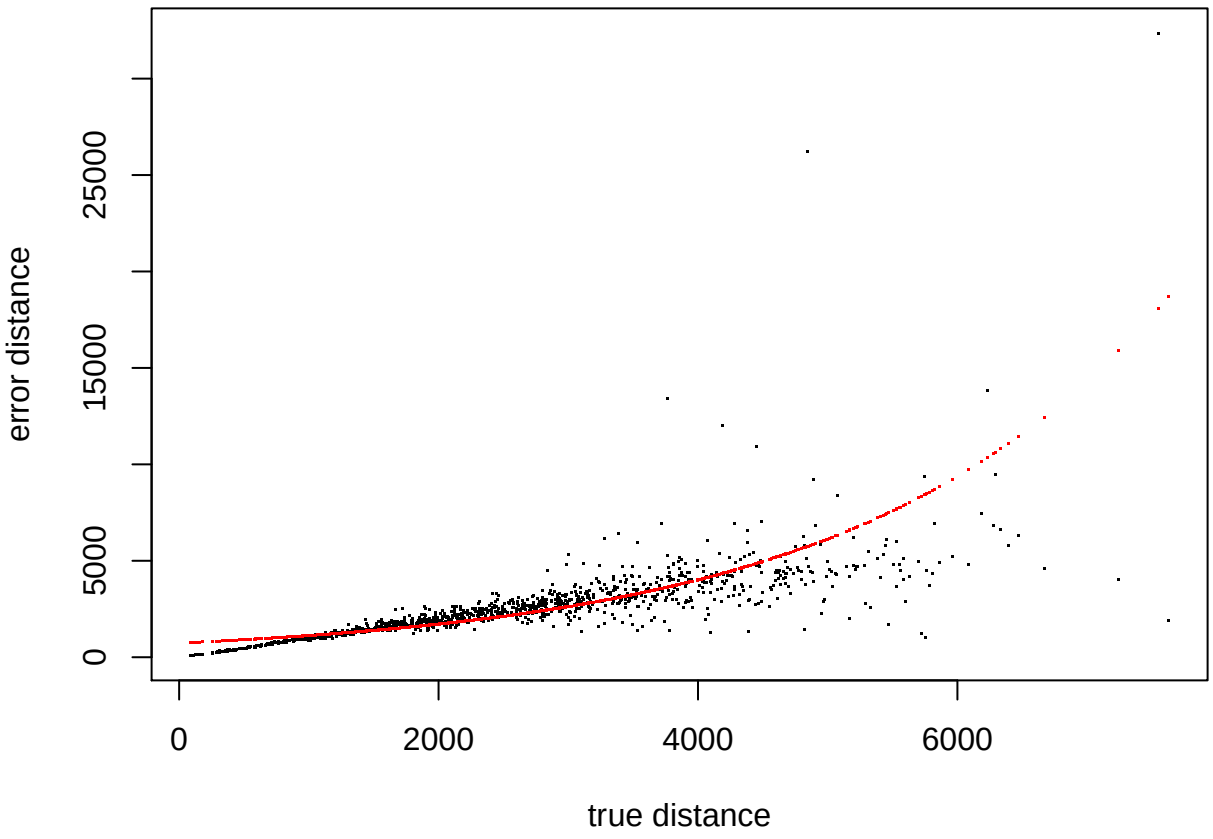

Figure 64: Fitting a gamma (log link) measurement error model to 10000 simulated pairs of true and error 2D distances to a virtual point transect. Model fit.

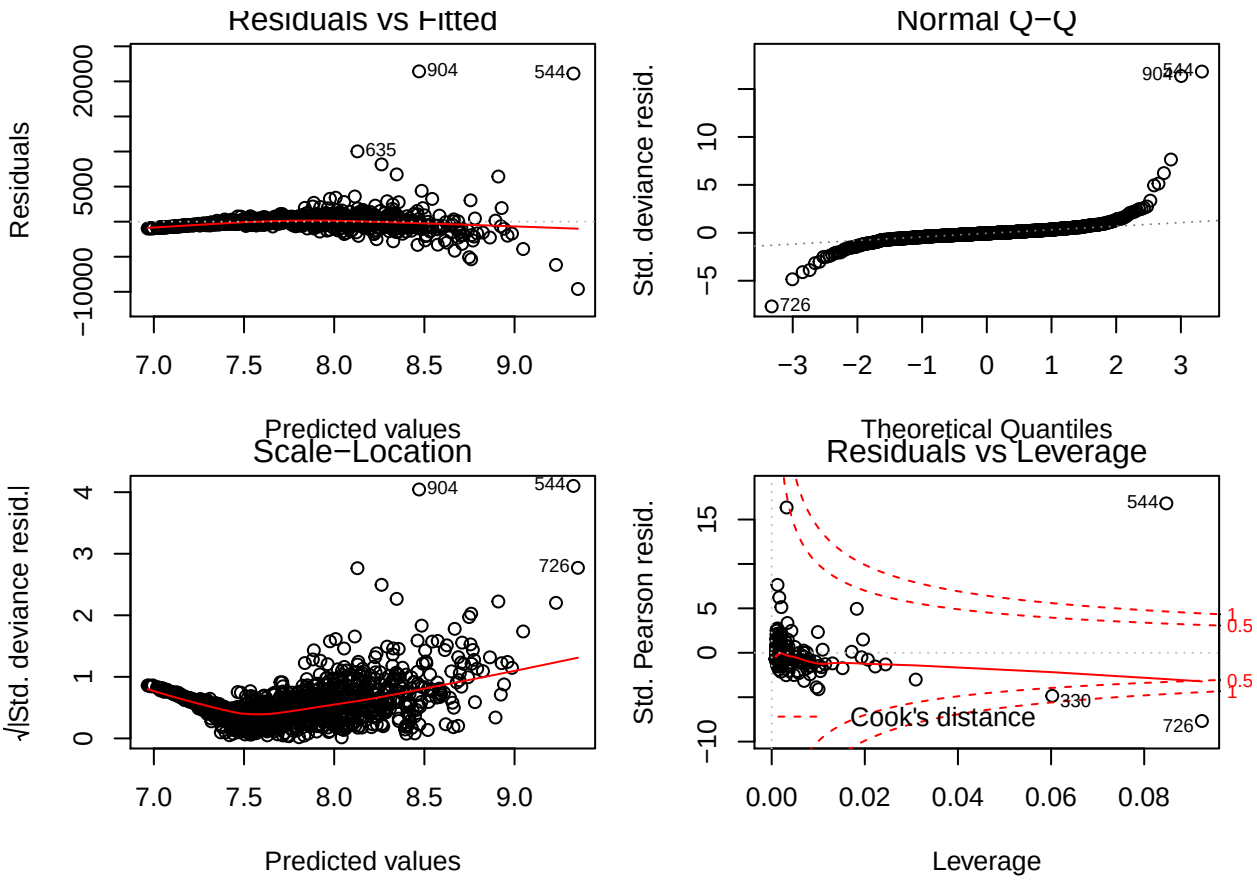

Figure 65: Fitting a Gaussian (with log link) measurement error model to 10000 simulated pairs of true and error 2D distances to a virtual point transect. Model diagnostics.

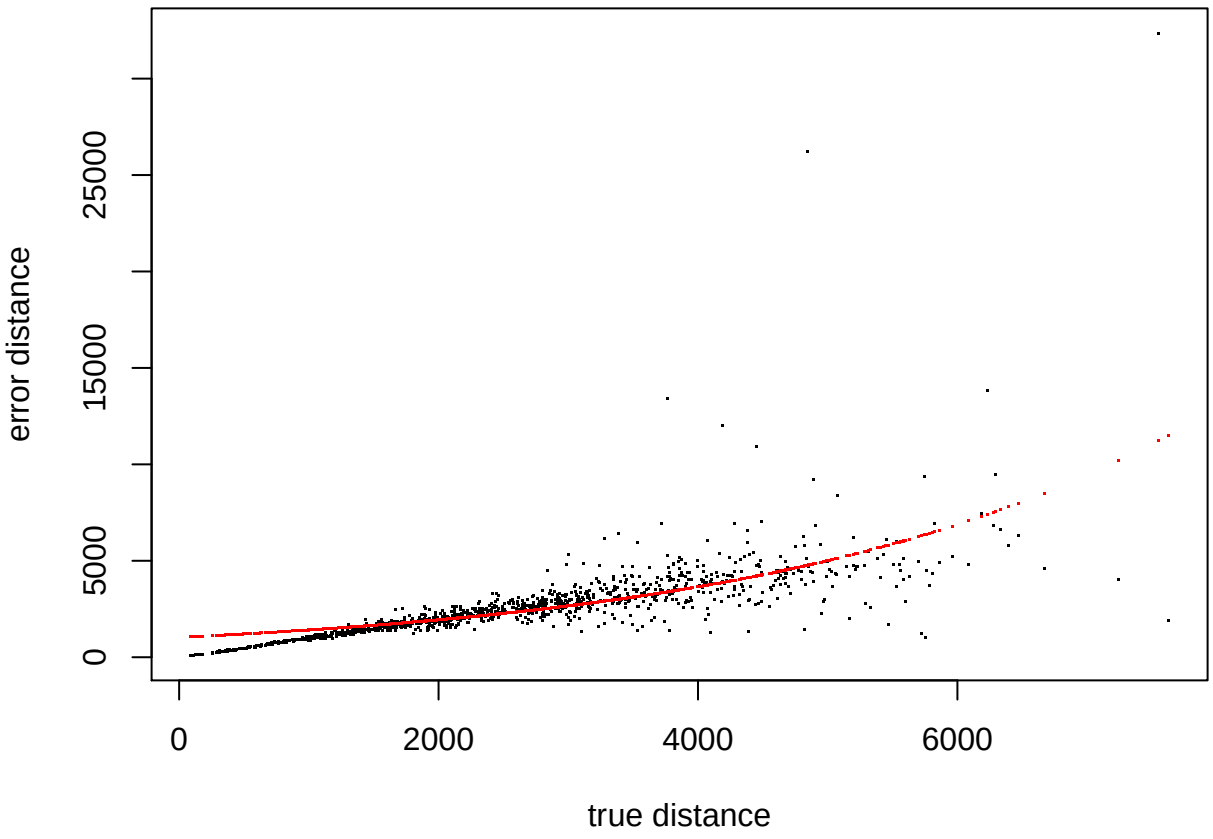

Figure 66: Fitting a Gaussian (with log link) measurement error model to 10000 simulated pairs of true and error 2D distances to a virtual point transect. Model fit.

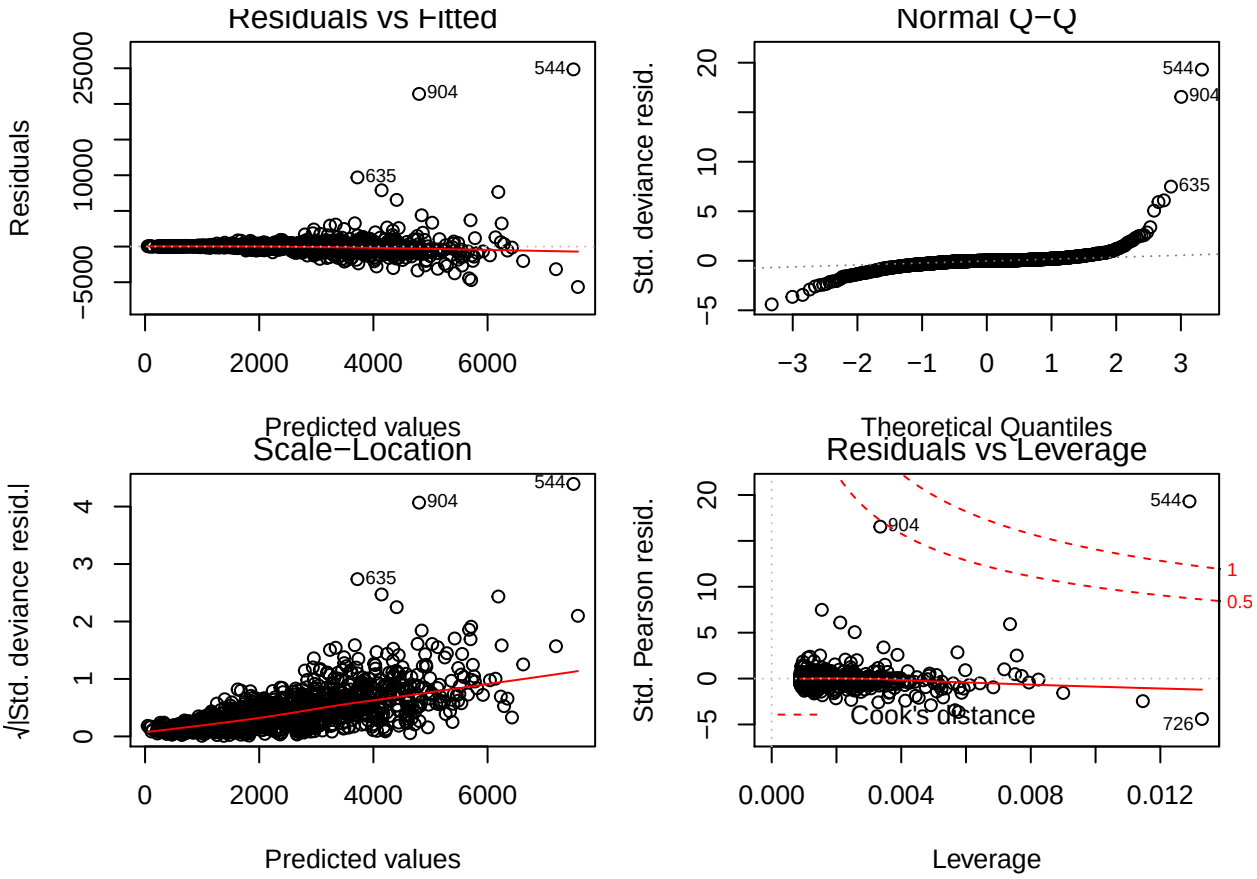

Figure 67: Fitting a Gaussian measurement error model to 10000 simulated pairs of true and error 2D distances to a virtual point transect. Model diagnostics.

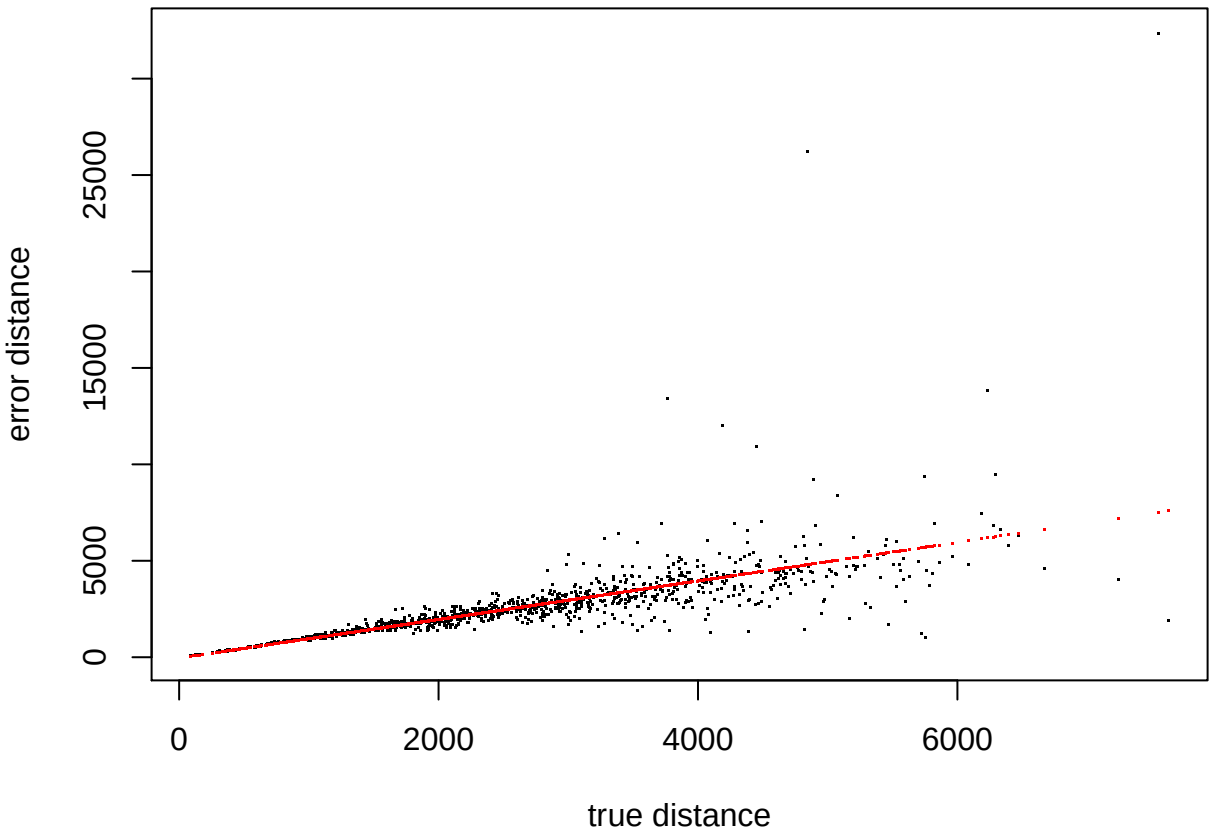

Figure 68: Fitting a Gaussian measurement error model to 10000 simulated pairs of true and error 2D distances to a virtual point transect. Model fit.

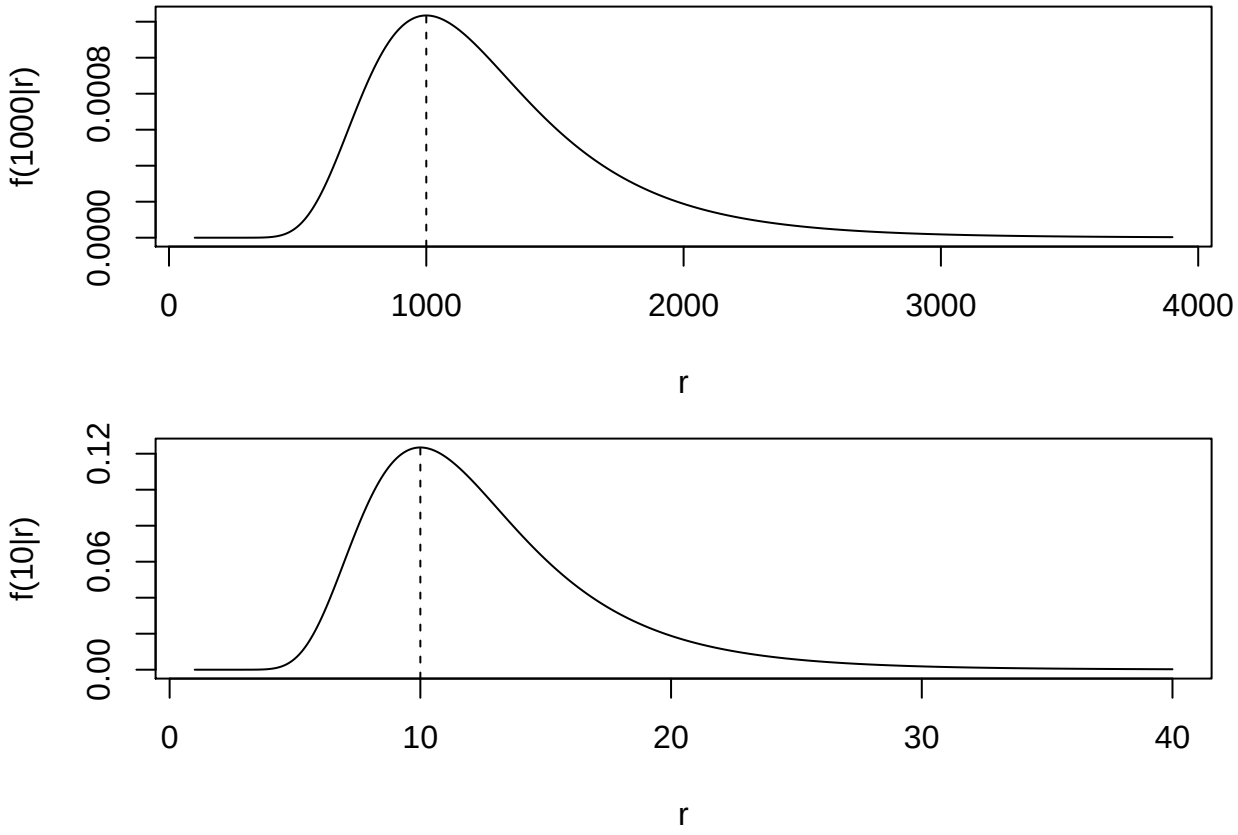

Figure 69: Estimated measurement error model for two example observed distances (10 and 1000 meters)

structure (we can think about the probability of the animal being in a given volume). That uncertainty volume will be dependent on the actual 3D location. Intuitively, a location along the line that crosses the two sensors would have its major axis (along that same line) much longer than if say the location was at the same distance between the two sensors. Similarly, the 3D volume shape will also be dependent on the difference in depth between the sensors and the whale. From the problem geometry, it seems clear that there are two axes of symmetry . Therefore, it is enough to characterize the process in one quadrant, under the assumption that errors are independent and equal in structure and magnitude for the two sensors.

Given that we observe the 3D bearing angles, as well as the distance between Q1 and Q2, and both of these should be related to measurement error, we can use that information as part of the measurement error model.

10 Conclusions

This report described the DECAF-TEA data collection setting, in particular regarding p-nodes from which the key parameter of detection probability will be estimated. The concept of a virtual point transect half way between the 2 4HUs was introduced. We also investigated potential ways of conceptualizing and simulating errors in the 3D bearings generated from each 4HU, and the implications of measurement error for the localization of sound sources, their corresponding estimated 2D distances to a virtual sensor, and the propagation of those errors to distance sampling density estimates of the sources of interest. It seems clear that measurement error could be a potential problem, leading to considerable bias if significant and ignored.

In the case where a single 4HU is considered for a n-node, we note here that the 3D bearing angles contain information about detectability, even if confounded with the distribution of depths at which the whales produce sounds. Assuming that an animal immediately above the sensor produces a 3D bearing angle of 0 degrees, then small angles (i.e. in the vicinity of 0) will be consistent with fast decreasing detectability. On the contrary, angles close to 90 degrees would imply very large detection distances, and hence non null detectability at large distances. It might therefore be possible to use the information on n-nodes to help in estimating P, which would make these nodes hybrid nodes (say np-nodes).

All the results and considerations made were based on reasonable assumptions about the data collection and potential models for the errors in 3D bearings. However, the next fundamental step will be the collection of empirical data on the trial DECAF-TEA deployment, scheduled for the spring of 2018. This will hopefully provide data which will allow us to move forward some of the ideas put forward here, in particular with a new set of simulations now considering estimated values for measurement error parameters instead of reasonable but essentially untested parameters values assumed here.

There are at least 3 sources of information on performance and measurement error derived from the trial deployment:

1. information on measurement error in 3D location from trials with sources at known locations
2. information on measurement error from potential redundancy in solutions, given that the trial deployment is planned to include 3 4HUs in the vicinity of each other
3. information on measurement error from observations of pairs of 3D bearings with error and the resulting distance between Q1 and Q2 (i.e. the shortest distance between the 2 3D bearings)

References

Borchers, D.L., Marques, T.A., Gunnlaugsson, T. & Jupp, P.E. (2010). Estimating distance sampling detection functions when distances are measured with errors. *Journal of Agricultural, Biological, and Environmental Statistics*, **15**, 346–361.

Buckland, S.T., Anderson, D.R., Burnham, K.P., Laake, J.L., Borchers, D.L. & Thomas, L. (2001). *Introduction to distance sampling: Estimating abundance of biological populations*. Oxford University Press, Oxford.

Buckland, S., Rexstad, E., Marques, T.A. & Oedekoven, C. (2015). *Distance sampling: Methods and applications*. Springer.

Duarte, P., Peixe, T. & Caissotti, T. (2013). Observar golfinhos. com trigonometria. *Gazeta de Matemática*, **169**, 16–22.

Gonzalez, R.P., Thomas, L. & Marques, T.A. (2017). Estimation bias under model selection for distance sampling detection functions. *Environmental and Ecological Statistics*, **24**, 399–414.

Marques, T.A. & Thomas, L. (2017). *Evaluating errors in estimated 2D distance given errors in 3D bearings*. DECAF-TEA internal report.

Marques, T.A., Duarte, P., Peixe, T. & 19/05/2017, L.T. (2017). *Estimating a 3D location from two 3D bearings from known location sensors ii*. DECAF-TEA internal report. CREEM Technical report.

Marques, T.A., Thomas, L., Martin, S.W., Mellinger, D.K., Ward, J.A., Moretti, D.J., Harris, D. & Tyack, P.L. (2013). Estimating animal population density using passive acoustics. *Biological Reviews*, **88**, 287–309.

Marques, T.A., Thomas, L., Ward, J., DiMarzio, N. & Tyack, P.L. (2009). Estimating cetacean population density using fixed passive acoustic sensors: An example with Blainville's beaked whales. *The Journal of the Acoustical Society of America*, **125**, 1982–1994.

Stimpert, A.K., DeRuiter, S.L., Falcone, E.A., Joseph, J., Douglas, A.B., Moretti, D.J., Friedlaender, A.S., Calambokidis, J., Gailey, G., Tyack, P.L. & Goldbogen, J.A. (2015). Sound production and associated behavior of tagged fin whales (*balaenoptera physalus*) in the Southern California Bight. *Animal Biotelemetry*, **3**, 23.